**BLOCK 7.**

**Poster exposition**

Impacts of agricultural activities on land degradation in a context of climate change: case of agricultural land deployed alongside the Bomboré river in Burkina Faso. J.N. KABORE et al.

**General topics presentation**

- The impact of drastic changes in soil moisture showcasing the genotypic variation in the adaptation of two wheat genotypes (Triticum durum Desf.) Afwa Thameur et al.
- Promoting sustainable irrigation management and non-conventional water use in the Mediterranean. Alarcón J.J.
- Alternate wetting and drying in the Center of Portugal: field assessment toward rice sustainability. Gonçalves J.M. et al.
- Water and solute mass balance and circulation model for the rice growing area on the right bank of the lower Guadalquivir River valley. Cuadrado-Alarcón B. et al.
- Effects of the implementation of the Alternate Wetting and Drying (AWD) irrigation strategy in an Italian rice district: lesson learned by applying a semi-distributed agro-hydrological model. Gilardi G. et al.
- Testing automatic irrigation in paddy rice fields: lesson learned in a northern Italy rice farm. Gangi F. et al.
- Water-saving irrigation techniques for rice cultivation in Baix Ter irrigation district. Cufí. S et al.
- Bucket water mass balance model applied to the rice growing areas of Lower Mondego (Portugal) and Bafra (Turkey) Irrigation Districts. Cuadrado-Alarcón B. et al.

# The impact of drastic changes in soil moisture showcasing the genotypic variation in the adaptation of two wheat genotypes (*Triticum durum* Desf.)

Afwa Thameur [1*], Wafa Gasmi [2]
[1]Higher Institute of Applied Biology, Road El Jorf Km 22.5, Medenine 4100, Tunisia
[2]Regional Center of Agricultural Research, BP 357 Road Gafsa Km 6, Sidi Bouzid 9100, Tunisia

* Correspondence: Afwa Thameur: afwa_thameur@yahoo.fr

**Abstract**
Although the breeding programs have enhanced the yield of cereal crops over the course of the last decades, the climate change effect is more and more challenging yield stability and is threatening farmer's livelihood. Among abiotic stresses, drought is the most devastating environmental factor causing yield loss. The objective of this research is to study the effect of water stress among two genotypes of durum wheat (*Triticum durum Desf*): the local variety "Bidi" and the commercialized variety "Om Rabiaa" grown in a pot experiment under greenhouse conditions. We focused on water status, morpho-physiological and biochemical parameters. For this purpose, a severe water deficit was induced by withholding irrigation for 15 days on the 35$^{th}$day after sowing. Concerning the water status, it was assessed through the relative water content (RWC) after 14 days of treatment. There was a reduction of 37% for Bidi and 23.26% for Om Rabiaa. Only the treatment (T) had a significant effect ($P<0.01$). As for the morphological parameters, the green leaf number (GLN) was affected by 58.27% for Om Rabiaa and 38.97% for Bidi after 14 days of withholding irrigation. The treatment (T) and the genotype (G) had a very significant effect ($P<0.01$). On the other hand, the plant height was reduced by 23.06 % for Om Rabiaa and only by 13.17% for Bidi after 14 days. A very highly significant effect ($P<0.0001$) of (T) was observed. Concerning the physiological parameters, the genotype had a highly significant effect ($P<0.01$) on SPAD values. At the same time, the net assimilation rate (A) has plummeted by 78.26% for Om Rabiaa. Whereas, we recorded a reduction of 55.25% for Bidi after 14 days and the (T) was very significant ($P<0.01$). The transpiration rate (E) was affected by 82% on average. Similarly, the stomatal conductance (gs) dropped clearly after 7 days of treatment, particularly for Bidi. The photochemical efficiency of PSII (Fv/Fm) was notably reduced for Om Rabiaa. The above-ground biomass accumulation was reduced in both genotypes and the (T) was highly significant ($P<0.01$). For root biomass, Bidi showed to be less affected by drought and the reduction was only about 19% compared to 48% for Om Rabiaa. Eventually, osmoregulation was important in both genotypes and high proline contents were recorded after 14 days of treatment.

## 1. Introduction

The vulnerability of modern crops to abiotic stresses causes wide annual yield fluctuations between bad years and good years. And there is a major global food deficit as the demand for food is higher than what is being produced. By 2025, the world farmers would have to produce about 3.0 billion tons of cereals to feed the earth's population of nearly 8.0 billion people. This means that worldwide, an average cereal yield of 4 t/ha is to be achieved and sustained (Nagarajan and Nagarajan, 2010). Cereals represent a major component of the human diet worldwide, either directly as baked goods derived from flour, or indirectly as components of animal feed (grain, brans, straws, and other residues). Global cereal production and trade are dominated by wheat and maize (Coombs and Hall, 1997). Average global yields increased from 1.4 t h $^{-1}$ during the 1970s to more than 2 t ha$^{-1}$ in recent years, leading to a great increase in total production. However, global production was curtailed in 2005 due to lower plantings in the major European producing countries combined with a severe drought affecting growing areas in the Mediterranean Basin (Royo et al., 2009). In Tunisia, yield decreased from 1.69 t/ha in 2004 to 1.53 t/ha in 2005 (USDA, 2005). Short periods of very high temperature (>35°C) are a common occurrence in many wheat-growing areas of North Africa. Actually, wheat is mainly grown under rainfed conditions, characterized by unpredictable rainfall and a large incidence of abiotic stresses. Drought and heat during the grain filling period, nutrient deficiencies, and soil problems are the main yield constraints. Tunisian Durum wheat landraces were later increasingly replaced by improved varieties. The introduction of productive varieties resulted in the abandon of the genetically diverse, locally well-adapted but unimproved landraces, and the extinction of genetic variability at the farm scale except for some limited clusters throughout the country (Royo et al., 2009).

Crop response to heat and drought stresses depends on the intensity and the duration of these stresses and the phenological stage of the crop at which they occur. Therefore, the selection of physiological traits for drought tolerance requires a comprehensive understanding of the nature of the trait and its contribution to yield as well as its response to the environment (Ludlow and Muchow, 1990) (Sheshshayee and Bindumadhava, 2003). When drought stress was imposed during the reproductive growth stage of wheat, pollen fertility was most affected. The most sensitive stage of wheat yield to drought stress is in the early spikelet development (Praba et al., 2009). Drought stress decreased the relative leaf water content, and the transpiration rate and concomitantly increased the leaf temperature in wheat and rice (Farooq et al., 2009; Siddique et al., 2001). The stomatal closure and the decrease in stomatal conductance and transpiration rate under drought stress have been related to higher water-use efficiency (the ratio of dry matter produced to water consumed) in wheat (Abbate et al., 2004). In the case of severe drought stress where plant growth and biomass accumulation are greatly diminished, the water-use efficiency is also reduced (Costa et al., 1997). Research focusing on the osmotic adjustment in wheat plants indicated that the osmotic adjustment was greater at the tillering stage than at the heading stage. It was not clear; however, whether the differences among cultivars in the allocation of biomass to grain under water stress were due to osmotic adjustment (Moustafa et al., 1996). Therefore, knowledge of morpho-physiological mechanisms involved in response to soil moisture depletion may contribute to a better selection of varieties adapted to different agro-climatic conditions. This study aimed to assess characteristics related to plant water use in durum wheat genotypes with contrasting yield performance under drought stress. Specifically, the work aimed at (i) assessing the morphophysiological response in local and enhanced wheat varieties and (ii) investigating how soil moisture depletion showcases drought tolerance traits.

## 2. Material and Methods

### *2.1. Plant Material and Growth Conditions*

Pot experiments were conducted in greenhouse semi-controlled conditions in a completely randomized design during the 2017/18 growing season at the Regional Center of Agricultural Research located in Sidi Bouzid, Tunisia. Plant materials consisted of two durum wheat (*Triticum durum* Desf.) genotypes Om Rabiaa (enhanced variety) and Bidi (local variety): Om Rabiaa: drought tolerant and subscribed in Tunisia in 1996. Issued of the cross of L0589 realized at ICARDA/Syria and introduced in Tunisia in 1987 (Deghais et al., 2007); Bidi: its multiplication for commercial purposes started in 1913/1914. Nowadays, it almost disappeared from field crop areas except for some clusters in central Tunisia (Deghais et al., 2007).

The pots were reshuffled weekly to minimize the position effect. Pots were filled with 5Kg of topsoil. Each pot was supplied with ample nutrition mainly comprising Potassium (K), Nitrogen (N), and Phosphorus (P) at 120-120-150. Sowing was performed at an average density of 6 seeds per pot spaced approximately 3 inches from all sides. Later on, replicates were thinned to 4 seedlings per pot. Genotypes were grown under well-watered and drought treatments using six replicates each.

*2.2 Water treatments*

Irrigated pots were watered after the appearance of seedlings, at the stem elongation, anthesis, and grain filling stages.

The plants were kept well-watered initially. The pots were weighed at 100% of field capacity regularly and the amount of lost water was added to maintain the required field capacity. Water-stressed pots were not watered starting from the beginning of tillering stage (stage 13, 21 Zadoks et al., 1974). After that, a drought was given for 14 days. Eventually, two different treatments were applied i.e., well-watered (C) and water-stressed plants (S).

*2.3. Measurements*

2.3.1. Relative water content

The flag leaf relative water content (RWC) was determined gravimetrically. The RWC was calculated using the following formula: RWC (%) = (FW-DW)/ (TW-DW) x 100, where FW-fresh mass, DW-dry mass, TW-turgid mass. The measurements of relative water content were conducted simultaneously to gas exchange parameters.

2.3.2. Gas exchange parameters

Gas exchange parameters (net assimilation rate: A, stomatal conductance: gs, and transpiration rate: E) were measured using the CI-340 handheld photosynthesis system. Measurements were carried out between 10:00 and 12:00 a.m. Data logging started after 45 s of the insertion of leaves into the chamber.

2.3.3. Chlorophyll content estimation

SPAD measurements were determined on flag leaf using a chlorophyll meter (Minolta-502).

2.3.4. Growth parameters

Plant height was measured in cm at 14 days after treatment with a ruler. The green leaf number (GLN) was determined. The fresh weights of the aboveground and root biomass were measured by harvesting four plants that were randomly selected from replicate pots for each water treatment. Finally, plants were harvested, and the dry weights of the above-ground and root biomass were determined.

2.3.5. Proline content

Proline content was determined following the method of Bates et al. (1973), with few modifications. About 0.5 g of leaves were homogenized in a pre-chilled pestle and mortar with 5 ml of 3% sulphosalicylic acid. Then, the homogenate was centrifuged at 3500 g for 15 min at 4°C. The supernatant (0.2 ml) was transferred to a plastic tube containing 3% ninhydrin (0.4 ml), and 0.2 ml of 96% acetic acid and 0.2 ml of 3% sulphosalicylic acid were added. Tubes were incubated for 1 h at 96°C in a water bath and 2 ml of toluene was added to each tube, then stirred, and centrifuged at 3500 g for 15 min at 4°C. The absorbance of the upper phase was measured at 520 nm. The determination of the proline was carried out with a calibration curve.

*2.4. Statistical analysis*

All the recorded variables were tested by applying a two-way analysis of variance (ANOVA). Then, Duncan's multiple range test (DMRT) was further applied for each of the variables to test the differences among the means of the treatments (Duncan, 1955). Data were analyzed on SPSS 16.0. Value $\leq 0.05$ was considered statistically significant.

## 3. Results

*3.1. Effect of water stress on plant water status*

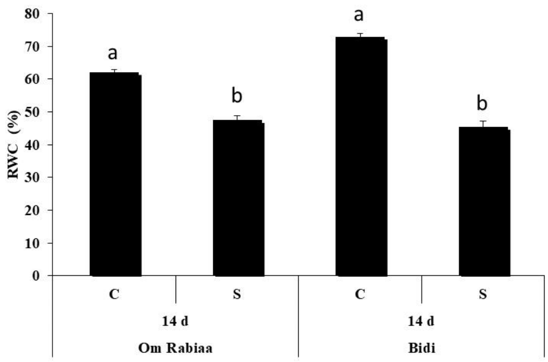


**Figure 1.** The relative water content (RWC) of two wheat varieties during waterlogging (S) and the well-watered treatment (C). Bars indicate the standard deviation of three replicates, and different letters represent the significant difference between the treatments.

Data showed that after 14 days of withholding irrigation, the highest values of relative water content (RWC) were recorded in control plants (Figure 1). RWC was about 72. 8% in control plants of var. Bidi. However, in stressed plants values were about 45.33% with a reduction of 37% compared to control. However, the RWC registered in control plants of Om Rabiaa was about 62%. While, stressed plants recorded 43.33%. A slight drop of 23.66% was observed. Statistical analysis using ANOVA test showed that the treatment had a highly significant effect ($P<0.01$) on the variation of the relative water content.

*3.2. Effect of water stress on growth parameters*

3.2.1. Plant height

After 14 days of withholding irrigation, height decreased by 23.06% for Om Rabiaa reaching 31.16 cm compared to the control 40.5 cm. For Bidi, the reduction was only about 7.05 %. (Figure 2A) Statistical analysis using the ANOVA test showed that the treatment and the genotype had a very highly significant effect ($P<0.001$) on the variation of the height after 14 days of treatment.

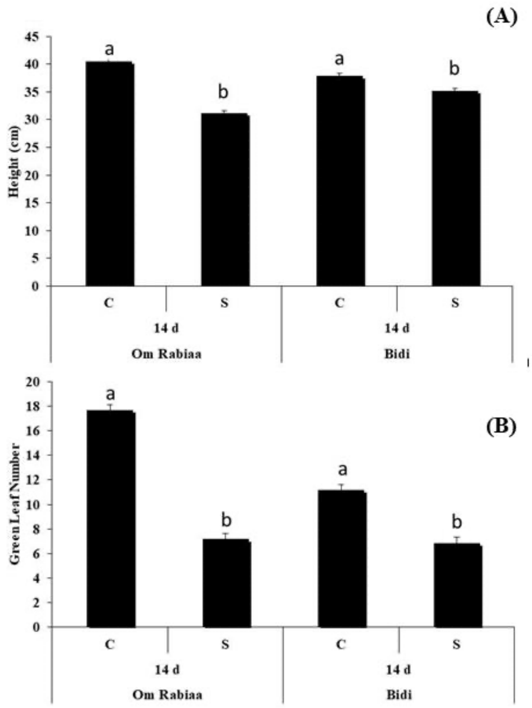


**Figure 2.** The plant height (A) and green leaf number (B) of two wheat varieties during waterlogging (S) and the well-watered treatment (C). Bars indicate the standard deviation of three replicates, and different letters represent the significant difference between the treatments.

3.2.2. The green leaf number

Following 14 days of waterlogging, the green leaf number (GLN) recorded 17.66 in control plants of var. Om Rabiaa. The stressed plants recorded a pronounced decrease of 59.45%. For var. Bidi, the GLN was reduced by 38.97% in stressed plants (Figure 2B). Statistical analysis using the ANOVA test showed that the treatment and the genotype had a highly significant effect ($P<0.01$) on the variation of the green leaf number after 14 days of treatment.

*3.3. Effect of water stress on gas exchange parameters*

3.3.1. The net assimilation rate

After 14 days of treatment, the net assimilation rate in control plants of Om Rabiaa was about 14.95 µmole $m^{-2}$ $s^{-1}$. While stressed plants recorded 3.28 µmole $m^{-2}$ $s^{-1}$ on the 14$^{th}$ day after treatment with a decrease of 78% compared to control (Figure 3A). For var. Bidi, A dropped to 7.49 µmole $m^{-2}$ $s^{-1}$ on the 14$^{th}$ day of treatment with a reduction of 55.25% compared to control. Statistical analysis showed that the genotype and the treatment had a highly significant effect ($P<0.01$) on the variation of the net assimilation rate.

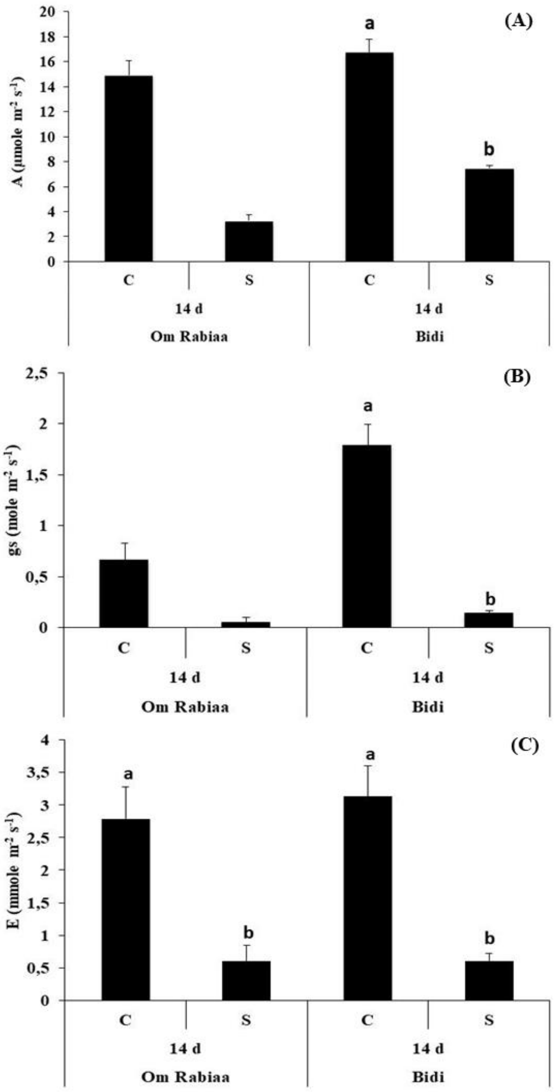


**Figure 3.** The net assimilation rate (A), stomatal conductance (B), and transpiration rate (C) of two wheat varieties during waterlogging (S) and the well-watered treatment (C). Bars indicate the standard deviation of three replicates, and different letters represent the significant difference between the treatments.

3.3.2. The stomatal conductance

After 14 days of treatment, stomatal conductance registered 0.31 mmole $m^{-2}$ $s^{-1}$ in control plants of var. Om Rabiaa. Values were reduced to 0.05 mmole $m^{-2}$ $s^{-1}$(Figure 3B). For var. Bidi, gs was about 1.7 mmole $m^{-2}$ $s^{-1}$ in control plants. In stressed plants, gs dropped to 0.14 mmole $m^{-2}$ $s^{-1}$ after 14 days of treatment. The genotype and treatment had a highly significant effect ($P<0.01$) on stomatal conductance.

3.3.3. The transpiration rate

After 14 days after treatment, the recorded values of transpiration rate were about 2.59 mmole $m^{-2}$ $s^{-1}$ s in control plants of var. Om Rabiaa. While in stressed plants, E was reduced to 0.61 mmole $m^{-2}$ $s^{-1}$ with a reduction of 78.13% (Figure 3C). The var. Bidi, recorded 3.13 mmole $m^{-2}$ $s^{-1}$ in control plants. While in stressed plants E values were reduced to 0.61 with a reduction of 80.51% compared to the respective control. The treatment had a significant effect ($P<0.05$) on the variation of transpiration rate.

*3.4. Effect of water stress on PSII photochemical efficiency*

After 14 days after treatment (DAT), the PSII photochemical efficiency (Fv/Fm) was about 0.74 in control of var. Om Rabiaa. While stressed plants registered 0.51 with a reduction of 32% compared to control. For var. Bidi, Fv/Fm recorded 0.66 in control (Figure 4). In stressed plants, values of 0.54 were recorded and the reduction was about 17% compared to control. The treatment had a significant effect on var. Om Rabiaa.

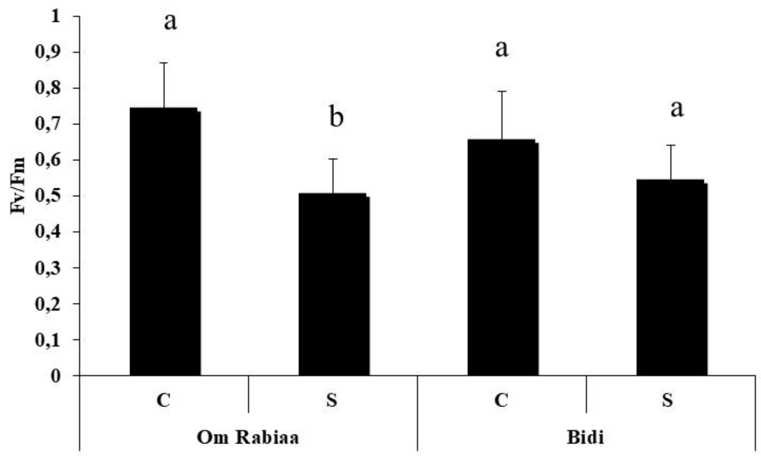


**Figure 4.** The photochemical efficiency of PSII (Fv/Fm) of two wheat varieties during waterlogging (S) and the well-watered treatment (C). Bars indicate the standard deviation of three replicates, and different letters represent the significant difference between the treatments.

*3.5. Effect of water stress on the biomass accumulation*

After 14 DAT, the fresh weight of the aboveground biomass (AGFW) recorded 1.89 g in stressed plants of var. Om Rabiaa with a reduction of 54.45% compared to control. For var. Bidi, the fresh weight was 3.11g in control plants and 1.94 g in stressed plants with a reduction of 37.62% (Figure 5A). Concerning the dry weight (AGDW), the highest values were about 0.68g and 0.57g respectively for var. Bidi and var. Om Rabiaa with the respective reductions of 30.61% and 38.7% compared to control.

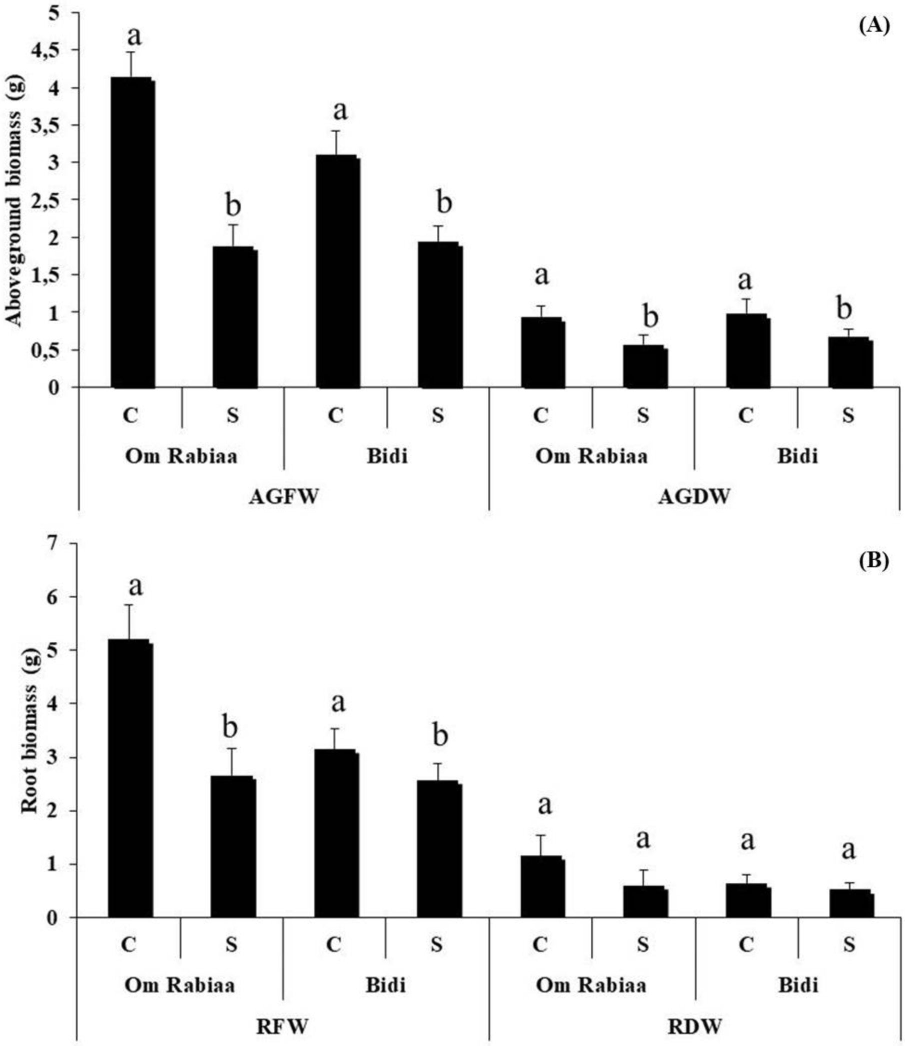


**Figure 5.** The aboveground biomass (A) and root biomass (B) of two wheat varieties during waterlogging (S) and the well-watered treatment (C). Bars indicate the standard deviation of three replicates, and different letters represent the significant difference between the treatments.

In stressed plants, root fresh weight (RFW) was about 2.56 g with a reduction of 50.76% in var. Om Rabiaa. While in var. Bidi the RFW was about 3.14g in control plants compared to 2.56 g in stressed plants with a reduction of 18.47% (Figure 5B). For var. Om Rabiaa, root dry weight was about 1.15g in control compared to 0.59g in stressed plants with a reduction of 48.69%. However, the reduction RDW was about 19.04% in var. Bidi with control plants recorded 0.63g and 0.51g in stressed plants. Statistical analysis showed that the treatment and the genotype had a highly significant effect ($P<0.01$) on the variation of the RFW. No significant effect was observed for RDW.

*3.6. Effect of water stress on the SPAD values*

After 14 DAT, SPAD values were slightly reduced for var. Om Rabiaa (30.31 in control and 30.16 in stressed plants) with a reduction of 0.49% (Figure 6). For var. Bidi, a reduction of 0.5% was observed compared to control after 14 days after treatment. The genotype had a highly significant effect ($P<0.01$) on the variation of the SPAD values.

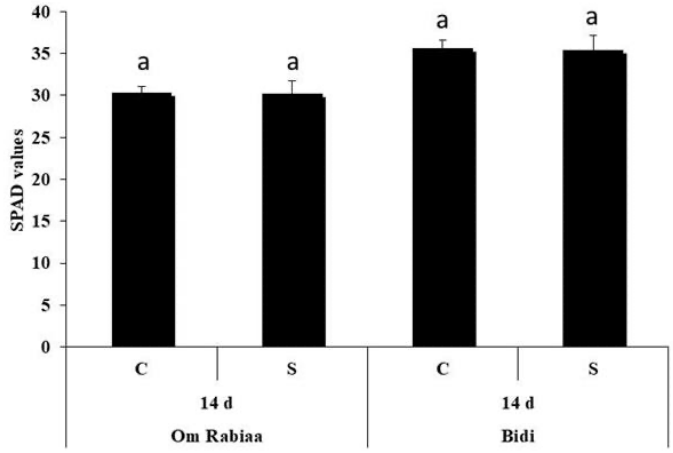


**Figure 6.** The SPAD values of two wheat varieties during waterlogging (S) and the well-watered treatment (C). Bars indicate the standard deviation of three replicates, and different letters represent the significant difference between the treatments.

*3.7. Effect of water stress on the proline content*

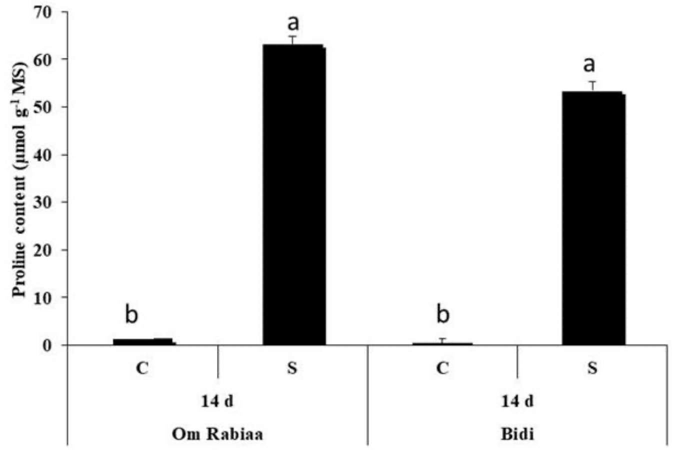


**Figure 7.** The proline accumulation of two wheat varieties during waterlogging (S) and the well-watered treatment (C). Bars indicate the standard deviation of three replicates, and different letters represent the significant difference between the treatments.

The highest proline content was recorded in stressed plants. The values in control plants for var. Om Rabiaa were about 1.38 µmol $g^{-1}$MS. (Figure 7). While in stressed plants values were about 63.26 µmol $g^{-1}$MS with an increase of 97.94% compared to control. On the other hand, for var. Bidi values were about 0.4 µmol $g^{-1}$MS in control plants. However, in stressed plants, values were about 53.48µmol $g^{-1}$MS with an increase of 99.26% compared to control. The treatment had a significant effect on proline content.

**4. Discussion**

The decrease in RWC was more pronounced in var. Bidi. Our results are similar to the findings of Houasli et al., 2014 showing that the relative water content was reduced under drought conditions. Thus, the RWC was rapidly reduced in susceptible genotypes (Thameur et al., (2012). Therefore, this reduction was directly correlated to the decrease in soil water content (Albouchi et al., 2000; Bajji et al., 2001).

Drought affected growth parameters substantially in var. Om Rabiaa. Similar results were obtained by Ferryra et al., (2004) who showed that morphological parameters were clearly affected. In barley, the reduction of green leaf number and leaf appearance rate (Thameur et al., 2011; Thameur et al., 2012) were recorded.

The decrease in leaf area might be due to the decrease in leaf expansion and/or accelerated leaf senescence (El Azeb et al., 2012; Hacini, 2014).

Ali Dib et al., (1992) and Elfakhri et al., (2008) showed that plant height is more affected in susceptible genotypes. In fact, this confirms an adaptation mechanism to reduce water loss by transpiration and maintain the water status of the whole plant (Boudjabi et al., 2017). SPAD values are used as an indicator to evaluate the integrity of the photosynthetic apparatus under drought conditions (Thapa et al., 2018). According to Hikosaka et al., (2006), the chlorophyll content can be influenced by the leaf age, leaf position, and environmental factors such as light, temperature, and water availability. Bousba et al., (2009) indicated that the stomata closure in stressed plants is a strategy to avoid water loss. Yet, it can cause the reduction of chlorophyll content. Siakhène, (1984) showed that the increase in chlorophyll content under drought is due to a reduction in cell size which leads to an increase in its content. This was observed in the genotype Bidi. According to Yuping Li et al., (2017) and Thapa et al., (2018), gas exchange parameters were notably affected by prolonged drought. According to Ali Dib et al., (1992) and Bousba et al., (2009), the drop in (A) was related to the decrease in chlorophyll content particularly in Om Rabiaa, and the increase of stomatal resistance to $CO_2$ penetration (a drop of gs) so as to provide the protection to plant water status through a decrease in transpiration rate (El Azab et al., 2012);

According to Bousba et al., 2009, the important reduction of the transpiration in both studied genotypes after 14 days of drought is related to stomata closure which is the preliminary strategy used to cope with water deficit. Hence, reducing water loss by transpiration through a prompt stomata closure is an efficient adaptation mechanism to water stress (Djekoun and Planchon, 1992). However, a firm stomata closure can cause disorders at the water status level.

Analysis of photochemical efficiency of PSII (Fv/Fm) showed that the decrease of this parameter was more important in var. Om Rabiaa. According to Jagtap et al., (1998), water deficit leads to a sharp decrease in the ratio (Fv/Fm) in five varieties of *Sorghum bicolor* L recording a more pronounced rate in susceptible genotypes. Accordingly, the analysis of chlorophyll fluorescence and its photochemical and non-photochemical components under drought showed a disturbance in the photochemical reactions of photosynthesis resulting in the blocking of electron transfer between LHC II et PS II (O'Neil et al., 2006).

Ali Dib et al., (1992) showed that a slight decrease in the chlorophyll fluorescence intensity in wheat varieties is due to an inhibition of the chloroplast photochemical activity which might be a result of the inhibition of the Calvin cycle ($CO_2$ fixation).

Accumulation of the root biomass was clearly affected by drought, particularly for Om Rabiaa which recorded a notable decrease. The variety Bidi was able to produce more root dry weight than Om Rabiaa after 14 days of drought.

According to Labdelli, (2011) and Thapa et al., (2018), the dry weight is one of the efficient indicators of the effect of water stress. In fact, drought reduced the elaboration of the AGDW more than RDW in durum wheat and bread wheat. Nevertheless, Boudjabi et al., (2017) reported that RDW accumulation is more important in stressed plants which is a way to produce new roots to enhance water uptake. The decrease of the above-ground biomass accumulation is more important in the genotype Om Rabiaa than in Bidi. These results are in accordance with those reported by Sassi et al., (2012) who showed that the wheat varieties replied similarly to drought with a reduction of the dry and fresh aboveground biomass with differences among varieties recording the highest accumulations in tolerant varieties.

Many authors showed that the increase of proline content is related directly to water deficit treatment application (Cechin et al., 2006; Mouellef, 2010). This increase is attributed to the degree, the duration of the applied stress, and the behavior of the genotype (Chaib et al., 2015). Other authors found that the increase of proline concentration is also considered an adaptation mechanism in certain varieties (Delauny and Verma, 1993; Hare and Cress, 1998); however, other authors proposed it as a breeding technique for the selection of drought-tolerant barley genotypes (Bellinger et al., 1991). Tahri et al., (1997) showed that the increase in proline content in wheat is negatively correlated with chlorophyll a and b content. This correlation is due to a competition between these two components to the common precursor which is glutamate. The latest becomes insufficient for the synthesis of both components due to the inhibition of the activity of the glutamate synthetase under drought.

## 5. Conclusion

The results of this study showed that genotypes with contrasting yield performance under drought stress differ significantly in their response to soil moisture variation. Drought tolerant genotype Bidi had a lower reduction rate for gas exchange parameters and photochemical efficiency, after 14 days of withholding irrigation as compared to Om Rabiaa. In addition, this resulted in lower biomass accumulation in Om Rabiaa where proline accumulation showed less increase compared to Bidi upon progressive exposure to water deficit. The tolerant genotype Bidi was able to extract water from dryer soil better than Om Rabiaa. This study suggests that the variety Bidi is more recommended in regions subjected to drastic changes in soil water availability.

### 6. References


Nagarajan S, Nagarajan S. 2010. Biotic Stress Adaptation in Plants: Physiological, Molecular and Genomic Foundation, pp.1–11. Springer Science + Business. Media B.V.

Coombs J, Hall K. 1997. The Potential of Cereals as Industrial Raw Materials. In: Campbell, G.M., Webb, C., McKee, S.L. (eds) Cereals. Springer, Boston, MA.

Royo C, Elias M.E, Manthey F.A. 2009. Durum Wheat Breeding. In: M.J. Carena (ed.), Cereals, pp 199. Springer Science + Business Media, LLC.

USDA, 2005. (http://www.fas.usda.gov/pecad/highlights/2005/07/durum2005/)

Ludlow MM, Muchow RC .1990. A critical evaluation of traits for improving crop yields in water-limited environments. Adv Agron 43:107–153.

Sheshshayee M. S, Bindumadhava H, Shankar A.G, Prasad T.G, Udayakumar M. 2003. Breeding strategies to exploit water use efficiency for crop improvement. J. Plant Bio. 30: 253–268.

Praba M.L, Cairns J.E, Babu R.C, Lafitte H.R .2009. Identification of physiological traits underlying cultivar differences in drought tolerance in rice and wheat. J Agron Crop Sci 195:30–46.

Farooq M, Wahid A, Kobayashi N, Fujita D, Basra SMA .2009. Plant drought stress: effects, mechanisms, and management. Agron Sustain Dev 29:185–212.

Siddique M.R.B, Hamid A, Islam M.S .2001. Drought stress effects on water relations of wheat. Bot Bull Acad Sinica 41:35–39.

Abbate PE, Dardanelli JL, Cantarero MG, Maturano M, Melchiori RJM, Suero EE .2004. Climatic and water availability effects on water-use efficiency in wheat. Crop Sci 44:474–483.

Costa LD, Vedove GD, Gianquinto G, Giovanardi R, Peressotti A .1997. Yield, water use efficiency and nitrogen uptake in potato: influence of drought stress. Potato Res 40:19–34.

Moustafa MA, Boersma L, Kronstad WE .1996. Response of four spring wheat cultivars to drought stress. Crop Sci 36 :982–986.

Deghais M, Kouki M, Gharbi MS, El Falah M. 2007. Les variétés de céréales cultivées en Tunisie. Imprimerie officielle.

Zadoks J.C , Chang T.T , Konzak C.F. 1974. A decimal code for the growth stage of cereals. Weed Res. 14, pp. 415-421

Houasli C, Nasserlhaq N, Elbouhmadi K, Mahboub S, Udupa S.2014. Effet du stress hydrique sur les critères physiologiques et biochimiques chez neuf génotypes de pois chiche (*Cicer arietinum* L.). Nature et Technologie.11:8-16.

Thameur A, Lachiheb B, Ferchichi A. 2012. Drought effect on growth, gas exchange, and yield, in two strains of local barley Ardhaoui, under water deficit conditions in southern Tunisia. J Env Manag. 113: 495-500.

Albouchi A, Sebei H, Mezni M.Y, EL Aouni M.H. 2000. Influence de la durée d'une alimentation hydrique déficiente sur la production de biomasse, la surface transpirante et la densité stomatique *d'Acacia cyanophylla.* Annales de l'INRGREF. 4 : 138- 61.

Bajji M, Lutts S, Kinet J.M. 2001. Water deficit effects on solute contribution to osmotic adjustment as a function of leaf aging in three durum wheat *(Triticum durum* Desf.) cultivars performing differently in arid conditions. Plant Sei. 160: 669 -681.

Ferryra R, Sellés G, Ruiz R.S, Sellés I.M. 2004. Effect of water stress-induced at different growth stages on grapevine cv. Chardonnay on production and wine quality. Acta Hort.664: 233-236p.

Thameur A. Ferchichi A, Lopez-Carbonell M. 2011. Quantification of free and conjugated abscisic acid in five genotypes of barley *(Hordeum vulgare* L.) under water stress conditions. S. Afr. J. Bot : 77. 222-228.
El Azab A, Molero G, Serret M.D, Araus J.L. 2012. Functional Plant Biology. 39:379-393.
Hacini N. 2014. Etude de l'interaction Génotype X Environnement et effet de l'origine de quelques cultivars de blé dur *(Triticum durum* Desf.) sur les aptitudes adaptatives et qualitatives. Thèse de Doctorat. Université de Baji Mokhtar Ennaba. l35p.
Ali Dib T, Monneveux M, Araus J.I.1992. Adaptation à la sécheresse et notion d'idéotype chez le blédur. II. Caractères physiologiques d'adaptation. Agronomie, EDP Sciences12 (5) :381-39 3
El Fakhri M, Nsarellah N, Mahboub S, Bidani A, El Bouhmadi K. 2008. Tests morphologiques et biochimiques pour la tolérance au stress hydrique chez le blé dur *(Triticum durum* Desf*).* Al Awamia : 123-12
Boudjabi S, Kribaa M, Chenchouni H. 2017. Sewage sludge fertilization alleviates drought stress and improves physiological adaptation and yield performances in Durum Wheat (*Triticum durum*): A double-edged sword. J of King Saud Uni - Science.1-9.
Thapa S., Reddy S. K, Fuentealba M.P, Xue Q, Rudd J.C, Jessup K.E, Devkota R.N, Liu S. 2018. Physiological responses to water stress and yield of winter wheat cultivars differing in drought tolerance. J Agro Crop Sei. :1-12.
Hikosaka K, Ishikawa K, Borjigidai A, Muller O, Onoda Y. 2006. Temperature acclimation of photosynthesis: mechanisms involved in the changes in temperature dependence of photosynthetic rate. J Exp. Bot. 57: 291-302.
Bousba R, Ykhlef N, Djekoun A. 2009. Water use efficiency and flag leaf photosynthesis in response to water deficit of durum wheat (*Triticum durum Desf).* World J of Agri Sci. 5 : 609 -616.
Siakhène N. 1984. Effet du stress hydrique sue quelques espaces de luzerne annuelle. Mémoire ing agr. INRAA. El Harrach : 90 p
Yuping L, Hongbin L, Yuanyuan L, Zhang S. 2107. Improving water-use efficiency by decreasing stomatal conductance and transpiration rate to maintain higher ear photosynthetic rate in drought-resistant wheat. Crop J: 1-16.
Djekoun A, Planchon C. 1991. Water status effect on dinitrogen fixation and photosynthesis in soybean. Agron. J. 83:316-322.
Jagtap V, Bhargava S, Streb P, Feierabend J. 1998. Comparative effect of water, heat and light stresses on photosynthetic reactions in *Sorghum bicolor (L.)* Moench. J Exp Bot 49:1715-1721.
O'Neill P.M, Shanahan J.F, and Schepers J.S. 2006. Use of Chlorophyll Fluorescence Assessments to Differentiate Corn Hybrid Response To Variable Water Conditions. Crop Sci. 46:681–687. Crop Physiol Meta.
Labedelli A. 2011. Etude des effets de variations morpho-structurales du système racinaire pour la tolérance du déficit hydrique du blé dur. *(Triticum durum* Desf.). Thèse de Doctorat. Université D'Oran ES-Sania. 120p.
Sassi K, Abid G, Jemni L, Dridi-AI Mohandes B, Boubaker M. 2012. Etude comparative de six variétés de blé dur *(Triticum durum* Desf.) vis-à-vis le stress hydrique. J An and Plant Sci. 5.2: 2157-2170.
Cechin 1, Rossi S.C, Oliveira V.C, Fumis T.F. 2006. Photosynthetic responses and proline content of mature and young leaves of sunflower plants under water deficit. Phtosynthethica 44 (1) : 143-146.
Mouellef A. 2010. Caractères physiologiques et biochimiques de tolérance du blé dur (*Triticum durum* Desf.) au stress hydrique. Mémoire magister, Faculté de biologie. Département de Biologie Végétale et Écologie, Université Constantine, 82 p.
Chaib G, Benlaribi M, Hazmoune T.2015. Accumulation d'osmoticum chez le blé dur *(Triticum durum* Desf) sous stress hydrique. Eu Sci J.24: 1857 - 7881.
Delauney A.J, Verma D.P.S.1993. Proline biosynthesis and osmoregulation in plants. Plant J. 4:215-223.
Hare P.D, Cress W.A, Van Staden J.1998. Detecting the roles of osmolytes accumulation during stress. Plant cell envi. 21: 535-553.
Bellinger Y, Bensaoud A, Larher F. 1991. Physiological significance of proline accumulation, a trait of use to breeding for stress tolerance. p. 449–458. In: E. Acevedo, A.P. Conesa, P. Monneveux and J.P. Srivastava (Eds). Physiology-Breeding of Winter Cereals for Stressed Mediterranean Environments. Montpellier, France, 3–6 July 1989. Colloques INRA n° 55.
Tahri E, Belabed A, Sedki K. 1997. Effet d'un stress osmotique sur l'accumulation de proline, de chlorophylle et des ARNm codant pour la glutamine synthétase chez trois variétés de blé dur *(Triticum durum).* Bulletin de l'Institut Scientifique, Rabat : 81-87.

# PROMOTING SUSTAINABLE IRRIGATION MANAGEMENT AND NON-CONVENTIONAL WATER USE IN THE MEDITERRANEAN – PROSIM

J.J. Alarcón*, F. Pedrero-Salcedo, A. Parra
Department of Irrigation, Centro de Edafología y Biología Aplicada del Segura (CEBAS-CSIC), P.O. Box 164, 30100 Espinardo-Murcia, Spain

*jalarcon@cebas.csic.es

**Abstract**

PROSIM project faces the challenge of water use for irrigation focusing on both water demand and supply for irrigation. The project brings innovative solutions combining water use efficiency and no conventional water resources (NCW) and build local capacities to adopt/upscale them. Cross-border capacity building and roadmaps and plans for improved water management based on project results will be carried out while enhancing public-private cooperation will be fostered together with investments for the adoption/upscale of the proposed solutions.

The project's main expected results are: • 4 national/regional institutions on water management involved and 80 extension agents trained to provide technical support to farmers • 237 pilot farmers (91 ha) equipped with tailored subsets of 9 innovative solutions, increasing water use efficiency (WUE) by 30% and substituting conventional by no conventional water (NCW) up to 100. They will act as change leaders in communities of about 50.000 farmers (100k ha) and beyond, reinforcing commitment to a more sustainable use of irrigation water at Mediterranean basin level

## 1. Introduction

In the context of climate change, the problem of water scarcity for agriculture has been accentuated during the last years.

The main water management problems in the Mediterranean countries are:

- Technical: important water losses in irrigation, due to non-efficient systems; limited water sources diversification and reliance on NCWs, still an untapped resource;
- Institutional: scarce capacities of institutions to enforce effective water management plans, involving Irrigation Practitioners-IPs (e.g. Extension Agents-EAs, water users' associations-WUAs, farmers) in planning and implementation;
- Social: scarce adoption of modern solutions at farmer's level enabling more efficient water-use and NCWs exploitation, due to the lack of awareness and knowledge and technology transfer initiatives.

The possible solutions are:

- To have available new/enhanced, more sustainable and context-tailored solutions for WUE and higher exploitation of NCWs in irrigation;

- To strengthen capacities of national/regional/local institutions to manage water sources efficiently and sustainably, cooperating with IPs and the private sector;
- To enhance capabilities of IPs to adopt, operate and maintain modern WUE and NCWs solutions.

In this sense, PROSIM answer focuses on both demand and supply side, bringing innovative solutions for improve of Water Use Efficiency (WUE) and NCWs and building local capacities.

## 2. General and specific objectives of PROSIM.

General objective: To contribute to environmental protection, climate change adaptation and mitigation in irrigation water management through water use efficiency and use of non-conventional waters.

Specific objectives:

| |
|---|
| To demonstrate new/enhanced, sustainable irrigation solutions that ensure an increased water-use efficiency and entail a larger use of NCWs, adapt their technical complexity to local conditions and capacities of target areas and make tailored solutions available to stakeholders at Med basin level |
| To strengthen cross-border cooperation, capacity building and engagement in sustainable irrigation water management of relevant local institutions and private stakeholders at Med basin level, by sharing and capitalising know-how; providing mutual support in the implementation of innovative solutions; |
| To support farmers' adoption of sustainable irrigation water management solutions combining environmental, technical and economic advantages and foster civil society engagement in environmental sustainability at Med basin level. |

## 3. Cross border impact and expected change

Cross-border Cooperation between different partners (from five Mediterranean countries) will allow to answer common water management challenges and specific needs of territories:

- Spain: to further progress in innovation in WUE and NCWs use, building best practices to transfer in the Med.
- Italy: to cope with technology innovation pace to face water scarcity of Southern regions, especially in Sicily.
- Jordan: to increase NCWs use, e.g. unexploited brackish waters.
- Tunisia: to upscale innovative desalination technologies combined with WUE to face increasing water scarcity in a way that is environmentally sustainable and cost-effective.
- Lebanon: to improve treated waste water (TWW) quality and use in irrigation to address environmental and health challenges.

Thanks to this cross border cooperation, the partners can exchange and capitalise knowledge, help and learn from each other in developing new competences on a multitude of irrigation solutions and improved agricultural practises (IAP).

Change at 5 levels in mid-long term are expected:

- Technological: increased adoption/upscale of 9 product innovations for WUE and NCWs, tailored to local context and farmer-oriented.
- Institutional: improved cooperation between institutions to manage water supply, plan and implement WM initiatives, including efficient and sustainable product innovations and involving the private sector.
- Social: more sustainable water demand by 237 pilot farmers; increased civil society engagement.
- Socio-Environmental: CWs savings thanks to +30% efficiency in water use and substitution up to 100% of CWs with NCWs in 51.5 ha in Lebanon, Jordan and Tunisia, increasing overall water availability.
- Economic: +5-10% investments in WUE and NCWs from governments, financial institutions, providers and farmers; improved agrofood production.
- Employment: we expect 20 new jobs created by farms and IS providers thanks to improved agrofood production and wider adoption of IS.

## 4. Brief description of the cross-cutting issues.

Gender equality: rural women are 70% of agriculture labour force in Jordan, 40% in Lebanon, 30% in Tunisia. Women will be represented at a higher percentage than their presence in comparable roles at national level and will be included equitably, showing that they are key for effective introduction of product innovations.

Democracy & human rights: the project has an inclusive approach linking up local-regional and national level and facilitating participation of groups as local farmer's associations/cooperatives to WM planning process. This reinforces the access to basic rights (e.g. right to higher quality water, to fair socio-economic conditions) and to public decision making process. Inclusion will be regardless of sex, nationality, religion, language.

Environmental sustainability: sustainable product innovations will have some positive environmental effects: -Effects of increased WUE in irrigation: reduced overexploitation and increased protection of groundwater; decreased groundwater salination. -Effects of higher use on NCWs for irrigation: reduced fresh water use; -Effects of improved NCWs quality will reduce soil pollution and salination, increasing crops safety and elimination of polluting irrigation practices.

## 5. Innovative Approach

The project has an overall approach based on partner's experience. Main lessons learned over time refers to process and organization:

- demonstrate solutions with farmers and let them fully experience their benefits is a must to really reach the goal, i.e. that other farmers overcome risk-aversion and progressively follow their peers in adopting innovations.
- successful initiatives combine introduction of technical solutions at farmers' site with support from research institutions and better coordination with local players as key for innovation adoption.

- long-lasting work with institutions at Med basin level opens the door to new solutions and related opportunities to address local needs, more effective ways of working locally and more supportive water management frameworks

Within this overall approach, partners will be concentrated in 9 product innovations (IS innovation stages are different: 1-development; 2-tuning, 3-field adoption).

- IS1: Sub-surface irrigation with treated waste water (JOR, LEB, ITA) – Stage 2
- IS2: Drip irrigation system with no conventional wastewater (all countries) – Stage 3
- IS3: New evaporation pan (JOR) – Stage 2
- IS4: New sensors for irrigation scheduling (JOR, LEB, TUN, ITA) – Stage 2
- IS5: New filtration systems to improve the wastewater reuse (JOR, LEB, TUN, ITA) –Stage 2
- IS6: Improvement of the reverse osmosis desalination (JOR, TUN) - Stage 2
- IS7: Improvement of the nano-filtration systems for desalination (TUN; JOR) - Stage 2
- IS8: Development of capacitive deionisation (JOR)–Stage 1
- IS9: Decision support system for mixing conventional and non-conventional water resources in compliance with national laws (JOR, LEB, TUN, ITA, SPA) – Stage 1.

Strong innovative results are expected for local territories, given their current situation: surface brackish water in Jordan Valley are unexploited and can significantly contribute to reduce pressure on other water sources; wastewater are used in Lebanon with poor treatment and dangerous consequences for the environment; wells excavation and use of groundwater is not sustainable in Tunisia; diffusion of innovation is low in Sicily; correctly mixing waters is a challenge in Spain; etc.

**Acknowledgements**

This research project "Promoting Sustainable Irrigation Management and Non-Conventional Water Use in the Mediterranean- PROSIM" has been funded the ENI CBC MED Programme 2014-2020.

# Alternate wetting and drying in the Center of Portugal: field assessment toward rice sustainability

**José Manuel Gonçalves [1,*], Manuel Nunes [1], António Jordão [2], José Paixão [3], Rui Eugénio [4], António Russo [3], Henrique Damásio [4], Sérgio Oliveira [1], Susana Ferreira [1], Isabel Maria Duarte [1,5], Kiril Bahcevandziev [1,5]**

[1] Instituto Politécnico de Coimbra, Escola Superior Agrária de Coimbra, 3045-601 Coimbra, Portugal; Portugal; jmmg@esac.pt; mnunes@esac.pt; susana.ferreira@esac.pt; iduarte@esac.pt; kiril@esac.pt
[2] Direção Regional de Agricultura e Pescas do Centro, Coimbra, Portugal; antonio.jordao@drapc.gov.pt
[3] Associação de Beneficiários da Obra de Fomento Hidroagrícola do Baixo-Mondego, Montemor-o-Velho, Portugal; jmjpaixao@gmail.com; dilarusso@gmail.com
[4] Associação de Regantes e Beneficiários do Vale do Lis, Leiria, Portugal; eugenio-rui@sapo.pt; hdamasio71@gmail.com
[5] CERNAS-Research Centre for Natural Resources, Environment and Society, 3045-601 Coimbra, Portugal

* Correspondence: jmmg@esac.pt; Tel.: +351 239802261

**Abstract:** Rice cultivation has an important economic and social value in Portugal, being traditionally cultivated under continuous flooding irrigation. High-water demand, water resources pollution and methane emissions are environmental problems of rice agroecosystems that claim effective agronomic changes to safeguard its sustainable production, facing the climate global changes and the raising of a social emergent consensus. Therefore, solutions in rice production that save water and environmentally friendly becomes a priority, to safeguard its sustainability. Alternate wetting and drying (AWD) consists of intermittent flooding irrigation through a sequence of flooding cycles, followed by drying periods. The recession is only due to infiltration and evaporation, leaving the soil surface layer in a non-saturated condition for a few days until the next reflooding cycle. The soil is kept dry until hairline cracks are visible, or the decrease in the soil water potential does not cause significant crop stress (AWD mild option). This communication presents a field study in farmer's paddies carried out for three consecutive years, from 2019 to 2021 with the objectives of: i) assessing the current rice irrigation practices, through a field monitoring, ii) testing AWD, and iii) preparing a AWD knowledge base to support its extension to rice farmers. The field experiments were carried out on the Lower Mondego and Lis Valley Irrigation Districts, Portugal, under Mediterranean Temperate climate, sponsored by the project MEDWATERICE (www.medwaterice.org). The field measurements included the soil hydrodynamics, water table level, field water level, irrigation scheduling and depths, agronomic operations, and rice productivity. This study confirmed the interest of the AWD irrigation of rice paddies in this region. It should be applied from the reproductive phase to the end of the season, through 2 to 4 wet-drying cycles with a dry period of 4-5 days, allowing water savings compared to the traditional continuous flooding, of about 10%, an additional 10-20 days with dry soil, being however expected a decrease in the production of about 5%. Furthermore, the need to carry out frequent and planned irrigation events during the AWD period, demands more accurate inflow control devices, making place for its automation, and leading towards rice modernization through smart flooding irrigation systems. In Portuguese conditions, AWD should be applied from the beginning of the reproductive stage. The traditional practice of waterlogging in the early stages of the crop should be kept, due to the particularly sensitive agronomic criteria, such as thermal control, weeds, wind, or phytosanitary treatments.

**Keywords:** Rice irrigation, Oryza sativa L., Alternate wetting and drying, MEDWATERICE

## 1. Introduction

Rice (*Oryza sativa* L.) has an important economic and social value in several regions, namely in Mediterranean countries [1]. In Portugal, rice is cultivated in about 30 thousand ha, especially in the Mondego, Tagus and Sado Valleys, in lowland areas and coastal wetlands, with a particular role in the preservation of the biodiversity and soil conservation [2]. In these valleys, rice is cultivated in traditional paddies, on lower soils with heavy texture and poor drainage, with a shallow and relatively saline groundwater table. Paddies are irrigated by continuous flooding (CF), with *ca*. 10 cm of ponding depth, and a frequency varying from daily to a few days. Paddies are highly water demanding due to a significant deep percolation, and surface drainage [3]. The flooding of paddies plays several determinant roles, namely, temperature regulation during the first weeks of crop development due to microclimatic imperatives, particularly during night-time in the initial phase of the cycle and during flowering; after sowing, to avoid seed collecting by wild birds; to control of weeds development; to control of the crop damage due to the strong wind; and the soil salt leaching in susceptible areas. In its turn, the initial drainage periods enable the application of phytopharmaceuticals, especially herbicides and fungicides, a good rooting of the seedlings, while avoiding soil hardening, and a reduction of algal proliferation on surface water.

Alternate wetting and drying irrigation (AWD) consists of intermittent flooding, through a sequence of flooding cycles with water depths of about 5 cm, followed by drying periods. The recession is only due to infiltration and evaporation, leaving the soil surface layer in a non-saturation condition for a few days (a condition called "dry soil", in contrast to "flooded soil"), until the next reflooding cycle [4,5]. The soil is kept dry until hairline cracks are visible, or the decrease of the soil water potential does not cause significant crop stress. The management of AWD must consider the referred the water thermoregulatory effect and weed control, to avoid compromising production. The benefits of AWD, when compared with CF, include the: i) irrigation water savings, by up to 30% [6], due to the decrease of deep percolation, facing a lower soil water potential, and a decrease of the soil evaporation.; ii) reduction of greenhouse gas emissions (methane plus nitrous oxide) by 45–90% [7]; iii) reduction of the arsenic accumulation in the grain by 50% [8], and iv) reduction of methylmercury concentrations in rice grain by 38–60% and in the soil [9]. The AWD management is based on two parameters: timing and threshold [6,10]: i) the timing is when in the growing season the drying cycles are imposed, namely by the vegetative, reproductive, or ripening phases, or then throughout the crop season; the crop sensitivity to water stress is a major factor to determine this timing; ii) the AWD threshold is the value of a soil water content that refers a limit condition of water deficit used to determine the time for reflooding.

This research aimed to provide knowledge to outline the guidelines to promote the development of AWD by rice farmers, by studying the effects of AWD on rice yield and water use relative to the actual practice of CF in the Central Region of Portugal.

**2. Materials and Methods**

The experimental study was carried out from 2019 to 2021 in the Lower-Mondego and in the Lis Valley Irrigation Districts, located in Coastal Center of Portugal, with a total irrigated area of about 14,000 ha, and a rice area of about 6,000 ha [2] (Figure 1a). This region has a Mediterranean climate, Csb and Csa of Köppen classification, with an annual average precipitation of about 800 mm to 900 mm. It has temperate and mild summers, with virtually no rainfall, and rainy winters with mild temperatures [12]. The soils are mainly alluvial with high agricultural quality, some of which are poorly drained, with waterlogging and salinization risks, particularly on the downstream areas where rice is cultivated in paddies. The river water used for irrigation is diverted and conveyed mainly by gravity, from weirs, through a collective system [13].

The experimental design, at each site, consisted of two rice plots located in identical edaphoclimatic conditions, one irrigated by CF and the other by AWD. Three trial sites were selected: Bico-da-Barca (BB) and Quinta-do-Canal (QC) in the Lower-Mondego, and Nuno-Guilherme (NG) in the Lis Valley, mapped in Figure 1b, being their geographic coordinates and soil characteristics presented in Table 1.

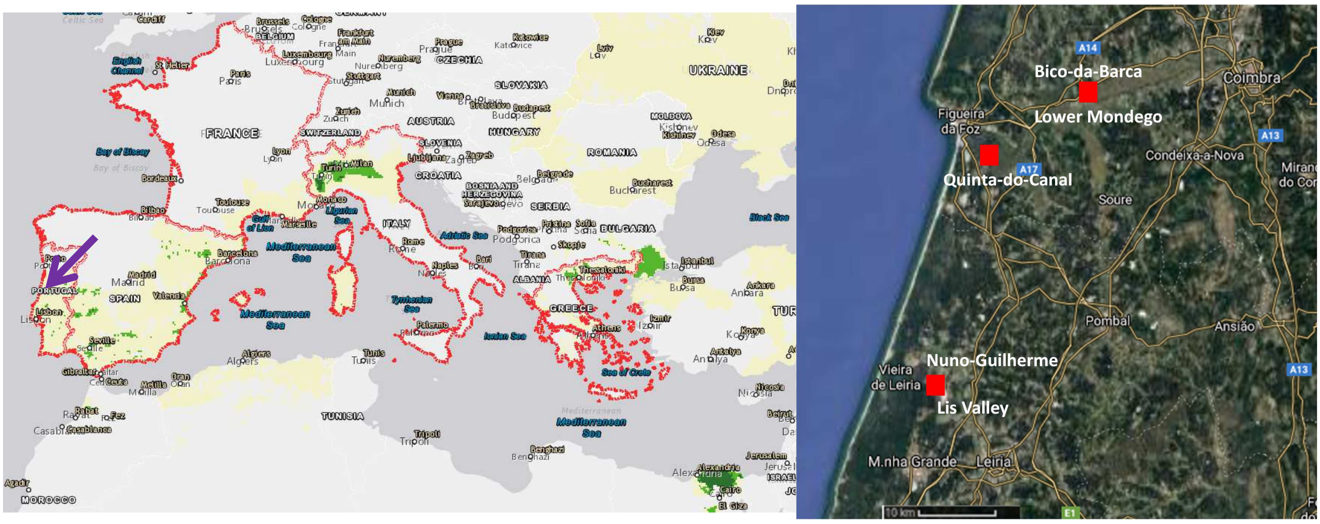


(a) **(b)**

**Figure 1.** Geographic location of: (a) Mediterranean rice growing areas, and the study area in Central Costal Region of Portugal (arrow); (b) the experimental fields (■), on the Lower-Mondego and Lis Valleys (source: (a) [11]; (b) Google Maps, https://maps.google.pt).

**Table 1.** Study site characteristics.

| | **Parameters** | **Experimental sites** | | |
|---|---|---|---|---|
| | | **BB** | **QC** | **NG** |
| Location | Latitude | 40°10′31′′ N | 40°06′54′′N | 39°52′17′′N |
| | Longitude | 8°39′40′′ W | 8°48′08′′ W | 8°52′58′′ W |
| | Altitude (m) | 5 | 2 | 8 |
| Type of farm | | State agricultural experimental station | Associative | Private |
| Area | Field plots (ha) | 0.11 | 4.8 | 3.0 |
| Texture (%) | Sand | 30.0 | 6.4 | 7.1 |
| | Silt | 49.3 | 59.2 | 37.3 |
| | Clay | 20.7 | 34.4 | 55.6 |
| Texture class | | Silt loam | Silty clay loam | Clay loam |
| Soil | pH ($H_2O$) | 5.9 | 7.6 | 7.2 |
| | Soil Organic Carbon (%) | 2.3 | 2.3 | 2.7 |
| | Bulk Density (g $cm^{-3}$) | 1.28 | 1.28 | 1.25 |
| Groundwater table level (bss, cm) | | 40-80 | 50-80 | 75-85 |
| Soil Water Content ($cm^3$ $cm^{-3}$) | Saturation | 0.519 | 0.517 | 0.520 |
| | Field Capacity | 0.484 | 0.471 | 0.385 |
| | Wilting Point | 0.090 | 0.188 | 0.204 |

* Texture classification according to Gomes and Silva [14]; Soil characteristics are relative to the superficial depth of 60 cm; bss—below the soil surface. Experimental sites: BB, Bico-da-Barca; QC, Quinta-do-Canal; NG, Nuno-Guilherme (source: [13]).

A single Italian rice cultivar, Ariete (japonica type) was used in all the sites. Ariete is classified as semi-early, with a cycle of about 139-150 days. It was sown in mid-May, and harvested throughout October, and was fertilized with doses of about 70-90 kg N/ha. Crop development and irrigation practices, and corresponding dates, are presented on Table 2 (example of NG site in 2020 campaign).

**Table 2.** Crop development and irrigation practices and corresponding dates (E.g. NG site 2020 data).

| Crop development and irrigation data | DAS* | Date |
|---|---|---|
| Initial soil flooding | -1 | 13 May |
| Wet sowing | 0 | 14 May |
| Start tillering | 34 | 18 June |
| Panicle differentiation | 60 | 13 July |
| Start AWD | 67 | 20 July |
| Flowering | 90 | 12 August |
| Last irrigation event | 128 | 19 September |
| Harvest | 148 | 9 October |

* DAS - Days after sowing

The experimental plots with the CF treatments were fully managed by the farmers. Traditional flooding practices were applied, which were used as reference to compare with the AWD. Identical agronomic practices were adopted in both treatments, namely the soil preparation, including the ploughing and harrowing, land levelling, fertilization, wet sowing, and crop protection treatments. Water from the river was supplied by gravity-fed systems, using open canals and buried pipes, which were manually controlled.

The methodology adopted in the AWD plots was based on the description by Bouman et al. [15], in the framework of the Mild version, with adjustments, according to the local experimental conditions [13]. In summary, the following steps were taken: i) An initial flooding for wet sowing, followed by an initial drying through a fast surface drainage event, to favor rice emergence, like the traditional practice; ii) Shallow ponding during the vegetative phase, considering the drying periods required for herbicide application, usually twice, like the traditional practice; iii) AWD technique applied after the vegetative phase, taken in account that: a) the target was a flood water depth not higher than 5-7 cm; b) the irrigation schedule considered was a minimum interval of 10 to 14 days between irrigation events; c) the water level should not fall to 15 cm below the soil surface, measured in a water tube; d) Particular attention was paid on the flowering period because at this phase plants are very sensitive to water stress; and iv) The last irrigation event took place about 20 days before the harvest.

The hydraulic monitoring system installed had two components: water tubes with automatic sensors, and water accounting devices with continuous record. The water tubes, consisting of PVC pipes, were placed on soil at 25 cm depth. These tubes, with 40 cm long and 10 cm in diameter, have holes with 1cm in diameter through which the soil water flows into its lumen, allowing the observation of the field water level (FWL) and the measurement with a piezometric head. The water tubes were equipped with automatic water level sensors, which data was complemented with the measurement of the atmospheric pressure though a barometer located nearby. Regularly, at least once a month, the loggers data were downloaded to a PC for further data analysis. During the crop season, manual FWL measurements were carried out in the water tubes with ruler, and the data was used for testing and calibrating the sensors.

The comparison of CF with the AWD practices was based on the water level recorded on water tubes, elucidating about the water level above the soil surface in the flooding irrigation plots, during the entire crop season. The meteorological observations were carried out with automatic weather stations, installed near the experimental sites, with a set of sensors for air temperature and humidity, solar radiation, and wind speed, a Class A pan evaporimeter, and remote communication tool via GSM to the several data users (Table 4). Daily reference evapotranspiration was calculated by Penman-Monteith method, based on Allen et al. procedure [16]. The daily crop evapotranspiration (ETc) was calculated through the crop coefficients of 1.25 for flooding condition, and 1.10 for dry periods.

These measurements allowed obtaining daily data from the system, necessary for the daily water balance method that enabled to calculate the deep percolation (DP), by applying the equation (1),

$$DP = P + I - ETc - SD - \Delta SW, \quad (1)$$

which requires the values of precipitation (P), irrigation (I), surface drainage (SD) and storage difference of surface or subsurface soil water ($\Delta SW$) [3].

The crop yield parameters were determined at harvest, collecting the aerial part of the total rice plants in diverse unit areas of 0.5 $m^2$, with about 5-unit areas per hectare. The biomass harvest was latter processed in the laboratory, determining the dry matter of grain with 14% of humidity and straw and the weight of 1000 grains.

Based on the irrigation water applied (I, $m^3$ $ha^{-1}$), precipitation (P, $m^3$ $ha^{-1}$) and yield (Y, kg $ha^{-1}$), the water productivity (WP, kg $m^{-3}$) was calculated through the equation (2),

$$WP = Y / (P + I). \quad (2)$$

## 3. Results

### *3.1. Soil flooding changes and crop development*

The characterization of the traditional CF practice, illustrated in Figure 2 with data from the NG site in the 2021 season, evidenced the contrast with the dry periods in the AWD treatment. The AWD technique was applied, making up to three wet-dry cycles, until the final period of 30 days before the harvest. These cycles corresponded to a three weeks period, with irrigation depths between 72 and 210 mm, and 4 to 6 days with dry soil, per cycle.

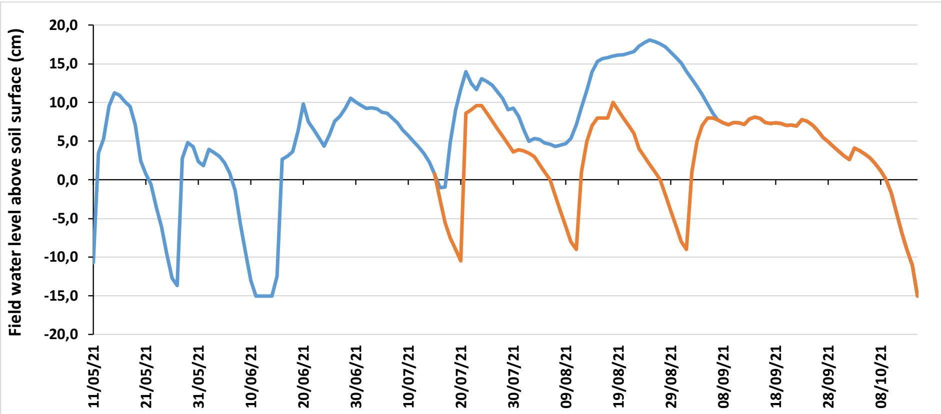


**Figure 2.** Water level above and below the soil surface (cm) of CF (blue line) and AWD (orange line) irrigation during 2021 rice crop season in NG site, Lis Valley.

The additional number of days with dry soil, comparing CF with AWD after the vegetative phase (average values of 2020 and 2021 seasons) was 5, 8 and 21 days, for QC, BB and NG, respectively (Table 3). Referring all cropping seasons, the total number of days with dry soil on cropping cycle was 38%, 54% and 29%, for QC, BB and NG, respectively.

**Table 3.** Number of days with wet and dry soil, in the experimental rice fields irrigated with CF with AWD (average and standard deviation values of 2020 and 2021 season).

| Experimental site | Soil condition | Crop season (days) | | After vegetative phase (days) | |
|---|---|---|---|---|---|
| | | CF | AWD | CF | AWD |
| QC | Wet | 96 ± 8 | 92 ± 14 | 50 ± 10 | 45 ± 16 |
| | Dry | 52 ± 6 | 57 ± 12 | 24 ± 9 | 29 ± 15 |
| | Total | 149 ± 2 | 149 ± 2 | 74 ± 1 | 74 ± 1 |
| BB | Wet | 72 ± 12 | 74 ± 6 | 32 ± 8 | 24 ± 4 |
| | Dry | 68 ± 16 | 77 ± 2 | 44 ± 4 | 52 ± 6 |
| | Total | 139 ± 4 | 139 ± 4 | 76 ± 3 | 76 ± 3 |
| NG | Wet | 126 ± 8 | 106 ± 16 | 76 ± 8 | 56 ± 16 |
| | Dry | 22.5 ± 1 | 44 ± 8 | 8 ± 1 | 28 ± 8 |
| | Total | 148 ± 8 | 148 ± 8 | 84 ± 8 | 84 ± 8 |

CF — Continuous flooding; AWD — Alternate Wetting and Drying; Experimental sites: BB, Bico-da-Barca; QC, Quinta-do-Canal; NG, Nuno-Guilherme.

The average irrigation water use (average values of 2020 and 2021 seasons) of CF was 1483 mm, 1865 mm and 1327 mm, for QC, BB and NG, respectively (Table 4). The correspondent deep percolation ratio for CF was 40%, 72% and 48%, which explain the high irrigation use of BB plot. The AWD relative water savings (compared with CF) was of 10%, 21% and 10%, for QC, BB and NG, respectively. The values for QC and NG could be considered a feasible target for most paddies, such as their soil representativeness. The AWD relative reductions in cultural evapotranspiration was 0.8%, 1.7% and 1.9%, and its reductions in deep percolation of 13.6%, 21.5% and 7.5%, for QC, BB and NG, respectively.

**Table 4.** Water use parameters in the experimental rice fields irrigated with CF with AWD, during the crop season, and after the vegetative phase (average and standard deviation values of 2020 and 2021 seasons).

| Experimental site | Water use (mm) | Entire cropping season | | After vegetative phase | |
|---|---|---|---|---|---|
| | | CF | AWD | CF | AWD |
| QC | ETc | 667.2 ± 29.0 | 661.6 ± 23.4 | 289.8 ± 9.1 | 284.2 ± 3.5 |
| | I | 1483 ± 104.5 | 1327 ± 61.0 | 634.3 ± 17.2 | 459.8 ± 34.6 |
| | P | 157.8 ± 27.4 | 157.8 ± 27.4 | 78.8 ± 1.2 | 78.85 ± 1.2 |
| | DP | 600.2 ± 61.8 | 518.4 ± 98.6 | 302.8 ± 41.4 | 223.6 ± 71.0 |
| | SD | 408.2 ± 108.2 | 345.4 ± 115.4 | 167.0 ± 44.6 | 77.5 ± 39.5 |
| BB | ETc | 594.2 ± 6.2 | 584.2 ± 16.1 | 279.0 ± 2.9 | 269.7 ± 6.3 |
| | I | 1865 ± 140.5 | 1473 ± 48.6 | 740.6 ± 1.5 | 467.8 ± 69.7 |
| | P | 131.6 ± 32.0 | 131.6 ± 32.0 | 84.0 ± 3.8 | 84.0 ± 3.8 |
| | DP[1] | 1342 ± 78.8 | 1027 ± 47.5 | 642.5 ± 8.9 | 436.7 ± 57.4 |
| NG | ETc | 677.9 ± 3.2 | 664.8 ± 8.5 | 358.8 ± 11.4 | 345.7 ± 16.7 |
| | I | 1327 ± 35.0 | 1194 ± 25.5 | 677.8 ± 38.6 | 545.6 ± 28.6 |
| | P | 102.2 ± 20.4 | 102.2 ± 20.4 | 74.0 ± 5.6 | 74.0 ± 5.6 |
| | DP | 638.1 ± 50.3 | 590.4 ± 84.2 | 374.0 ± 43.8 | 327.2 ± 78.6 |
| | SD | 135.0 ± 19.8 | 112.8 ± 5.45 | 41.0 ± 4.5 | 18.8 ± 18.8 |

ETc — Crop Evapotranspiration(mm); DP — Deep percolation (mm); P — Precipitation (mm); I — Irrigation (mm); SD — Surface Drainage (mm); CF — Continuous flooding; AWD — Alternate Wetting and Drying; Experimental sites: BB, Bico-da-Barca; QC, Quinta-do-Canal; NG, Nuno-Guilherme. [1] Includes a small fraction of surface drainage

The average rice yield (unhusked grain with 14% of moisture) was higher in the plots irrigated by CF than in those with AWD. The relative yield decrease of AWD was 5.2%, 7.3% and 2.7%, for QC, BB and NG, respectively. The relative WP increase of AWD was 5.9%, 12.5% and 6.6%, for QC, BB and NG, respectively. However, yield varied significantly between the sites, due to the effects of local edaphoclimatic conditions (Table 5).

**Table 5.** Rice and water productivity of CF and AWD plots (average and standard deviation values of 2020 and 2021 seasons).

| Experimental site | Method | Y (t/ha) | WP (kg/m³) | G (g) | RS (t/ha) |
|---|---|---|---|---|---|
| QC | CF | 8.542 ± 1.041 | 0.541 ± 0.062 | 27.0 ± 1.95 | 5.595 ± 0.11 |
| | AWD | 8.101 ± 1.151 | 0.573 ± 0.094 | 26.4 ± 2.50 | 5.910 ± 0.29 |
| BB | CF | 6.613 ± 1.489 | 0.353 ± 0.117 | 27.7 ± 3.30 | 4.560 ± 0.11 |
| | AWD | 6.128 ± 1.996 | 0.397 ± 0.137 | 28.3 ± 2.70 | 4.735 ± 0.55 |
| NG | CF | 6.149 ± 0.156 | 0.401 ± 0.035 | 28.1 ± 3.95 | 4.145 ± 0.02 |
| | AWD | 5.986 ± 0.327 | 0.428 ± 0.024 | 27.5 ± 3.35 | 3.825 ± 0.18 |

Y – Yield (t unhusked rice grain, 14% of humidity/ha); WP — Water Productivity (Y(kg/ha) / (I+P, m³/ha) (kg/m³); G — Weight of 1000 grãos, with 14% of humidity (g); RS — Rice Straw (dry matter, t/ha); CF — Continuous flooding; AWD — Alternate Wetting and Drying; Experimental sites: BB, Bico-da-Barca; QC, Quinta-do-Canal; NG, Nuno-Guilherme.

The water savings and the impacts on production due to AWD, recorded in this study are, in general, in agreement with the values indicated in the literature [17,18]. Therefore, this experiment confirmed the importance of AWD for water saving in rice irrigation, especially from the reproductive phase onwards, which occurs after mid of July. This water saving allows the Water Users Associations to mitigate the water scarcity in this period at district level, which corresponds to the maximum demand of most irrigation crops, such as corn, widely grown in Portugal. However, the successful application of AWD requires several changes on the rice production system, namely on precise land levelling (PLL), weeds control and fertilization scheme. PLL is a crucial complementary aspect to the success of AWD, so that the water depth on the soil is uniform throughout the entire plot. This is a condition for adopting a thinner water layer which, therefore, allows for a reduction in water use [19]. To this end, a regular and rigorous practice of level maintenance and monitoring should be encouraged.

Irrigation management in the alternating flooding period can be carried out in several ways. Gonçalves et al. [13] presented the main issues related to the application of AWD to rice irrigation to Center of Portugal. The AWD negative impacts on yield raises the question of the farmer's economic income, making this technique unattractive, especially when the water supply is sufficient for CF. This issue claims for a political strategy to promote rice production sustainability because the governmental support to change the rice irrigation system should guarantee the farmer's income.

## 4. Conclusions

This study confirmed the interest of the AWD irrigation of rice paddies in the Center of Portugal, a technique to be applied after the vegetative phase of the crop. AWD should be applied after the reproductive phase, through 2 to 4 drying cycles, with a dry period of 4-5 days in each cycle, allowing water savings in relation to the traditional continuous flooding of about 10%, an additional 10-20 days with dry soil, without significantly compromising rice production with a decrease in production about 5%. It was also concluded that the process of application and extension of AWD must be guided by a progressive adaptation of irrigation techniques, to obtain consolidated knowledge and adapted to local conditions, to limit the risks of loss of income and to build up the confidence in farmers for technological change.

The practice of waterlogging in the early stages of the crop is highly conditioned by particularly sensitive agronomic criteria (thermal control, weeds, wind, and phytosanitary treatments). Therefore, changes of the conventional procedure are not recommended until the beginning of the reproductive stage. Furthermore, the need to carry out frequent and planned irrigation events during the AWD period, demands for more accurate inflow control devices, making place for its automation, leading towards to rice modernization through smart flooding irrigation systems.

**Funding:**

Project MEDWATERICE: Towards a sustainable water use in Mediterranean rice-based agro-ecosystems. The project is financed in the context of the PRIMA Programme (PRIMA-Section-2018; Topic: 1.1.3: Irrigation technologies and practices) (MEDWATERICE-PRIMA-0005-2018, www.medwaterice.org).

## References

1. MEDWATERICE Homepage, http://www.medwaterice.org/, last accessed 2022/03/23.
2. GPP - Gabinete de Planeamento, Políticas e Administração Geral. Available online: https://www.gpp.pt/ (accessed on 20 March 2022).
3. Pereira, L.A. Management of rice irrigation. PhD Thesis, ISA, Technical University of Lisbon, Lisbon, 1989 (in Portu-guese).
4. Tuong, T.P., Bouman, B.A.M. Rice production in water-scarce environments. In Kijne, J.W., Barker, R. Molden, D. (eds.) Water Productivity: Limits and Opportunities for Improvement. CABI Pub., Oxon, pp. 53-67 (2003).
5. Richards, M., Sander, B.O. Alternate wetting and drying in irrigated rice. Implementation guidance for policymakers and investors. Info Note, CGIAR, CCAFA, IRRI, 2014.
6. Carrijo, D.R., Lundy, M.E., Linquist, B.A. Rice yields and water use under alternate wetting and drying irrigation: A meta-analysis. Field Crops Research 2017, 203, 173–180; doi: 10.1016/j.fcr.2016.12.002.

7. Runkle, B.R.K., Suvoscarev, K., Reba, M.L., Reavis, C.W., Smith, S.F., Chiu, Y.L., Fong, B. Methane emission reductions from the alternate wetting and drying of rice fields detected using the eddy covariance method. Environ. Sci. Technol. 2019, 53, 671-681.
8. Linquist, B., Anders, M.M., Adviento-Borbe, M.A.A., Chaney, R.., Da Roda, E.F.F., Van Kessel, C. Reducing greenhouse gas emissions, water use, and grain arsenic levels in rice systems. Glob. Change Biol. 2014, 21, 407-417.
9. Tanner, K.C., Windham-Myers, M., Marvin-DiPasquale, M., Fleck, J.A., Linquist, B.A. Alternate Wetting and Drying Decreases Methylmercury in Flooded Rice (Oryza sativa) Systems. Soil Sci. Soc. Am. J. 2018; doi:10.2136/sssaj2017.05.0158.
10. Mote, K., V Praveen Rao, V.P., Anitha, V. Alternate wetting and drying irrigation technology in rice. Indian Farming 2020, 70(04), 06–09.
11. USDA – US Department of Agriculture – Foreign Agricultural Service. Available online: https://ipad.fas.usda.gov/cropexplorer/ (accessed on 20 March 2022).
12. IPMA. IPMA Home Page. Available online: www.ipma.pt (accessed on 10 November 2018).
13. Gonçalves, J.M., Nunes, M., Ferreira, S., Jordão, A., Paixão, J., Eugénio, R., Russo, A., Damásio, H., Duarte, I.M., Bahcevandziev, K. 2022. Alternate Wetting and Drying in the Center of Portugal: Effects on Water and Rice Productivity and Contribution to Development. Sensors, 22, 3632.
14. Gomes, M.P.; Antunes-da-Silva, A. A new triangle diagram for basic soil texture classification. Estudos Agronómicos 1962, 3 (1), 1-9, Lisbon (in Portuguese).
15. Bouman, B.A.M., Humphreys, E., Tuong. T.P., Barker. R., 2007. Rice and water. Adv. Agron. 92, P.187-237.
16. Allen, R.G., Pereira, L.S., Raes, D., Smith, M. Crop Evapotranspiration. In Guidelines for Computing Crop Water Re-quirements; FAO Irrigation and drainage paper 56; FAO: Rome, Italy, 1998; 300p.
17. Datta, A., Ullah, H., Ferdous, Z. Water management in rice. In: Chauhan, B.S. (eds.) Rice Production Worldwide, pp. 255-277. Springer Int. Pub. AG (2017).
18. Jalindar, M.K., Rao, V.P., Ramulu, V., Kumar, K.A., Devi, M.U. Effectiveness of field water tube for standardization of alternate wetting and drying (AWD) method of water management in lowland rice (Oryza Sativa L.). Irrig. and Drain. 2019, 68: 679-689.
19. Evangelista, G.K.M. Land Gradient Effects on Water Productivity in Rice Production; Crop Science, University of Philippines: Los Banos, Philippines. 2019.

**Water and solute mass balance and circulation model for the rice growing area on the right bank of the lower Guadalquivir River valley**

**Authors:** *Blanca Cuadrado-Alarcón[1], Sébastien Guery[2], Luciano Mateos[1]*

**Affiliation:** [1] Instituto de Agricultura Sostenible, CSIC, 14004 Córdoba, Spain; [2] Optiriego Consulting, 41015 Sevilla, Spain.

**Abstract**

The rice-growing area in the right riverbank of the Lower Guadalquivir Marshes (Spain) comprises about 22,000 ha. Land productivity in the region is high due to a favourable environment and high cropping intensity. The rice fields require about 10,000 m$^3$/ha/year of flood irrigation at a district scale, although individual fields may receive four times as much due to a high rate of surface drainage and water recirculation. Irrigation water is pumped from the Guadalquivir estuary. Salinity is therefore a potential problem which severity depends on the rate of water released from the river reservoirs located upstream and the ocean tides.

A 'bucket' mass balance with capacity constraints has been applied to model daily water, salts balances and circulation in the rice area. The model computes both balances in single irrigation units considering the components evapotranspiration, precipitation, percolation, surface drainage, and irrigation. The connections between the irrigation units requires a conceptualization of the system in a mesh (looped) layout of the distribution network with connection nodes consisting of drains that collect return flows from the irrigation units and supply reused water for irrigation.

Water mass and salt concentration are monitored in specific points of the rice growing area. These measurements were compared with the model outputs. The model was validated by comparing measurements and simulation results from year 2020.

**Keywords:** 'bucket' model, water balance, salt balance, irrigation, rice.

## 1. Introduction

Water resources governance needs simple tailormade models adapted to the requirements of each area. This study addresses water management and planning in the rice growing area in the right riverbank of the lower Guadalquivir Marshes, Spain (Figure 1). The area comprises about 22,500 ha between the estuary of the Guadalquivir River and the Doñana National Park. Land productivity in the region is high due to a favourable environment, high cropping intensity and professionalized practices. Rice production is traditional in the region and generates a significant amount of rural employment. The economic activity associated to rice production includes rice industry, agrochemical suppliers, transport, agricultural machinery dealers, and red swamp crayfish (*Procambarus clarkii*) industry.

The fields require about 10,000 m$^3$/ha/year of irrigation water at a district scale, although individual fields may receive four times as much. This difference is due to a high rate of surface drainage and water recirculation. Irrigation water is pumped from the Guadalquivir estuary.

Water scarcity is the most important limitation to rice production in the Guadalquivir Marshes. The water storage in the basin allowed cultivation of only 50% of the area in 2021 and about 30% in 2022. Moreover, salinity is an additional problem which severity depends on the influence of the ocean tides (greater the further downstream), the water released from the river reservoirs located upstream, and how water is circulated across the district. The water that is not consumed or percolated down to the underlying water table returns to the estuary with an increased concentration of salts. Therefore, salt concentration is spatially distributed across the rice growing area, increasing downstream along the estuary and as the number of upstream water reuses increases.

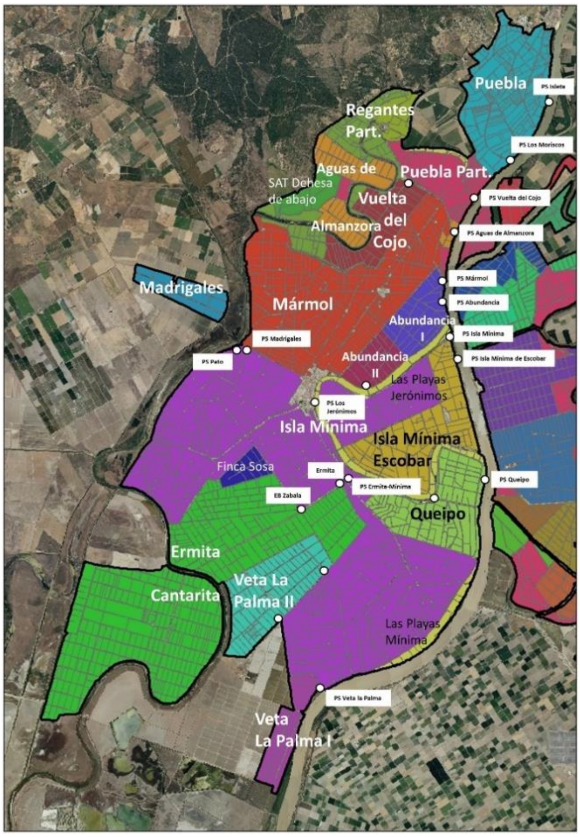


**Figure 1. Right riverbank of the rice growing area in the lower Guadalquivir River valley (Spain)**

The objective of this paper is the development of a model to predict water and salt distribution in the rice growing area on the right bank of the lower Guadalquivir River, in response to water management and planning decisions.

## 2. Materials and methods

We developed a model of balance and circulation of water and salt with capacity restrictions to compute daily water and salts distribution in the study area. The model approach (Mateos et al., 2000, Mateos, 2008) computes the water balance in each irrigation and drainage unit in the system considering the components evapotranspiration, precipitation, percolation, surface drainage and irrigation.

The connection between both types of units requires topological conceptualization of the system. In the study case, the arrangement of the units was determined by its mesh layout. Once the water fluxes are computed, salts mass balance equations are formulated for each unit according to its flow diagram, and the unknown salt concentration in every unit is calculated daily.

Volumes of irrigation and drainage are calculated in the irrigation units according to irrigation needs and the management of the drainage outlets. Irrigation and drainage volumes flow from and to different drainage units or the river according to the topological diagram of the system, which is formulated mathematically through two correspondence matrices (Figure 2). The Irrigation Correspondence Matrix ($ICM$) contains factors that indicate the proportion of irrigation that flows from the water sources (columns) to the irrigation units (rows). The Drainage Correspondence Matrix ($DCM$) contains factors that indicate the proportion of drainage that flows from each irrigation unit (rows) to the main water source and each drainage units (columns). In the matrices, $n$ is the number of irrigation units represented with the $j$ subscript throughout the model, $m$ is the number of drainage units represented with the $k$ subscript throughout the model, and $r$ is the main water source (Guadalquivir River for this case study).

Irrigation Correspondence Matrix ($ICM$)

| $j \backslash k$ | $r$ | 1 | 2 | 3 | ⋯ | $m$ |
|---|---|---|---|---|---|---|
| 1 | $f_{1r}$ | $f_{11}$ | $f_{12}$ | $f_{13}$ | ⋯ | $f_{1k}$ |
| 2 | $f_{2r}$ | $f_{21}$ | $f_{22}$ | $f_{23}$ | ⋯ | $f_{2k}$ |
| 3 | $f_{3r}$ | $f_{31}$ | $f_{32}$ | $f_{33}$ | ⋯ | $f_{3k}$ |
| ⋮ | ⋮ | ⋮ | ⋮ | ⋮ | ⋮ | ⋮ |
| $n$ | $f_{jr}$ | $f_{j1}$ | $f_{j2}$ | $f_{j3}$ | ⋯ | $f_{jk}$ |

Drainage Correspondence Matrix ($DCM$)

| $j \backslash k$ | $r$ | 1 | 2 | 3 | ⋯ | $m$ |
|---|---|---|---|---|---|---|
| 1 | $g_{1r}$ | $g_{11}$ | $g_{12}$ | $g_{13}$ | ⋯ | $g_{1k}$ |
| 2 | $g_{2r}$ | $g_{21}$ | $g_{22}$ | $g_{23}$ | ⋯ | $g_{2k}$ |
| 3 | $g_{3r}$ | $g_{31}$ | $g_{32}$ | $g_{33}$ | ⋯ | $g_{3k}$ |
| ⋮ | ⋮ | ⋮ | ⋮ | ⋮ | ⋮ | ⋮ |
| $n$ | $g_{jr}$ | $g_{j1}$ | $g_{j2}$ | $g_{j3}$ | ⋯ | $g_{jk}$ |

**Figure 2. Correspondence matrices derived from the conceptualization of the system**

Factors $f$ and $g$ must meet conditions:

$$\forall\, j\,; \qquad f_{jr} + \sum_{k=1}^{m} f_{jk} = 1 \qquad (1a)$$

$$\forall\, j\,; \qquad g_{jr} + \sum_{k=1}^{m} g_{jk} = 1 \qquad (1b)$$

### 2.1. Water balance in the irrigation units

The water mass balance equation for an irrigation unit is:

$$\boldsymbol{V_{ij}} = \boldsymbol{V_{(i-1)j}} - \boldsymbol{ETc_{ij}} + \boldsymbol{R_{ij}} + \boldsymbol{I_{ij}} - \boldsymbol{D_{ij}} - \boldsymbol{P_{ij}} \qquad (2)$$

Where the $i$ subscript represents the day in the balance, the *j* subscript represents the irrigation unit, $\boldsymbol{V_{ij}}$ and $\boldsymbol{V_{(i-1)j}}$ are the volumes of water in the unit *j* on the day of concern and the previous day, respectively, and $\boldsymbol{ETc_{ij}}$, $\boldsymbol{R_{ij}}$, $\boldsymbol{I_{ij}}$, $\boldsymbol{D_{ij}}$,and $\boldsymbol{P_{ij}}$ are the volumes of crop evapotranspiration, rainfall, irrigation, surface drainage, and percolation, respectively, in the irrigation unit *j* on day *i.*

$\boldsymbol{ETc_{ij}}$ was calculated with the FAO Penman-Monteith method (Allen et al., 1998). Daily reference evapotranspiration ($ETo_i$) was taken from the Isla Mayor weather station part of the Agroclimatic Information Network of Andalusia (RIA, acronym of the name in Spanish, www.juntadeandalucia.es/agriculturaypesca/ifapa/ria/), which is located in the study area. The daily crop coefficient ($kc_{ij}$) was considered to be 1.05 when the irrigation unit is flooded and before rice plants emerge above the water surface, 1.20 when the crop is fully developed, and 0.6 just before harvest (Allen et al., 1998). Satellite Sentinel-2 images of the study area, downloaded from the Copernicus open-access website (https://sci-hub.copernicus.eu), were used to derive unit specific crop coefficients derived from the vegetation index NDVI (Mateos et al., 2013; González-Dugo et al., 2013). During the water filling period, that in large irrigation units may take several days, a filling factor (varying from 0 to 1) simulating the flooding progression is multiplied by the corresponding $ETc_{ij}$. The daily filling progression factor ($FillF_{ij}$) is calculated based on the pumping capacity in the irrigation unit and the irrigation needs of the day.

$$ETc_{ij} = ETo_i * kc_{ij} * Area_j * FillF_{ij} \qquad (3)$$

$\boldsymbol{R_{ij}}$ was calculated from rainfall data recorded at the Isla Mayor weather station.

$\boldsymbol{V_{ij}}$, $\boldsymbol{I_{ij}}$, $\boldsymbol{D_{ij}}$,and $\boldsymbol{P_{ij}}$ are functions of the water depth in the irrigation unit **($\boldsymbol{h_{ij}}$)**, which is the water depth in the soil profile ($\boldsymbol{h_{SWCij}}$) plus the water depth in the free water layer above the soil surface ($\boldsymbol{h_{FWDij}}$):

$$\boldsymbol{h_{ij}} = \boldsymbol{h_{SWCij}} + \boldsymbol{h_{FWDij}} \qquad (4)$$

The value of $\boldsymbol{h_{SWCij}}$ can vary between the soil water depth in the soil profile at wilting point ($h_{WPj}$) and at saturation water content ($h_{SATj}$), passing by that at field capacity ($h_{FCj}$). Wilting point, saturation water content and field capacity are soil parameters specific of each irrigation unit. The soil profile was considered 1 m deep for this specific application of the model purpose. Thus:

$$V_{ij} = Area_j * h_{ij} \qquad (5)$$

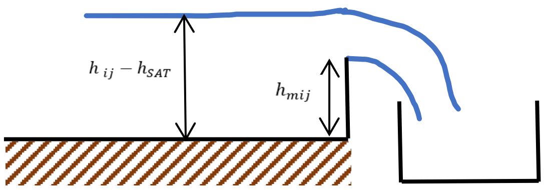


**Figure 3. Sketch of an outlet in the Guadalquivir case study irrigation unit**

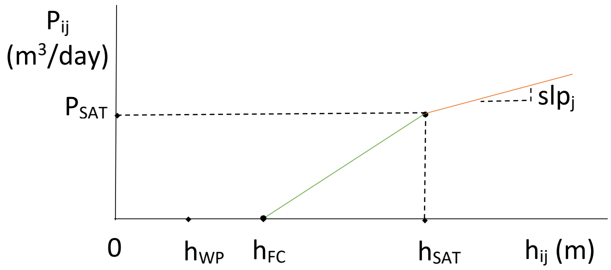


**Figure 4. Relationship between percolation and water height**

$\boldsymbol{D_{ij}}$ for the Guadalquivir case study is calculated using the discharge equation of a rectangular weir with $h_{ij}$ as independent variable (Fig. 4):

$$D_{ij} = 86400 * \frac{3}{2} * \sqrt{2g} * C_d * B_{tj} * \left(h_{ij} - h_{SATj} - h_{mij}\right)^{3/2} \quad \text{If } h_{ij} > \left(h_{mij} + h_{SATj}\right) \qquad (6a)$$

$$D_{ij} = 0 \quad \text{If } h_{ij} \leq \left(h_{mij} + h_{SATj}\right) \qquad (6b)$$

Where $D_{ij}$is expressed in m$^3$ day$^{-1}$, $B_{tj}$ is the width of weir crest (m) in unit *j*, estimated as 0.20 m ha$^{-1}$, $C_d$ is the discharge coefficient of the weir, and $h_{mij}$ is a management parameter equal to de height of the weir crest on day *i*, unit *j*.

$\boldsymbol{P_{ij}}$ is calculated using a three-branch linear equation with $h_{ij}$ as independent variable (Figure 4):

$$P_{ij} = 0 \quad \text{If } h_{ij} < h_{FCj} \qquad (7a)$$

$$P_{ij} = FillF_{ij} * P_{SATj} * \left(h_{ij} - h_{FCj}\right)/\left(h_{SATj} - h_{FCj}\right) \quad \text{If } h_{SATj} > h_{ij} \geq h_{FCj} \qquad (7b)$$

$$P_{ij} = FillF_{ij} * \left(P_{SATj} + slp_j * \left(h_{ij} - h_{SATj}\right)\right) \quad \text{If } h_{ij} \geq h_{SATj} \qquad (7c)$$

Where $slp_j$ is the slope for the increase in percolation rate due to a free water layer above the saturated soil (Fig. 5). Note that the filling factor used to adjust $ETc_{ij}$ during the flooding progression is also applied to $P_{ij}$.

$\boldsymbol{I_{ij}}$ is calculated as the amount of water needed to reach the target free water depth ($TFWD_{ij}$), which is a management daily input value representing the depth of water above the soil surface that is desired in the irrigation unit. $\boldsymbol{I_{ij}}$ is constrained by the pumping capacity ($B_{maxj}$) in the irrigation unit. Thus, $\boldsymbol{I_{ij}}$ can be expressed as a function of the independent variable $h_{ij}$ as:

$$I_{ij} = 0 \quad \text{If } h_{ij} \geq \left(TFWD_{ij} + h_{SATj}\right) \text{ or } TFWD_{ij} = 0 \qquad (8a)$$

$$I_{ij} = \left(TFWD_{ij} + h_{SATj} - h_{ij}\right) * Area_j \quad \text{If } h_{ij} < \left(TFWD_{ij} + h_{SATj}\right) \qquad (8b)$$

$$I_{ij} = B_{maxj} \quad \text{If } I_{ij} > B_{maxj} \qquad (8c)$$

$I_{ij}$ and $D_{ij}$ are divided according to their sources and destinations using the factors in $ICM$ and $DCM$, respectively:

$$I_{ij} = \sum_{k=1}^{m}(I_{ij} * f_{jk}) + I_{ij} * f_{jr} \qquad (9a)$$

$$D_{ij} = \sum_{k=1}^{m}(D_{ij} * g_{jk}) + D_{ij} * g_{jr} \qquad (9b)$$

Substituting equations 5, 6, 7 and 8 into equation 2, the later becomes a non-linear function that can be solved for $h_{ij}$ applying the Newton-Raphson method.

## 2.2. Water balance in the drainage units

The drainage ditches act as water reservoirs, accumulating drainage water from the irrigation units to be evacuated or reused for irrigation. The dimensions of the drainage units are input to the model. The water balance of the drainage units may be expressed as:

$$V_{ik} = V_{(i-1)k} - E_{ik} - P_{ik} + R_{ik} + \sum_{j=1}^{n} D_{ij} * g_{jk} - \sum_{j=1}^{n} I_{ij} * f_{jk} + F_{in\ ik} - F_{out\ ik} \quad (10)$$

Where the subscript $i$ indicates the daily step and the subscript $k$ indicates the drainage unit. $\boldsymbol{V_{ik}}$ and $\boldsymbol{V_{(i-1)k}}$ are the volumes of water in the unit $k$ on days $i$ and $i$-1, respectively. $\boldsymbol{E_{ik}}$, $\boldsymbol{R_{ik}}$, and $\boldsymbol{P_{ik}}$ are the volumes of evaporation from the drain water surface, rainfall on the drain and percolation through the drain wetted perimeter, respectively, for drainage unit $k$ on day $i$. $\boldsymbol{F_{in\ ik}}$ and $\boldsymbol{F_{out\ ik}}$ are the daily water flows in drainage unit $k$ entering from and discharging to the main source (the river in the case study), respectively.

$V_{ik}$, $E_{ik}$, $P_{ik}$, $F_{in\ ik}$ and $F_{out\ ik}$ are functions of the water depth in the drainage unit ($h_{ik}$), which is the water depth stored in the drainage ditch. The drains are assumed of trapezoidal cross-section (Figure 5). Values for the base of the cross-section ($b_k$), slope of the sides ($z_k$), maximum water depth ($y_k$), maximum width ($T_k$), and length of the unit ($L_k$) are input parameters. $R_{ik}$ is calculated with surface $T_k$, and the precipitation of the weather station mentioned in section 2.1.

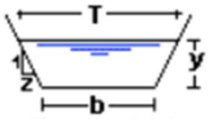


**Figure 5. Trapezoidal cross section of a drainage unit**

$\boldsymbol{V_{ik}}$ is expressed as:

$$V_{ik} = (b_k + z_k * h_{ik}) * h_{ik} * L_k \quad (11)$$

$\boldsymbol{E_{ik}}$ is calculated from $ET_0$, an open water evaporation coefficient ($k$), $L_k$, and the free water surface, which is a function of $h_{ik}$:

$$E_{ik} = ET_{0_i} * k * L_k * (b_k + 2 * z_k * h_{ik}) \quad (12)$$

$\boldsymbol{P_{ik}}$ is estimated from a rate of percolation for the saturated drains ($K_{sat\ k}$), $L_k$ and the wetted perimeter, which is a function of $h_{ik}$.

$$P_{ik} = K_{sat\ k} * \mathrm{L}_k * \left(b_k + 2 * h_{ik} * \sqrt{1 + z_k^2}\right) \quad (13)$$

$\boldsymbol{F_{out\ ik}}$ is the volume of water that exceeds the drainage unit capacity ($V_{max\ k}$), and thus it is returned to the source:

$$F_{out\ ik} = V_{ik} - V_{max\ k} \qquad \text{If } V_{ik} > V_{max\ k} \quad (14a)$$

$$F_{out\ ik} = 0 \qquad \text{If } V_{ik} \leq V_{max\ k} \quad (14b)$$

During periods of high tides, the drainage units can take up water from the source. This flow ($\boldsymbol{F_{in\ ik}}$) is computed as the volume needed to fill the drainage in one day up to a fraction ($q$) of $V_{max\ k}$:

$$F_{in\ ik} = 0 \qquad \text{If } V_{ik} \geq q * V_{max\ k} \quad (15a)$$

$$F_{in\ ik} = q * V_{max\ k} - V_{ik} \qquad \text{If } V_{ik} < q * V_{max\ k} \quad (15b)$$

The fraction $q$ is assumed to be 0.1 in all the drainage units. Equation 15 is a very rough approximation justified by the current limited knowledge of the drains hydraulics.

Substituting equations 11, 12, 13, 14 and 15 into equation 10, the later becomes a non-linear function on $h_{ik}$ that can be solved applying the Newton-Raphson method.

## 2.3. Solute balance equations and salt concentration calculation

The solute mass conservation equation for the irrigation and drainage units are:

$$V_{ij} * c_{ij} = V_{(i-1)j} * c_{(i-1)j} - P_{ij} * c_{ij} - D_{ij} * c_{ij} + \sum_{k=1}^{m}(I_{ij} * f_{jk} * c_{ik}) + I_{ij} * f_{jr} * c_{ijr} \qquad (16)$$

$$V_{ik} * c_{ik} = V_{(i-1)k} * c_{(i-1)k} - P_{ik} * c_{ik} + F_{in\,ik} * c_{ikr} - F_{out\,ik} * c_{ik} - c_{ik} * \sum_{j=1}^{n}(I_{ij} * f_{jk}) + \sum_{j=1}^{n}(D_{ij} * g_{jk} * c_{ij}) \qquad (17)$$

Where $\boldsymbol{c_{ij}}$ is the solute concentration in the irrigation unit $j$ on day $i$, and $\boldsymbol{c_{ik}}$ is the solute concentration in the drainage unit $k$ on day $i$. $\boldsymbol{c_{ijr}}$ or $\boldsymbol{c_{ikr}}$ are the concentration of solutes on day $i$ for the stretch of the external source (the river water) where the irrigation unit $j$ or drainage unit $k$ are connected.

There are as many solute balance equations as there are irrigation plus drainage units, while the unknowns are the concentration of solutes in each unit. The system of linear equations is solved applying the Gaussian elimination method using the LAPACK routine (Anderson et al., 1999) in the NumPy library linear algebra submodule (Harris et al., 2020).

## 3. Results and discussion

The topological diagram of the hydraulic arrangement for the 'bucket' modelling approach applied to the rice growing area in the right riverbank of the Lower Guadalquivir valley is in Figure 6.

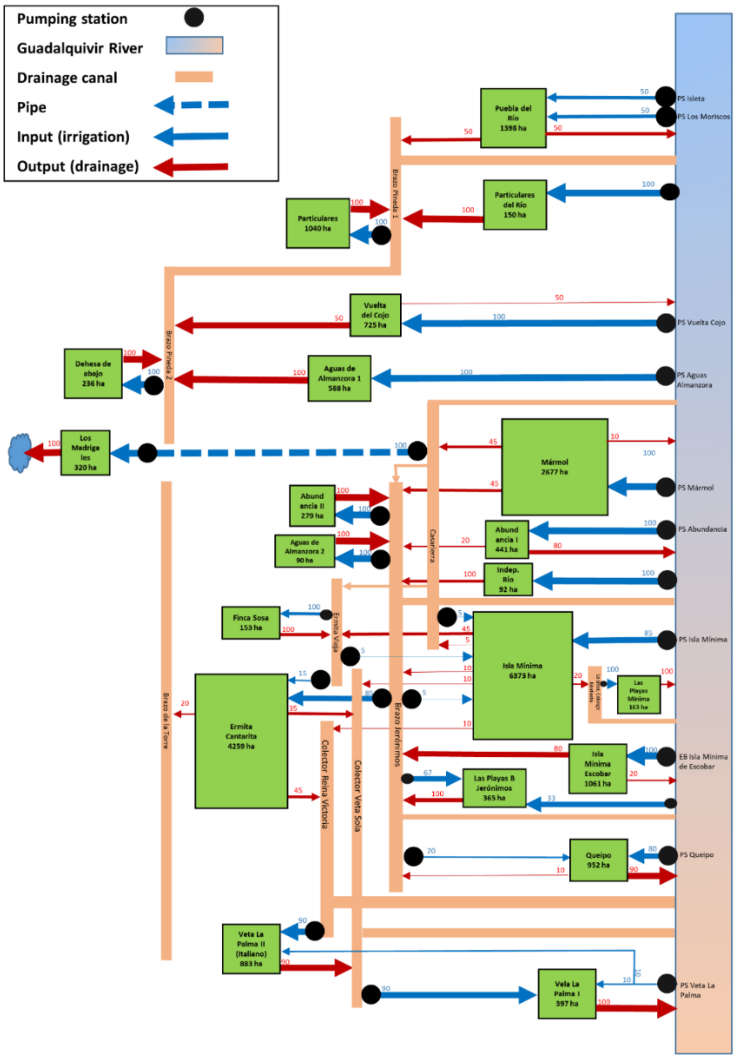


**Figure 6. Conceptual layout for the bucket mass balance model in the Guadalquivir case study**

Figure 7 shows the daily evolution of the water balance components and input and output salt concentrations in one example irrigation unit. The sharp initial increase of irrigation corresponds to the filling of the irrigation unit, while the other sudden changes are due to variations of the management free water depth and the management height of the drainage weir crest ($TFWD_{ij}$ and $h_{mij}$, respectively). Water balances for every irrigation unit during irrigation season 2020 (Table 1) resulted on average irrigation of 2500 mm, and average surface drainage fraction (SDF) of 0.52. SDF is calculated as the fraction of irrigation that leaves the unit by surface drainage, and thus is susceptible for water recirculation.

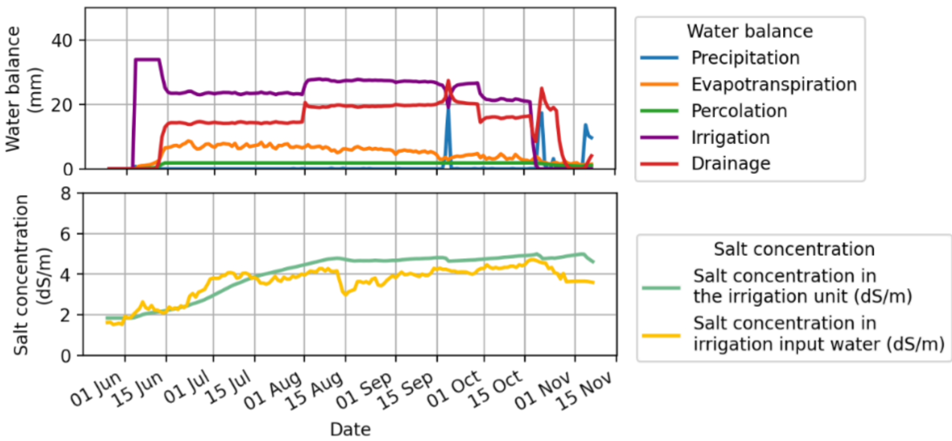


**Figure 7. Results of the daily evolution of water and salinity in the irrigation unit called Isla Minima for the irrigation season 2020**

**Table 1. Modelled total values for the water balance during year 2020**

| Irrigation unit | ETc (mm) | Rainfall (mm) | Percolation (mm) | Surface drainage (mm) | Irrigation (mm) | SDF |
|---|---|---|---|---|---|---|
| **IslaMinima** | 796 | 97 | 266 | 2,365 | 3,474 | 0.68 |
| **AbundanciaI** | 853 | 97 | 279 | 1,917 | 3,091 | 0.62 |
| **AbundanciaII** | 770 | 97 | 267 | 922 | 2,008 | 0.46 |
| **IslaMinimaEscobar** | 779 | 97 | 266 | 2,146 | 3,240 | 0.66 |
| **Poblado** | 824 | 97 | 272 | 2,630 | 3,771 | 0.70 |
| **Marmol** | 809 | 97 | 268 | 2,617 | 3,740 | 0.70 |
| **ErmitaCantarita** | 796 | 97 | 267 | 2,609 | 3,720 | 0.70 |
| **PueblaRio** | 818 | 97 | 276 | 894 | 2,032 | 0.44 |
| **Madrigales** | 757 | 97 | 259 | 1,654 | 2,718 | 0.61 |
| **VueltaCojo** | 770 | 97 | 265 | 476 | 1,557 | 0.30 |
| **VetaPalmaII** | 784 | 97 | 273 | 1,380 | 2,489 | 0.55 |
| **PartRio** | 790 | 97 | 270 | 891 | 1,997 | 0.45 |
| **Particulares** | 777 | 97 | 268 | 900 | 1,992 | 0.45 |
| **AguasAlmanzoraA** | 806 | 97 | 271 | 848 | 1,967 | 0.43 |
| **VetaPalmaI** | 887 | 97 | 291 | 1,169 | 2,389 | 0.49 |
| **DehesaAbajo** | 770 | 97 | 268 | 884 | 1,970 | 0.45 |
| **PlayasJeronimos** | 757 | 97 | 266 | 891 | 1,963 | 0.45 |
| **PlayasMinima** | 763 | 97 | 267 | 895 | 1,974 | 0.45 |
| **AguasAlmanzoraB** | 770 | 97 | 267 | 913 | 1,999 | 0.46 |
| **FincaSosa** | 757 | 97 | 266 | 890 | 1,962 | 0.45 |

The percentages of water inputs and outputs in the study area are in Figure 8. 77.6% of the inputs was water pumped from the river, and 45.1% of the outputs was flowed back to the Guadalquivir River.

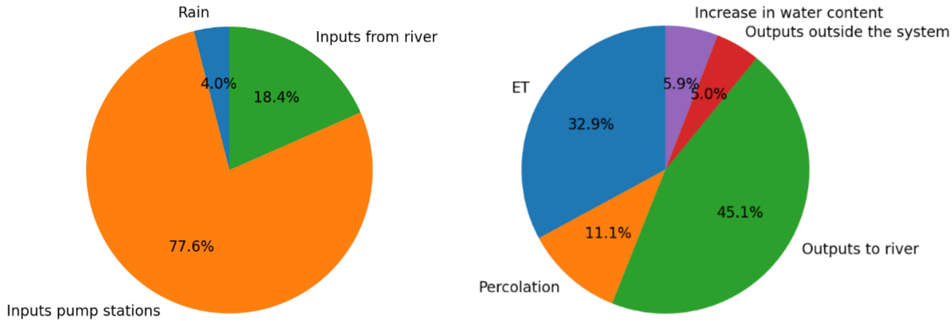


**Figure 8. Modelled fractions inputs and outputs in the rice growing right riverbank of the Guadalquivir lower valley for year 2020**

To validate the water balance model, measured data of water inputs from the 9 pumping stations located in the Guadalquivir River (https://www.chguadalquivir.es/saih/) were compared with the corresponding model outputs (Table 2). A difference of a 6 % in total volumes measured and modelled is observed.

**Table 2. Comparison of measured and simulated values**

| River pumping stations | Measured values (m3) | Simulated values (m3) | River pumping stations | Measured values (m3) | Simulated values (m3) |
|---|---|---|---|---|---|
| **PueblaRio** | 28,750,288 | 21,528,785 | **IslaMinima** | 185,008,048 | 172,896,432 |
| **VueltaCojo** | 9,944,227 | 9,702,694 | **IslaMinimaEscobar** | 32,358,298 | 32,608,715 |
| **AguasAlmanzoraA** | 11,298,381 | 9,453,351 | **Ermita** | 148,443,905 | 147,381,739 |
| **Marmol** | 96,584,383 | 89,784,852 | **Poblado** | 28,381,226 | 25,845,170 |
| **Abundancial** | 15,902,765 | 12,558,145 | | | |

Salt concentration in the irrigation units increases during the irrigation season, and starts decreasing with precipitations in November (Figure 7). This is because salinity of the water that enters the system increases during the summer season, and the evaporation process concentrates salt content. Table 3 contains simulated mean concentration of salt in the irrigation water and in the irrigation unit.

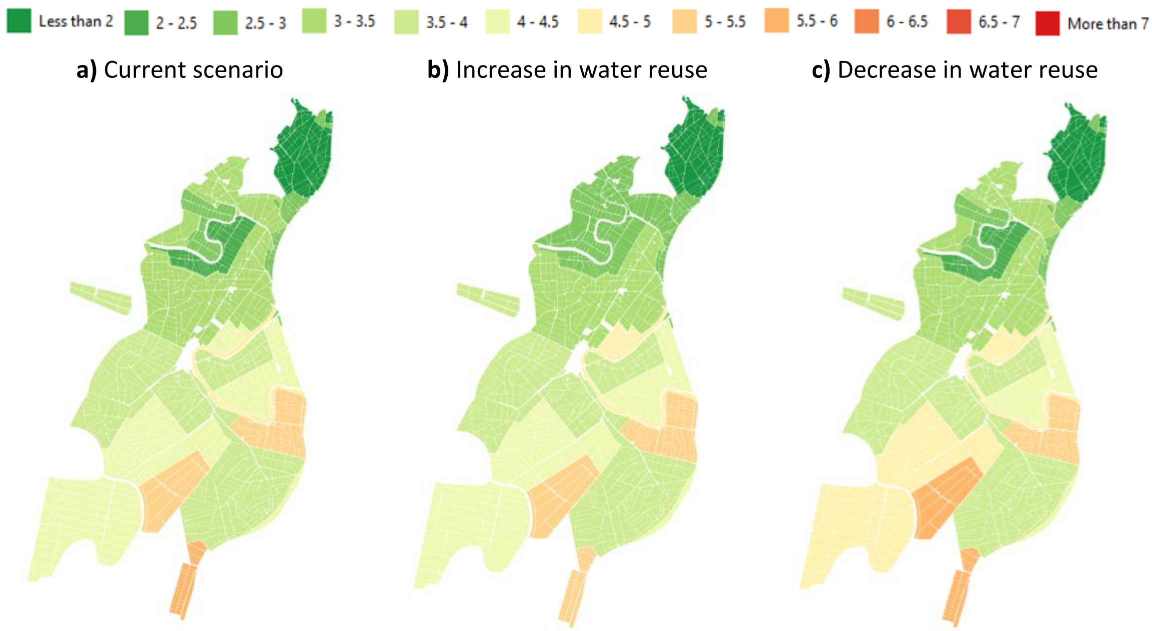


**Figure 9. Spatial distribution of salinity in the input water for irrigation. Average value for year 2020 (dS/m). Rice growing right riverbank of the lower Guadalquivir valley.**

**Table 3. Modelled salt concentration values for the water balance during year 2020**

| Irrigation unit | Irrigation input (dS/m) | Irrigation unit (dS/m) | Irrigation unit | Irrigation input (dS/m) | Irrigation unit (dS/m) |
|---|---|---|---|---|---|
| **IslaMinima** | 3.7 | 4.0 | **VetaPalmalI** | 5.4 | 6.5 |
| **AbundanciaI** | 3.3 | 3.8 | **PartRio** | 2.5 | 3.0 |
| **AbundanciaII** | 4.4 | 4.9 | **Particulares** | 3.1 | 3.4 |
| **IslaMinimaEscobar** | 4.5 | 4.8 | **AguasAlmanzoraA** | 2.8 | 3.4 |
| **Poblado** | 5.0 | 5.4 | **VetaPalmal** | 5.6 | 7.0 |
| **Marmol** | 3.2 | 3.5 | **DehesaAbajo** | 3.1 | 4.6 |
| **ErmitaCantarita** | 4.4 | 4.7 | **PlayasJeronimos** | 4.6 | 4.6 |
| **PueblaRio** | 1.9 | 2.4 | **PlayasMinima** | 4.3 | 4.6 |
| **Madrigales** | 3.74 | 3.99 | **AguasAlmanzoraB** | 4.44 | 4.57 |
| **VueltaCojo** | 2.50 | 3.11 | **FincaSosa** | 4.13 | 4.58 |

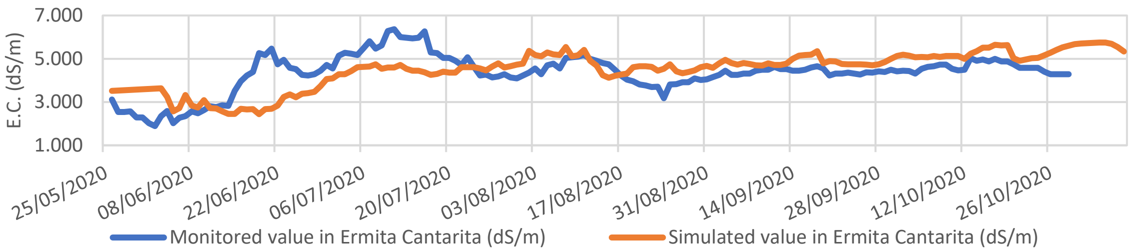


**Figure 10. Monitored and simulated salinity in Ermita Cantarita, year 2020**

Figure 9a shows the distribution of averaged salinity for the growing season under the management practices in 2020. Overall, it may me observed an increase of salinity from north to south, determined by the salinity of the river water and irrigation reusing drainage water.

Simulated daily measurements of salinity at the pumping station Ermita Cantarita, that reuses drainage water (Figure 1), were compared with daily measurements (Figure 10). Mean seasonal simulated and measured salinity were equal (4.4 dS/m).

Alternative management practices may be simulated to evaluate potential improvements. Figure 9 shows also simulated salinity results assuming an increase in water reuse, obtaining an average input irrigation in the irrigation units of 4005 mm and a surface drainage fraction of 0.72 (Figure 9b) and a reduction on water reuse (Figure 9c), obtaining an average input irrigation in the irrigation units of 1940 mm and a surface drainage fraction of 0.4. Comparing the three maps in Figure 9, there is a clear effect of salt redistribution when we increase water reuse within the system. Salinity in areas with higher concentration is attenuated, and areas with relatively low salinity increase their value.

## 4. Conclusions

A 'bucket' water and salt mass balance model has been set up for the rice growing area in the right riverbank of the Guadalquivir lower valley, with an area of 22,500 ha. The main difficulty was found in the interconnections of the system, being a large and complex network with supply, drainage and water reuse.

Results show good agreement with measured values, the average irrigation input in the irrigation units is 2500 mm with a surface drainage fraction of 0.52, which indicates fraction of irrigation that leaves the unit by surface drainage, and is susceptible for recirculation within the system. Average salinity is 4.4 dS/m, with a value of 1.9 dS/m in the irrigation unit located upsteam, and increasing downstream along the Guadalquivir River.

The model allows the simulation of different water management practices to evaluate possible improvements in the performance of the entire area.

**Acknowledgements:** This work is included in the framework of the MEDWATERICE project *Towards a sustainable water use in Mediterranean rice-based agro-ecosystems*, funded by the PRIMA program (Agencia Estatal de Investigación, PCI2019-103714), the ORYZONTE project, and the WAGRINNOVA project *Co-innovations across scales to enhance sustainable intensification in water-managed agricultural systems in West Africa*, funded by LEAP-Agri (Agencia Estatal de Investigación, PCI2018-093051).

## References

Allen, R.G., Pereira, L.S., Raes, D. and Smith, M., (1998). Crop evapotranspiration - Guidelines for computing crop water requirements. *FAO Irrigation and Drainage Paper 56*. FAO, Rome.

Anderson, E., Bai, Z., Bischof, S., C. and Blackford, Demmel, J., Dongarra, J., J. and Du Croz, Greenbaum, A., … Sorensen, D. (1999). LAPACK Users' Guide (Third). Philadelphia, PA: Society for Industrial and Applied Mathematics.

González-Dugo, M.P., Escuin, S., Cano, F., Cifuentes, V., Padilla, F.L.M., Tirado, J.L., Oyonarte, N., Fernández, P. and Mateos L., (2013) Monitoring evapotranspiration of irrigated crops using crop coefficients derived from time series of satellite images. II. Application on basin scale. *Agricultural Water Management*. 125: 92-104

Harris, C. R., Millman, K. J., van der Walt, S. J., Gommers, R., Virtanen, P., Cournapeau, D., … Oliphant, T. E. (2020). Array programming with NumPy. *Nature*, 585, 357–362.

Mateos L, Young CA, Wallender WW, Carlson HL (2000) Simulating spatially distributed water and salt balances. *J Irrig Drain Engrg* 126:288–295

Mateos, L. (2008) Identifying a new paradigm for irrigation system performance. Irrigation Science 27:25-34

Mateos, L., González-Dugo, M.P., Testi, L., Villalobos, F.J., (2013) Monitoring evapotranspiration of irrigated crops using crop coefficients derived from time series of satellite images. I. Method validation. *Agricultural Water Management*. 125: 81-91

**Effects of the implementation of the Alternate Wetting and Drying (AWD) irrigation strategy in an Italian rice district: lesson learned by applying a semi-distributed agro-hydrological model**

Authors: Giulio Gilardi[1], Alice Mayer[1], Michele Rienzner[1], Giovanni Ottaiano[1], Marco Romani[2], Elisa Cadei[2], Olfa Gharsallah[1], Arianna Facchi[1]

Affiliation: [1]Department of Agricultural and Environmental Sciences - Production, Landscape, Agroenergy (DiSAA), Università degli Studi di Milano, via Celoria 2, 20133 Milan (Italy); [2]Centro Ricerche sul Riso, Ente Nazionale Risi (ENR), 27030 Castello D'Agogna (Italy)

**ABSTRACT**

The north-western part of the Padana Plain in northern Italy is the most important rice district in Europe and the second in the Mediterranean basin after Egypt (230,000 ha in Italy and 450,000 ha in Egypt). Traditionally, rice irrigation was based on wet seeding and continuous flooding until to approximately three weeks before harvesting. Recently, due to an increased frequency of water scarcity periods and competition for water among agricultural and non-agricultural uses, water saving techniques are being introduced. Although these techniques must be firstly tested on a field scale, it is important to estimate their effects on the overall water resources system. In fact, especially in rice areas characterized by shallow aquifers, the strong interaction between traditional irrigation methods and phreatic aquifer levels leads to a re-use of the irrigation water which contributes to water flows in rivers and irrigation networks thus increasing the overall irrigation efficiency of rice areas.

An experimental platform was set up in the core of the Italian rice area (Castello D'Agogna, PV) to compare three rice irrigation management strategies over two agricultural years (2019-2020): wet seeding and traditional flooding (WFL), dry seeding and delayed flooding (DFL), and a 'safe' wet seeding and alternated wetting and drying irrigation (AWD-safe). Irrigation water use was monitored by the installation of flow meters, and all the other soil water balance components were quantified. At the field scale, water savings of AWD and DFL were found to be about 20% and 14% compared to WFL without penalizing rice production, while the temporal distribution of irrigation water needs and percolation fluxes changed as a function of the irrigation strategy.

Results achieved in the experimental fields were used in the parametrization of a semi-distributed and physically-based agro-hydrological model aimed at stimulating the overall irrigation system efficiency of a rice district (about 1000 ha) located close to the experimental platform. The modelling framework consists of three sub-models: i) one for the agricultural area, based on the physically-based SWAP model; ii) one for the channel network percolation; iii) one for the groundwater level dynamics. After investigating the current water dynamics and irrigation system efficiency for the period 2013-2020, the modelling system was used to explore the effects on the water resources system of some 'what-if scenarios', such as the adoption of a AWD-safe rice irrigation strategy in the whole district. The AWD-safe technique after wet seeding seems to be a good compromise solution in terms of recharging groundwater and reducing the peak irrigation request for rice.

This research was developed in the context of the MEDWATERICE (PRIMA-Section2 2018; https://www.medwaterice.org/) project.

**Keywords:** irrigation district; rice irrigation requirement; water-saving technology; agro-hydrological model; groundwater level; irrigation network efficiency

## 1. INTRODUCTION

Italy, with over half of the total European production grown on an area of more than 200 thousand hectares, is the most important rice producer in Europe and the second in the Mediterranean basin after Egypt. The most important rice-growing area of the country, located between Lombardy and Piedmont Regions, is featured by many peculiarities: an historical abundance of surface water, an extensive network of unlined irrigation and drainage channels and the presence of one of the largest aquifers in Europe.

Traditionally, rice irrigation was based on wet seeding and continuous flooding (WFL) up to about 30 days before harvesting. Recently, due to an increased frequency of water scarcity periods and competition for water among agricultural and non-agricultural uses, water saving techniques are being introduced in the area. However, their effectiveness over the territory need to be assessed.

Water Application Efficiency, which is computed as the ratio between evapotranspiration and water inputs (WAE, %; Bouman et al., 2005), is a well-known index used to evaluate the irrigation management efficiency. However, WUE depends on the spatial scale at which the hydrological processes are observed. In fact, water fluxes which are considered non-beneficial losses at the field scale, such as percolation from the agricultural fields and from the irrigation channel network, can be partially recovered and reused on larger scales by fields located downhill, where shallow groundwater levels allow the reduction of percolation losses and the activation of capillary rise.

The objective of the hydrological modelling activity presented in this paper is to explore water dynamics and water use efficiencies of different irrigation management alternatives in a 1.000 ha irrigation district prevalently cropped with rice and located in the Lombardy portion of the Italian rice basin (Lomellina). In order to allow a clear illustration of the results, years 2013, 2016 and 2019, characterized by different agro-climatic conditions and availability of water resources in the district, are considered in the paper.

**2. STUDY AREA AND DATA COLLECTION**

The pilot rice district is located within the administrative boundary of San Giorgio di Lomellina (Pavia), about 45 km southwest of the city of Milan and extending over an area of about 1.000 hectares. The rice growing area of the district covers about 90% of the agricultural surface while the remaining 10% is mainly cropped with maize and poplar. Spatial distribution of the crops in the area were retrieved from the annual SIARL land-use raster maps provided by the Lombardy regional authority (ERSAF; 20 m x 20 m). The MNDWI index (Modified Normalized Difference Water Index; Xu, 2016) was calculated starting from satellite images (Landsat 7/8 and Sentinel 2) downloaded for the period April-May with the objective of identifying wet seeded and dry-seeded rice, following the procedure described in Mayer et al. (2019). Since the poplar area in the pilot district is very limited, poplar was randomly split into young (irrigated) and mature (rainfed), following a 40-60% ratio on the basis of indications from AIES.

A Ground Degree Days (GDD) model was developed and applied for dry seeded and wet seeded rice, using ground-based information provided by Ente Nazionale Risi (ENR). Rice crop biometric parameters were provided by ENR technicians, while crop coefficients were measured in a former experiments (Cesari de Maria et al., 2016, Chiaradia et al., 2015). Development stages and crop parameters for the other crops (maize and poplar) were defined according to the information reported in Mayer et al. (2019).

Soil hydraulic properties for the five most abundant types of soil in the area were estimated through PedoTransfer Functions (PTFs) based on the information reported in the 1:50.000 Lombardy Soil Map (ERSAF; 1: 50,000). The chosen PTFs were: i) Tomasella et al. (1998) for the soils Bulk Density (BD, not available in the Lombardy Soil Map); ii) Ungaro et al. (2005) for the soil water retention curve parameters and the saturated hydraulic conductivity. To take into account the compaction characterizing paddy soils, both BD and saturated hydraulic conductivity obtained by the PTFs were corrected following Mayer et al. (2019).

The agro-meteorological data were recorded at the ARPA station in Castello D'Agogna (a few kilometres from the district). The amount of rain fell from April to September in 2013, 2016 and 2019 was found to be 283, 331 and 281 mm, respectively. For the same years, in July the rainfall registered was 5, 75 and 54 mm.

The channel network within the district is managed by the Associazione Irrigazione Est Sesia (AIES); irrigation water comes almost exclusively from surface water bodies. Daily irrigation discharges conveyed to the district and used in this study were provided by AIES.

During the last years, dry seeding followed by an alternation of flooding and dry periods (a sort of rough Alternate Wetting and Drying - AWD - in which flooding periods are dictated by the irrigation turns scheduled by AIES on the basis of water availability in rivers) took the place of the traditional WFL practice. This change was triggered by new environmental conditions (e.g. greater probability of dry years) but, despite the simplified agronomic management and consequently the economic saving that dry seeding has brought to the farmers, this change is leading to different unexpected problems such as a lowering in GWL and increasing in competition for the water resources with other crops (especially maize) in June and July. The change (%) in rice irrigation management among the years 2013, 2016 and 2019 is shown in Table 1.

The phreatic groundwater surface varies in space and time and is very shallow in some areas of the district. Four piezometer wells were installed in the district area, and the groundwater level (GWL) was measured weekly from 2015 by AIES. Figure 1 shows the average daily GWL measured by the piezometers installed in the district (the 2013 GWL was reconstructed using the modelling system described in this paper; see Mayer et al. 2019). The figure clearly shows how the rice irrigation management conversion in the district affected the daily average GWL values, with a general lowering of the groundwater table and an evident delay in reaching high GWLs at the beginning of the agricultural season (April-June).

| Year | Dry seeded (%) | Wet seeded (%) |
|---|---|---|
| 2013 | 40.1 | 59.9 |
| 2016 | 92.5 | 7.5 |
| 2019 | 100.0 | 0.0 |

Table 1. Irrigation management strategies adopted in the years 2013, 2016 and 2019. Percentage where computed from the soil land use raster maps used in the simulations (see Section 2 for more details).

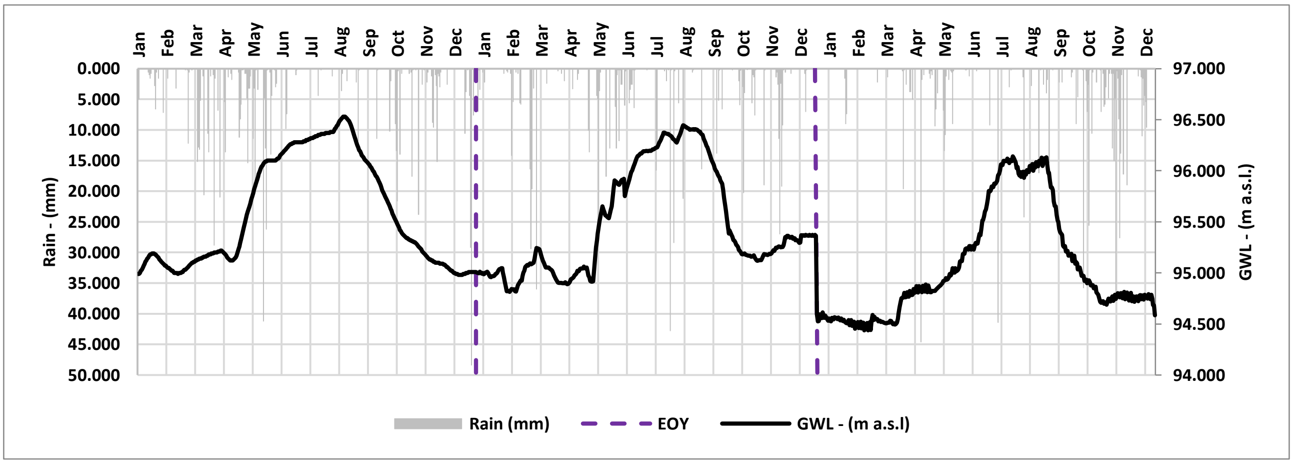


Figure 1. Average daily GWL over the district in the years 2013, 2016 and 2019. The 2013 GWL was reconstructed using the modelling system described in the paper after its calibration.

## 3. MODELLING SYSTEM AND SIMULATED SCENARIOS

In the modelling framework developed, the SWAP model (Soil, Water, Atmosphere and Plant; Kroes et al., 2008; 2017) is applied to the irrigation district following a semi-distributed approach (SMDAA). The district area is divided into 40 different homogeneous zones, considering: 4 crop types cultivated in the area (rice, maize, young and old poplar), 5 soil types and 2 groundwater level conditions.

With respect to GWL conditions, two zones having shallow and deep GWLs are defined by attributing to the first zone the areas that, in the daily spatial interpolation obtained using all data measured in GW wells, showed a GWL shallower than -1 m on July 15$^{th}$ of each year. Two groundwater depth series (shallow and deep) are moreover generated for the two zones averaging the daily GWLs in each zone (further details are reported in Mayer et al., 2019).

Two empirical models complete the modelling framework, the former is used to estimate the monthly irrigation channel network percolation (PC) and the latter to simulate the mean monthly GWL over the district (PGL) depending on the district percolation. In this way, by following a recursive computation scheme (5 iterations are generally sufficient to obtain stable GWL series), the modelling system is able to simulate scenarios and/or past years for which GWL data series are not available (e.g. GWLs for 2013).

The PC model has the following characteristics:

$$Pc(t) = Qc(t) \cdot a(t); \quad \text{with } t = \text{monthly time index} \tag{1}$$

where the monthly irrigation channel network percolation Pc(t) is a function of the mean monthly irrigation discharge Qc(t) and of a loss factor a(t), which varies between 0.0 and 0.4 depending on the GWL during the agricultural season, while it is set to 0.2 outside the irrigation season when the smaller canals are dry. In the scenarios, in which irrigation discharges are not measured and only the field irrigation requirements simulated by SWAP (Ir(t)) are known, equation 1 is converted into:

$$Pc(t) = [a(t) \cdot Ir(t)] / [1 - a(t)] \tag{2}$$

The theoretical formulation of the PGL model is illustrated below:

$$Yd(t) = f(Pd(t); Yupstream(t); Yd(t-1)); \quad \text{with } t = \text{monthly time index} \tag{3}$$

where Yd(t) is the mean monthly GWL over the district, Pd(t) is the district total monthly percolation (i.e. sum of Pc(t) and the percolation from the agricultural fields), Yupstream(t) is the regional monthly GWL data measured at the Cascina Stella piezometer located NE, upstream of the district, along the main groundwater flow direction with respect to the study area (being a sort of NE boundary condition).

The entire framework was calibrated considering the historical soil use, irrigation management and irrigation water availability for the period 2013-2016. Further details about the calibration of the three models presented here and about the developing of the PC and PGL models can be found in Mayer et al. (2019).

The objective of this study was to compare the following rice irrigation management scenarios: i) fixed turn irrigation (FTI) after a dry seeding, ii) wet seeding and continuous flooding (WFL), iii) a safe AWD technique following a wet seeding. The FTI scenario, characterized by a turn of 8 days and 120 mm per irrigation event, is designed accordingly to AIES information, to be representative for the FTI strategy proposed by AIES in condition of good water availability. For the traditional WFL irrigation management, 120 mm of ponding water is kept on the fields from a few days before the emergence to rice maturity, apart from three dry periods needed for the agronomic practices. In the case of AWD, rice irrigation is managed as for WFL in the first part of the season and undergoes intermittent flooding from the tillering stage; in particular, after tillering flooding is applied to reach 120 mm of ponding water only when the soil reaches a critical moisture level (set in SWAP as: pore water pressure -100 cm at 5 cm below the soil surface). As a matter of fact, this irrigation strategy was tested directly in experimental parcels set up at Ente Nazionale Risi during the 2019-2020 agricultural seasons and led to an average water saving of about 20% for safe-AWD with respect to WFL.

Water Application Efficiency (WAE) was calculated as:

$$WAE = (E + T) / (I + R) \times 100 \tag{5}$$

where E, T, I and R are evaporation, transpiration, net irrigation and rainfall, respectively. It shall be noted that WAE is the inverse of the Relative Water Supply (RWS) indicator, defined as the available water (I + R) over the crop evapotranspiration (E+T) within the agricultural season (Yildirim et al. 2007; Kuscu et al. 2009).

Channel Efficiency (CE) was computed as the ratio between the irrigation water reaching the agricultural fields ($Q_{DEL}$) and the water entering the district through the irrigation conveyance network ($Q_{IN}$):

$$CE = Q_{DEL} / Q_{IN} \times 100 \tag{6}$$

In the scenario analysis, $Q_{IN}$ is not known since it is not possible to rely on historical measures. Because of that, $Q_{IN}$ is set to be equal to the sum of the simulated irrigations and the estimated channel percolation, while $Q_{DEL}$ is set equal to the simulated irrigations. Thus, in this case, $Q_{IN}$ must be considered as the minimum amount of water that the district would need to guarantee the simulated water requirements ('minimum' because it is assumed that the irrigation water conveyed to the district is used with maximum efficiency in all months, so that it is never discharged into drainage channels exiting the district).

## 4 RESULTS

The simulated groundwater table depth (GWD = GWL minus level of the soil surface taken by a Digital Terrain Model) for all the scenarios are shown in Figure 2, while net irrigation and channel percolations for the years 2013, 2016 and 2019 are reported in Table 2 and 3. Figure 2 shows that the dry seeding technique adopted in FTI leads to a dramatic decrease in GWD in first months of the season, slowing the rise of the water table towards its maximum peak values of about one-two months. On the contrary, the GWD values under the AWD irrigation strategy overlap with WFL in the first part of the season, starting to diverge in June.

With respect to the net irrigation demand (Table 2), the WFL scenario shows the highest irrigation water required, not only during the entire irrigation season (April-September) but also for the critical month of July. AWD seasonal values of WAE are strongly influenced by the wet seeding technique, however AWD performs better in July when compared to FTI as a result of a more efficient use water (irrigations are scheduled to take place only when soil reaches a critical moisture level). Shallow groundwater has a strong effect on WAE values, especially in WFL scenarios where it never falls under 40% both in April-September and July (see in Table 2 the values reported in brackets on the left).

When considering the percolation from the channel network, the AWD scenario shows to produce the highest values of percolation from the channel network during the period April-September, even if they are not very dissimilar to FTI values. However, in July FTI values of percolation overtake both AWD and WFL. Channel Efficiency (CE) values show obviously an opposite trend: channel network percolation depends not only on the irrigation discharge conveyed in the channel network, but also from the GWD; thus, the higher CE values for WFL can be explained by the GWD behaviour in the three years (Figure 2).

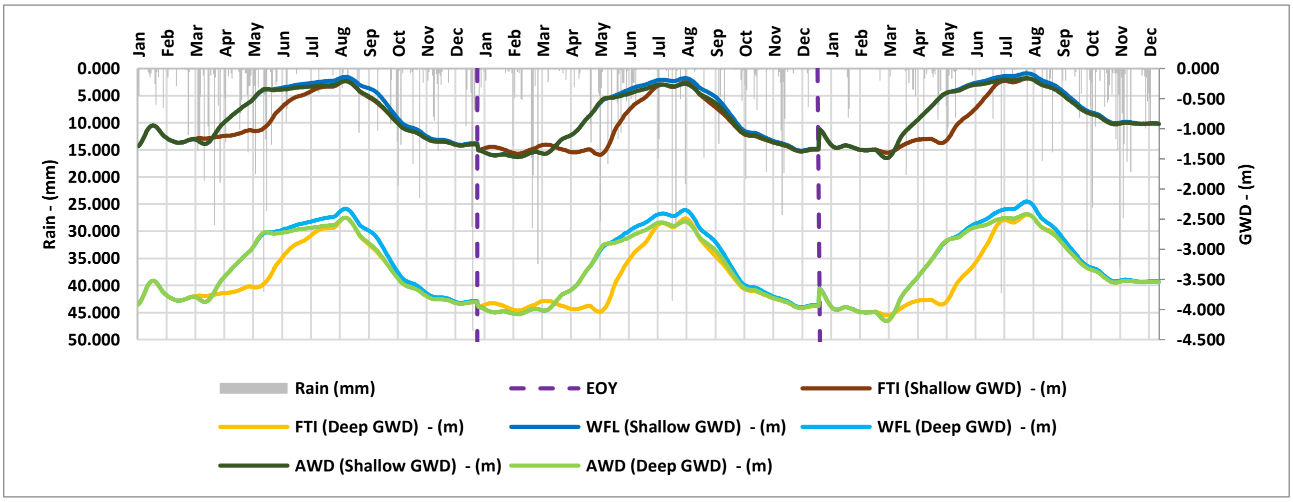


Figure 2. Groundwater depths (GWD) calculated by the PGL model for the years 2013, 2016 and 2019 and provided to the SDMAA model during the last iteration adopted in the simulation (five iterations were used for every year in all the scenarios).

Table 2. Net irrigation and WAE values for the agricultural fields within the district, both for the whole season (April to September) and for July only. In brackets: WAE indices computed separately for shallow and deep GWL zones, respectively.

| Scenario | Year | Seasonal Net Irrigation (mm) | Seasonal WAE (%) | Net Irrigation of July (mm) | WAE of July (%) |
|---|---|---|---|---|---|
| FTI | 2013 | 991.3 | 43.0 (46.9, 41.1) | 310.8 | 49.3 (58.6, 45.3) |
| | 2016 | 919.9 | 43.7 (50.0, 40.8) | 368.7 | 34.9 (42.6, 31.8) |
| | 2019 | 923.9 | 46.0 (51.0, 43.8) | 395.2 | 36.6 (42.3, 34.3) |
| WFL | 2013 | 1954.5 | 28.3 (41.8, 24.0) | 499.6 | 33.0 (51.6, 27.6) |
| | 2016 | 1930.4 | 28.0 (41.2, 23.8) | 432.8 | 31.6 (50.9, 26.2) |
| | 2019 | 1931.5 | 29.1 (42.6, 25.1) | 470.1 | 32.8 (53.6, 27.5) |
| AWD | 2013 | 1554.9 | 34.4 (48.8, 29.6) | 408.0 | 40.4 (55.4, 35.2) |
| | 2016 | 1539.6 | 33.8 (44.7, 29.9) | 327.9 | 39.9 (51.1, 35.7) |
| | 2019 | 1594.3 | 34.3 (47.1, 30.2) | 309.4 | 47.3 (77.5, 39.5) |

Table 3. Channel percolation and CE values for the whole season (April to September) and for July only.

| Scenario | Year | Seasonal Channel perc. (mm) | Seasonal CE (%) | Channel perc. of July (mm) | CE of July (%) |
|---|---|---|---|---|---|
| FTI | 2013 | 402.6 | 71.1 | 114.0 | 73.2 |
| | 2016 | 382.4 | 70.6 | 114.2 | 76.4 |
| | 2019 | 336.6 | 73.3 | 122.2 | 76.4 |
| WFL | 2013 | 546.3 | 78.2 | 56.5 | 89.8 |
| | 2016 | 652.8 | 74.7 | 29.9 | 93.5 |
| | 2019 | 577.4 | 77.0 | 16.1 | 96.7 |
| AWD | 2013 | 613.5 | 71.7 | 102.4 | 79.9 |
| | 2016 | 738.8 | 67.6 | 74.2 | 81.6 |
| | 2019 | 652.5 | 71.0 | 51.1 | 85.8 |

Figure 3 illustrates a comparison between the simulated $Q_{IN}$ (irrigation discharge entering the district, obtained as the sum of net irrigation and percolation from the channel network) and the corresponding discharge conveyed to the district by AIES in 2016 ($Q_{IN-AIES}$). The idea is to verify the difference in gross irrigation needed under the three different irrigation management strategies, compared to the real irrigation water availability for the district. For sake of simplicity, only year 2016 is shown in Figure 3. As shown in Table 1, in 2016 only the 7.5% of the rice surface was still irrigated by wet seeding and continuous flooding; moreover, based on personal communications of AIES, during the central months of the 2016 season irrigation turns had to be extended up to 10-12 days because irrigation water was not sufficient for 8-day turns. This explains why the red lines is above the black line in June and July. Figure 3 shows that the FTI gross irrigation requirement significantly differs from WFL and AWD in the months of April and May because of the dry seeding technique adopted.

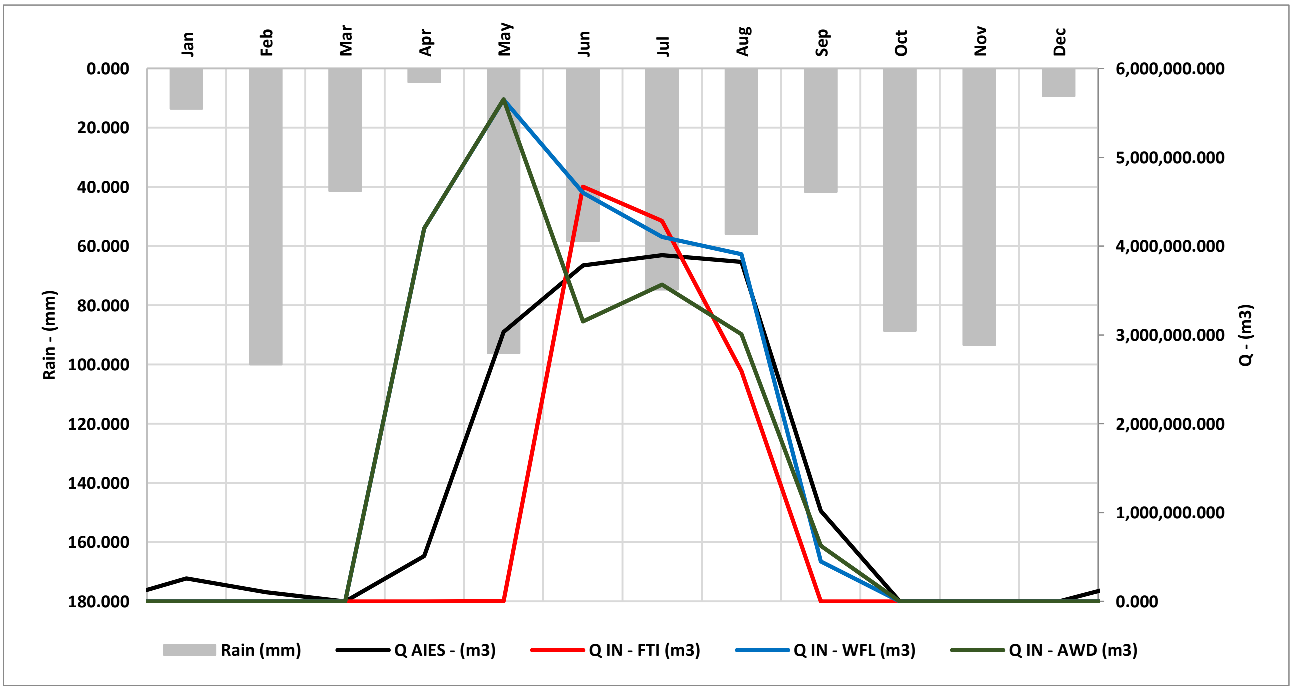


Figure 3. Simulated gross irrigation requirements ($Q_{IN}$) for the year 2016 for all the scenarios simulated (FTI, red; WFL, blue; AWD, green). In black, the discharges conveyed to the district by AIES ($Q_{IN-AIES}$) in the same year.

The great difference between $Q_{IN-AIES}$ and WFL and AWD in these two months is obviously explained by the fact that only a small percentage of wet seeded rice was still cultivated in 2016, and the dry seeding of rice was heavily prevalent in the district. However, $Q_{IN-AIES}$ is higher than FTI in the first months of the season, and this is due to the fact that even with a turned irrigation after a dry seeding, the irrigation channel network needs to reach a sufficient water discharge availability well in advance with respect to the irrigation season.

Both FTI and WFL irrigation requirements in the central part of the irrigation season (June-July) are higher than the available ones, while AWD would guarantee a lower use of the water resource if compared to the irrigation water availability. In the last months of the irrigation season, $Q_{IN\text{-}AIES}$ generally is higher than the irrigation requirement of the agricultural territory; water in excess is discharged in the drainage network exiting the district.

## 5 CONCLUSIONS

The modelling activity conducted in the context of MEDWATERICE highlights, once more, the strong connection existing between irrigation and groundwater table depth in rice areas, and how complex is to estimate the actual irrigation water need and efficiency of an irrigation strategy when considering large portions of agricultural territory.

Recently, the study area is facing a lowering in GWLs due to the massive conversion to dry seeding and turned irrigation. However, even if the FTI strategy can reduce the overall irrigation volume used during the agricultural season, it does not allow to decrease the irrigation need in the central months of the season, leading to an even higher irrigation requirement compared to the WFL in June and July for the three years covered by this study. This is explained by the fact that, although the field irrigation requirement decreases in June and July adopting FTI, the lowering of the GWLs leads to an increase in the channel network percolation losses.

The AWD-safe technique after wet seeding, currently tested only in experimental plots, seems able to reduce irrigation requests starting from the rice tillering phase (first half of June), thus constituting a compromise solution in terms of recharging the water table and reducing the peak irrigation request for rice. When compared to WFL, AWD-safe leads to a water saving of about 20% for the period April-September and 25% for the month of July.

## REFERENCES

Papers

Bouman, B. A. M., Peng, S., Castañeda, A. R., & Visperas, R. M. (2005). Yield and water use of irrigated tropical aerobic rice systems. Agricultural Water Management, 74(2), 87–105.

Cesari de Maria, S., Rienzner, M., Facchi, A., Chiaradia, E. A., Romani, M., & Gandolfi, C. (2016). Water balance implications of switching from continuous submergence to flush irrigation in a rice-growing district. Agricultural Water Management, 171, 108–119.

Chiaradia, E. A., Facchi, A., Masseroni, D., Ferrari, D., Bischetti, G. B., Gharsallah, O., Cesari de Maria, S., Rienzner, M., Naldi, E., Romani, M., & Gandolfi, C. (2015). An integrated, multisensor system for the continuous monitoring of water dynamics in rice fields under different irrigation regimes. Environmental Monitoring and Assessment, 187(9).

Kuscu, H., Bölüktepe, F. E., Demir A. O., 2009. Performance assessment for irrigation water management: A case study in the Karacabey irrigation scheme in Turkey. African Journal of Agricultural Research Vol. 4 (2), pp. 124-132. http://www.academicjournals.org/AJAR

Mayer, A., Rienzner, M., Cesari de Maria, S., Romani, M., Lasagna, A., & Facchi, A. (2019). A Comprehensive Modelling Approach to Assess Water Use Efficiencies of Different Irrigation Management Options in Rice Irrigation Districts of Northern Italy. Water, 11(9), 1833.

Tomasella, J., & Hodnett, M. G. (1998). Estimating soil water retention characteristics from limited data in Brazilian Amazonia. Soil science, 163(3), 190-202.

Ungaro, F., Calzolari, C., & Busoni, E. (2005). Development of pedotransfer functions using a group method of data handling for the soil of the Pianura Padano–Veneta region of North Italy: water retention properties. Geoderma, 124(3-4), 293–317.

Xu, H. (2006). Modification of normalised difference water index (NDWI) to enhance open water features in remotely sensed imagery. International Journal of Remote Sensing, 27(14), 3025–3033.

Yildirim, M., Cakmak, B., Gokalp, z., 2007. Benchmarking and Assessment of Irrigation Management Transfer Effects on Irrigation Performance in Turkey. Journal of Biological Sciences 7(6). DOI: 10.3923/jbs.2007.911.917

Manuals/Books

de Wit, A.J.W., System description of the WOFOST 7.2 cropping systems model, Wageningen: Wageningen Environmental Research. 2020.

DiSAA – Department of Agricultural and Environmental Sciences, IdrAgra Technical manual - version 2.0, University of Milan, 2021.

Kroes, J. G., van Dam, J. C., Groenendijk, P., Hendriks, R. F. A., & Jacobs, C. M. J. Swap version 3.2: theory description and user manual. Wageningen: Alterra, 2008.

Kroes, J. G., van Dam, J. C., Bartholomeus, R. P., Groenendijk, P., Heinen, M., Hendriks, R. F. A., Mulder, H. M., Supit, I., & van Walsum, P. E. V. (2017). SWAP version 4. Wageningen: Wageningen Environmental Research, 2017.

Institutions/Web sites

AIES, https://www.estsesia.it/.

ARPA, https://www.arpalombardia.it/.

ENR, https://www.enterisi.it/.

ERSAF, https://www.ersaf.lombardia.it/.

# Testing automatic irrigation in paddy rice fields: lesson learned in a northern Italy rice farm

**Authors:** Fabiola Gangi[1], Giorgio Scotti[1], Giovanni Ottaiano[1], Andrea Galli[1], Rodolfo Ceriani[1], Olfa Gharsallah[1], Arianna Facchi[1], Daniele Masseroni[1]

**Affiliation:**
[1] Department of Agricultural and Environmental Sciences, University of Milan, Via Celoria 2, 20133 Milan (Italy)

**Contact:** Fabiola Gangi, Department of Agricultural and Environmental Sciences, University of Milan, Via Celoria 2, 20133 Milan (Italy). Phone: +39 02503 16903, Mail: fabiola.gangi@unimi.it

**ABSTRACT**

Rice is one of the major staple food crops in the world. In Europe, Italy is the main rice producer, with almost all of the production concentrated in the north-east of the country. Traditionally rice is grown in fields flooded from before seeding to close to harvest. This water management technique requires a huge labor for farmers who have to manually adjust inlet and outlet gates in order to maintain a constant ponding water level in the fields. A new water soft-path strategy based on the introduction of automatic water flow rate regulation systems is under investigation in a rice farm of about 40 ha located south of Milan, in northern Italy. The general purpose of the experimental activity is: (i) to test their reliability in a traditional rice context, and (ii) to assess their environmental and economic sustainability. The installed instrumentation is constituted by four PikoGate® automatic gates positioned in strategic points of the farm irrigation canal network and Ferit® water level sensors installed in five groups of fields. To date, automatic gates and water level sensors have been installed and tested, and a new irrigation algorithm has been implemented to allow the automatic management of a predetermined ponding water level in the fields, which may change in time based on site-specific conditions. Results achieved so far will be presented describing the adopted automatic solutions and their responsiveness to the site-specific conditions.

**Keywords**: irrigation management, automatic system for irrigation, remote-controlled gate, water level sensor, real-time monitoring.

## 1. INTRODUCTION

Italy is the leading rice producer in Europe, accounting for more than half of the total production of this high-quality crop (Masseroni et al., 2018; Facchi et al., 2018). Typically, rice is grown in fields that have been flooded from planting to pre-harvest, and this traditional irrigation technique (i.e. continuous submersion) is considered an important water resource sink. This technique dominates in most areas and is characterized by low irrigation efficiencies (Cesari de Maria et al. 2016). Additionally, the irrigation management requires a lot of human labor because, to date, it is still based on maintaining a predetermined water level in the paddies through the manual regulation of the irrigation inflow rate (Masseroni et al., 2017).

In this context, the application of flexible, automated regulation devices for managing irrigation in paddy fields appears as a viable solution that can be exploited to (i) increase water use efficiency of rice cultivation and (ii) decrease efforts dedicated to the irrigation flow rate regulation at field and farm scale, without changing the traditional irrigation flooding practices. More in detail, hydraulic infrastructures based on a

system of coordinated automatic gates located in strategic points of the farm irrigation network can allow to maintain optimal water levels within the farm channels, providing more consistent and reliable irrigation fluxes through at the farm service points.
In light of the developments on the application of automation systems in irrigation, Lombardy region (which is the most important region in Italy both from the industrial and agricultural point of view, with over 7000 $km^2$ of irrigated surfaces) is promoting bottom–up initiatives in the form of 'information and pilot project actions' with the main purpose to demonstrate the potential of innovative irrigation management systems at the farm and district scales, fostering the collective sharing of the modernization objectives. Therefore, in this work we examine and discuss the results obtained in one of these demonstration projects, consisting in the first example in Europe of a transition to a flexible and remote-controlled management of irrigation in a paddy rice farm. In particular, the new technological solutions adopted for a coordinated flow rate regulation will be described and the algorithm implemented for maintaining a predetermined ponding water level in the fields according to on site-specific conditions will be presented.

**2. THE CASE STUDY**

The flexible and remote-controlled system of gates has been installed and tested in the 'Cascina Ca' Granda Milano' which is a paddy rice farm (40 ha in size) located in south Milan and consisting of 10 fields of about 4 ha each, on average (Fig. 1).

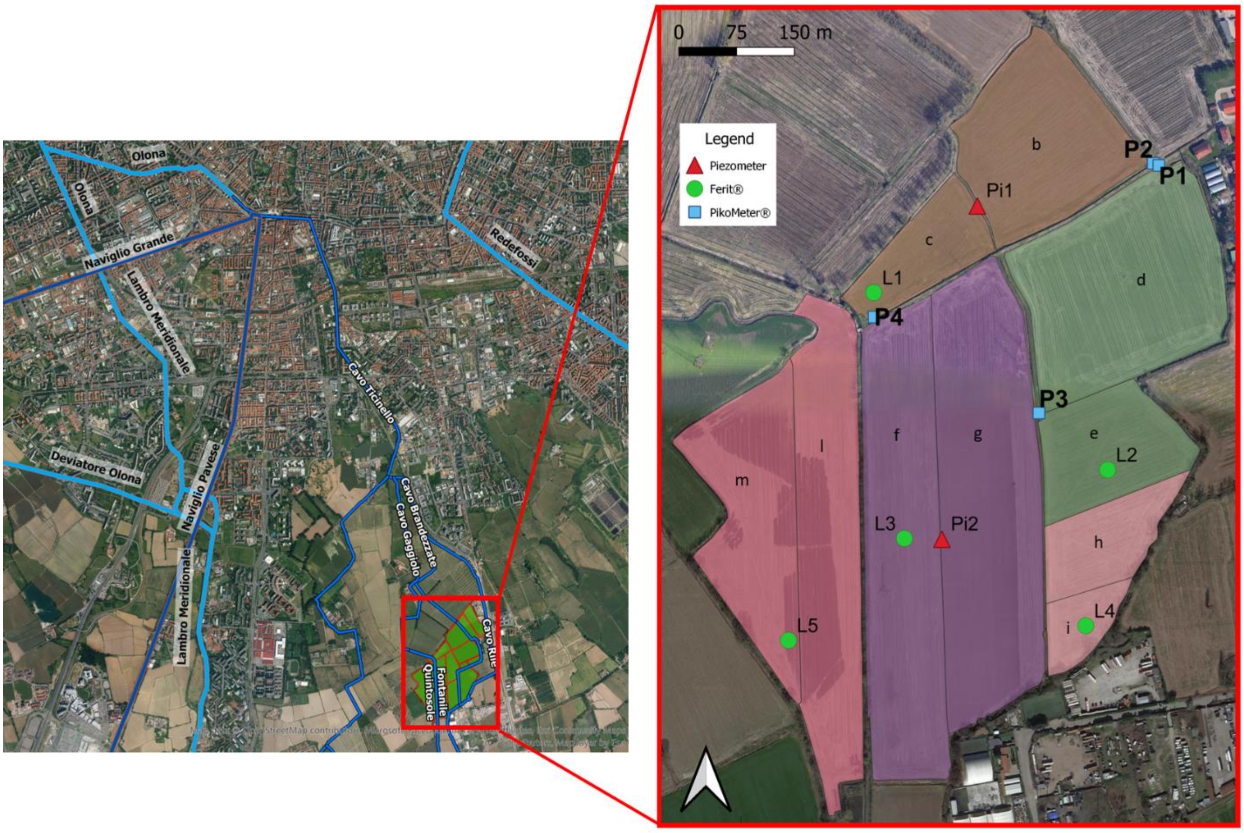


*Fig.1. Cascina Ca' Granda Milano rice farm. In the picture, the field subdivision in blocks and the position of the instrumentation is shown.*

The fields are characterized by a toposequence (from north to south) that facilitates the watering procedures. More in detail, the fields are subdivided in five different blocks (i.e. *bc, de, hi, fg, lm*) which are characterized by a single water flow entry point. For instance, in the block *bc* the only inlet point is located in *b*. From *b* the water flows in *c* since it is topographically more depressed than *b*. According to the toposequence, the fields are irrigated as follow: block *bc* is submerged first, then follows the block *de,* as third the block *hi* and then the block *fg,* finally the block *lm.*

All fields have been seeded with rice and the adopted irrigation practice is the continuous flooding. In particular, rice is seeded in dry soil at the end of April and the fields are flooded when rice is approximately around the three-leaf stage (i.e. about one month after the seeding). The harvesting is typically planned in mid-September, whereas the water into the fields is drained at the end of August. The nominal flow rate delivered to the farm from the irrigation consortium is about 250 l/s in continuous during the irrigation season (i.e. from April to September). The water is delivered to the farm from north, i.e. upstream of the gates P1 and P2. No drainage points are present in the fields, whereas only one farm drainage point is activated in case of overflows.

## 3. INSTRUMENTATION INSTALLED

In strategic points of the farm canals (P1-4 in Fig. 1) four automatic and remote-controlled PikoMeter® gates (Rubicon Water, AU) were installed (Fig. 2a) for managing watering into the fields. The PikoMeter® are constituted by three main components i.e. an ultrasonic level sensor inside the frame of the gate, a flow meter and a steel gate. The flow meter measures flow rate across the gate; hence the volume integrating the flow rates during irrigation. This meter consists of a cylindrical box with 20 ultrasonic transducers across 5 planes of measurement. The flow meter can measure with an accuracy of +/- 2.5% for velocities greater than 25 mm/s. The water level obtained by the ultrasonic level sensor is measured with an accuracy of 0.5 mm and a resolution of 0.1 mm. The gates are equipped with a adaptative control software that allows managing their operation through three different setpoint levels of configuration i.e. maintaining a fixed (i) gate opening, (ii) upstream water level (U/S) or (iii) downstream flowrate (D/S).

In addition to the PikoMeter® five ultrasonic water level sensors (Ferit®) were installed in each fields block (Fig. 2b). The Ferit® position in the field was decided according to the farmer's experience i.e. where its measurement would be representative of the water level in the block (L1-L5 in Fig. 1).

a b

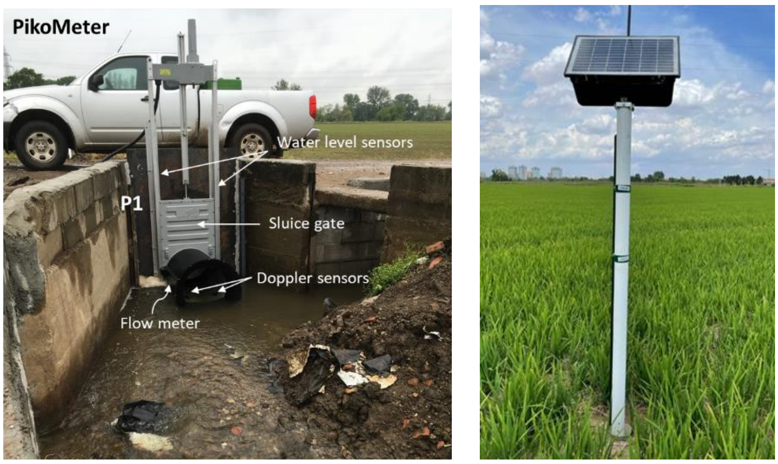


*Fig.2 – Instruments installed in the experimental field of Cascina Ca' Granda Milano. (a) PikoMeter® gate, (b) Ferit® water level sensor.*

Each Ferit® continuously monitors the water level in paddy field and sends the information to a master control system (FarmConnect® Gateway – Rubicon Water AU) that provides instructions, through a tailored algorithm developed in the context of this experimentation, to maneuver the gates as required to maintain a predetermined water level in the field. Finally, the FarmConnect® Gateway provides an interface between cellular networks and PikoMeter® and Ferit®. This interface uses the Telstra NextG protocol to routinely upload the data [through a global system for mobile (GSM) connection] to a Host Server for remote monitoring and control.

## 4. GATE CONTROL ALGORITHM

A tailored gate control algorithm written in Python 3 and running on PythonAnywhere® environment was implemented to provide instructions to maneuvering the PikoMeter® gates from information monitored by Ferit® sensors. The algorithm was able to send HTTP requests to the "Rubicon Site Operations" Application Programming Interface (API), this latter based on RESTful architectural style. The algorithm architecture is presented in Fig. 3 and briefly described in the following.

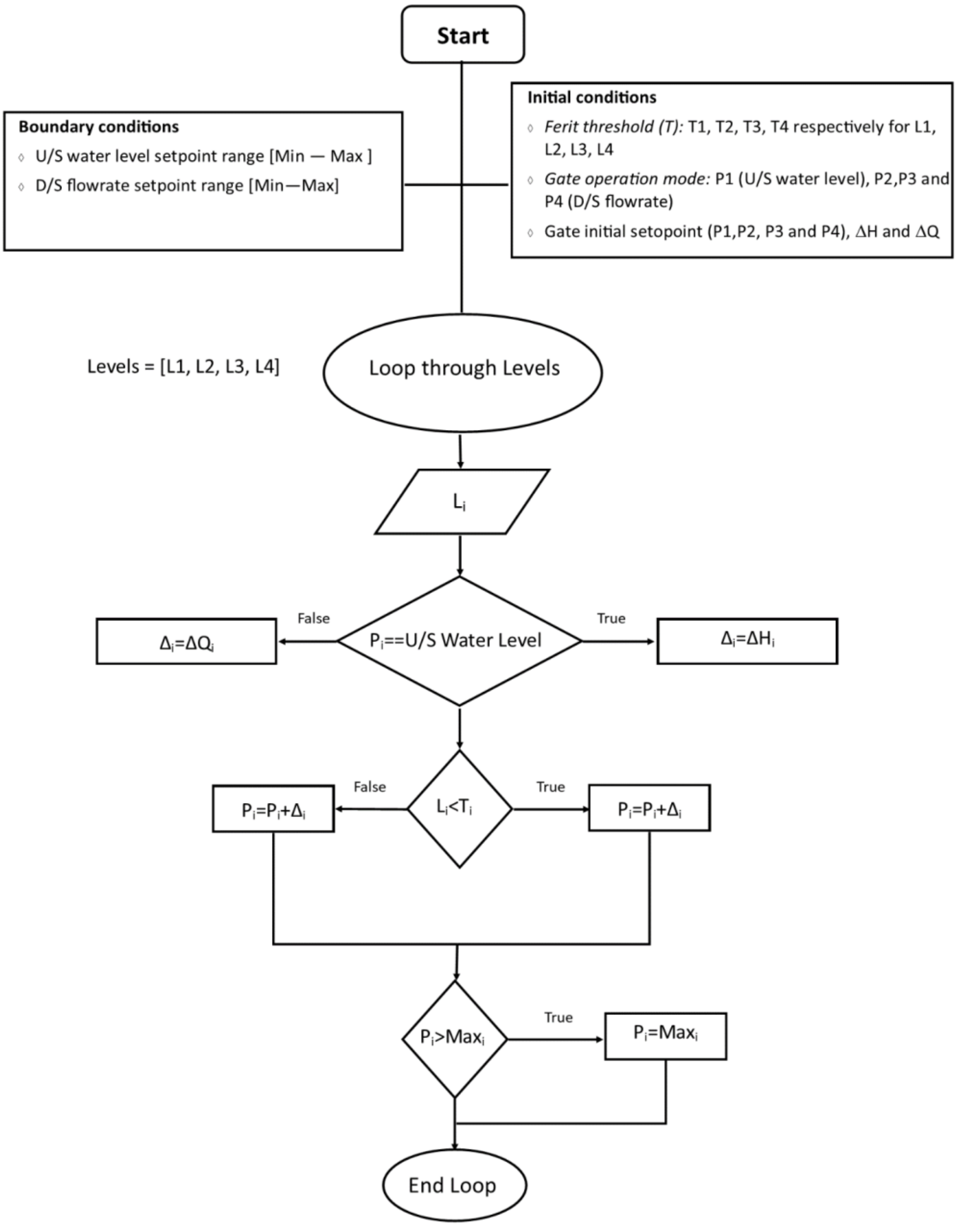


*Fig. 3-Algorithm architecture.*

At the beginning, P1, P2 and P4 are close, whereas P3 is open. P1 works for maintaining a fixed upstream water level, while P2, P3 and P4 a fixed flowrate. An optimal water level that would be maintained into the fields is chosen before irrigation (hereafter threshold - T) and compared with the measurements performed by the Ferit® sensors.

The farm canal upstream of P1 and P2 fills up when the water is delivered by the irrigation consortium, and once a suitable level is reached, it enters into the block *bc*. Until the water level in the first block is less than the threshold, the P1 U/S water level setpoint increases of 5 cm at a time ($\Delta$H) up to the maximum allowed value. If the water into the field exceeds the threshold (with a tolerance of about 10 mm), the P1 U/S water level setpoint decreases of $\Delta$H up to the minimum allowed value. This control is done with a time scheduling of 3 min. During the maintenance phase of the U/S water level, water excess from P1 is released downstream in the block *de.* Once the water level registered by L2 reaches the threshold, the P2 is opened. In particular, if the water level registered by L2 exceeds the threshold, the D/S flowrate setpoint of P2 is increased of 1 l/s at a time ($\Delta$Q) up to the maximum allowed value, while if the water level measured by L2 is less than the threshold, the D/S flowrate setpoint of P2 is decreased up to the minimum allowed value. Downstream P2, the water flows toward block *hi.* In this case the gate (P3) is already opened and the water enters into the field *h* and then *i*. Once the water level registered by L4 reaches the threshold, the P3 is closed. More in detail, if the water level registered by L4 exceeds the threshold, the D/S flowrate setpoint of P3 is decreased of $\Delta$Q up to the minimum allowed value, while if the water level measured by L4 is less than the threshold, the D/S flowrate setpoint of P3 is increased up to the maximum allowed value. After the submersion of *hi*, it is the turn of *fg* block. In this case, when the water level registered by L3 reaches the threshold, the P4 is opened and the water flows in the last block *lm*. The submersion phase of *fg* follows the same philosophy of that applied to submerge the block *de*. Ferit® L5, located in the last block, notifies (through an alarm) potential irrigation problems as, or even before, they occur.

## 5. RESULTS AND DISCUSSION

The effect of the gate control algorithm on the water level inside the fields is shown in Fig. 4, where the evolution of water level in the block *bc* (L1) is reported for a brief period of time (about 12 hours).

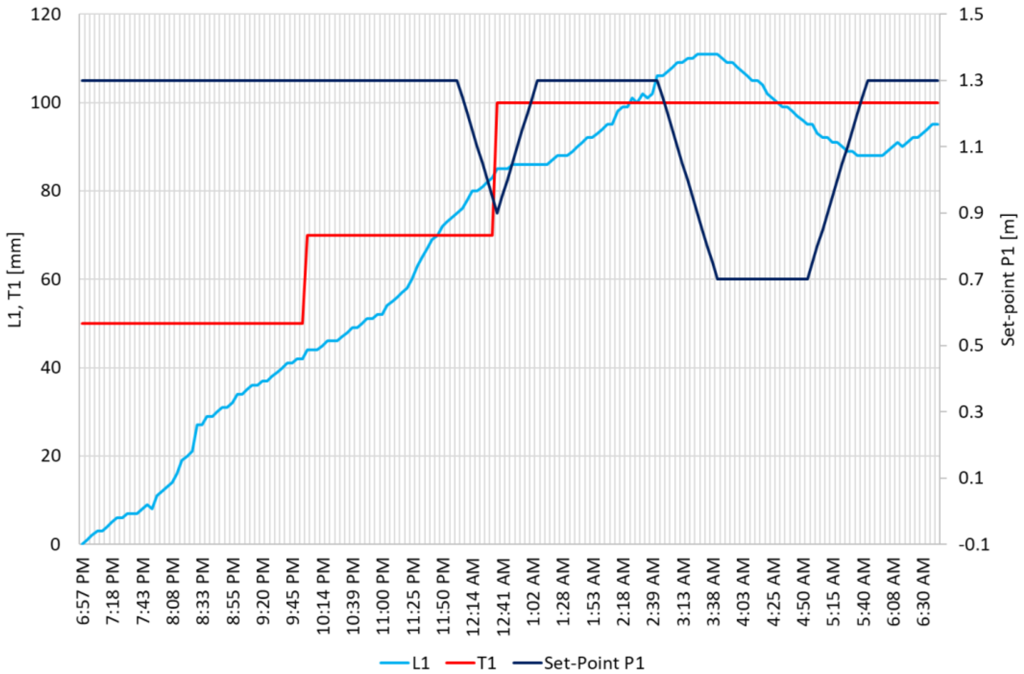


*Fig. 4 – Time evolution of (i) water level into the block (bc) (L1), (i) gate setpoint (P1) and (iii) water level threshold (T1).*

In this example of flow regulation, the water level threshold (T1) was set at about 50 mm for the first 3 hours (from 7:00 PM to 10:00 PM), 70 mm for the next 2 hours (from 10:00 PM to 12:00 AM) and finally at 100 mm. After the algorithm run, the gate setpoint (P1) rapidly increased up to the maximum value set up in the algorithm (1.3 m) until the water level in the field resulted in less than T1. At about 11:25 PM, the water level L1 reached the threshold T1 (50 mm) and the gate P1 automatically decreased its setpoint up to about 0.9 m. Water level into the field stopped to increase for some instant of time, then the T1 was increased at 100 mm and the gate responded increasing its setpoint up to the maximum allowed value (1.3 m). The water level into the field increased up to the new threshold (at about 2.39 AM) and then decreased.

As a result of this algorithm configuration, a lag-time has to be taken into consideration before that the water level into the field changes its pattern as a consequence of the modification of setpoint value. In fact, if we pay attention on the trend of L1 just after the modification of the gate setpoint (P1) occurred at about 2.39 PM, we can observe that the water level still increases for about half an hour and then decreases. This behavior is due to the fact that water needs of a time to flow from the inlet point of the field to the end of the field (where the Ferit® sensor is installed), and a too large range of allowed gate setpoints can cause wide fluctuations of water levels into the field. For instance, in the right part of Fig. 4 is evidenced as the water level oscillates of about +/- 10 mm around the threshold.

**6. CONCLUSIVE REMARKS**

In this work an innovative automatic system designed to support the traditional rice irrigation was presented. The system is composed by four PikoMeter® gates for automatic and remote-controlled flow regulation in the farm canals and five Ferit® sensors for the real-time monitoring of water levels into the fields. A new algorithm was implemented (run through an API interface) to create a connection (currently non-existent) between water level measurements into the fields and gate maneuvering. In general, the automatic irrigation system was robust and did not reveal any mechanical malfunctioning during the examined irrigation seasons. The algorithm resulted stable and guaranteed a robust and continuous connection between Ferit® sensors and PikoMeter® gates. One of the lessons learned during the experimentation is that the way to change the gate setpoints should be improved. The change should be proportional to the water level registered by the Ferit®, without waiting to reach a certain threshold. This might limit the oscillation of the water level in the field around the threshold, decreasing the number of gate maneuvering.

# References


Cesari de Maria, S., Rienzner, M., Facchi, A., Chiaradia, E. A., Romani, M., & Gandolfi, C. (2016). Water balance implications of switching from continuous submergence to flush irrigation in a rice-growing district. *Agricultural Water Management*, *171*, 108-119.

Facchi A., Rienzner M., Cesari de Maria S., Mayer A., Chiaradia E.A., Masseroni D., Silvestri S., Romani M. (2018) Exploring scale-effects on water balance components and water use efficiency of toposequence rice fields in Northern Italy. Hydrology Research, 49(6), 1711-1723. ISSN: 0029-1277. DOI:10.2166/nh.2018.125.

Masseroni, D., Uddin, J., Tyrrell, R., Mareels, I., Gandolfi, C., & Facchi, A. (2017). Towards a smart automated surface irrigation management in rice-growing areas in Italy. *Journal of Agricultural Engineering*, *48*(1), 42-48.

Masseroni, D., Moller, P., Tyrell, R., Romani, M., Lasagna, A., Sali, G., Facchi A. & Gandolfi, C. (2018). Evaluating performances of the first automatic system for paddy irrigation in Europe. *Agricultural water management*, *201*, 58-69.

**Water-saving irrigation techniques for rice cultivation in Baix Ter irrigation district**

**Authors**: Sílvia Cufí[1], Gerard Arbat[1], Jaume Pinsach[1], Miquel Duran-Ros[1], Jaume Puig-Bargués[1], Joan Pujol[1], Josep M Villar[2], Luciano Mateos[3], Arianna Facchi[4], Francisco Ramírez de Cartagena[1]

**Affiliation**: [1] Department of Chemical and Agricultural Engineering and Agrifood Technology, University of Girona, Carrer de Maria Aurèlia Capmany, 61, 17003 Girona, Catalonia, Spain; [2] Department of Environmental and Soil Sciences, Universitat de Lleida, Lleida, 25003, Spain; [3] Instituto de Agricultura Sostenible, CSIC, Alameda del Obispo, 14004 Córdoba, Spain; [4] Department of Agricultural and Environmental Sciences – Production, Landscape, Agroenergy (DiSAA), Università Degli Studi di Milano, Via Celoria 2, 20133 Milan, Italy

**Abstract**

Rice is the main staple food in many countries and, because of its particular irrigation water management, it provides complementary ecosystem services where it is cultivated. In the Mediterranean area, rice is traditionally cultivated under flooding conditions (WFL, water sowing and continuous flood irrigation), which are maintained with a variable ponding water level until 2 – 4 weeks before harvest. Because of the increasing fresh water scarcity, other irrigation methods are being tested to reduce water use while maintaining yield. Some of these techniques, such as dry seeding and delayed flood irrigation (DFL) and subsurface drip irrigation (SDI), have been studied as part of MEDWATERICE project to assess their viability in Baix Ter rice area (Girona, Spain).

Water balances to evaluate the effects of water-saving irrigation techniques and to support water-management decisions were carried out for 3 different irrigation management practices (WFL, DFL and SDI) as part of the tests performed in Baix Ter rice production area during 2020 and 2021. Three commercial rice fields of 1.16, 1.15 and 0.38 ha with silty-clay-loam, loam and silty-clay textured soils were selected for WFL, DFL and SDI testing, respectively. Irrigation water, soil water contents, ponding water level and meteorological variables were continuously monitored in all cases. No water runoff from the paddies was observed due to the irrigation management carried out by rice producers in the fields. Percolation plus lateral seepage (SP) was computed as water balance closure term.

No irrigation water reduction was registered in DFL when compared to WFL. In both cases, about 1,300 mm of irrigation water were applied during both agricultural seasons. SDI irrigation water application was 44% and 38% lower than in WFL during 2020 and 2021, respectively. The largest water output from DFL and WFL was SP, which averaged 77% of the irrigation input in both campaigns. When using SDI, SP accounted for 52% of the irrigation inputs, almost the same proportion as crop evapotranspiration, which accounted for 48% of irrigation. Yields were not significantly different when using different irrigation methods, and they were close to the average one in the area. DFL, however, showed slightly higher yields during both seasons due to agronomic reasons other than irrigation management.

**Keywords**: Rice; Irrigation; Water-saving; Aerobic rice; Water productivity

## 1. Introduction

Rice (*Oryza sativa L.*) is a staple food in many countries and is critical for global food security (Maclean et al., 2013). As stated in Food and Agriculture Organization of the United Nations (2021), almost 90% of rice is produced in Asia. In Europe, Spain is the second major producer after Italy, with a total surface of 102,060 ha in 2020.

**Bucket water mass balance model applied to the rice growing areas of Lower Mondego (Portugal) and Bafra (Turkey) Irrigation Districts**

**Authors:** *Blanca Cuadrado-Alarcón*[1], *Melih Enginsu*[2], *Isabel Pedroso de Lima*[3], *Özgür Azapoglu*[2], *Romeu Gerardo*[3], *Luciano Mateos*[1]

**Affiliation:** [1] Instituto de Agricultura Sostenible, CSIC, 14004 Córdoba, Spain; [2] Black Sea Agricultural Research Institute, PK. 39 Samsun, Turkey; [3] University of Coimbra, 3041 Coimbra, Portugal.

**Abstract**

The MEDWATERICE project includes upscaling of the on-farm irrigation management improvements to the irrigation district scale. A 'bucket' mass balance approach was applied to two study cases in the project: i) Quinta do Canal, in the Lower Mondego irrigation district (Portugal), with 322 ha of rice production and supplied by the Mondego River; and ii) the west side of the Bafra irrigation district (Turkey), with 6200 ha of irrigated land (5100 ha devoted to rice cultivation), and supplied by the Kızılırmak River. In the two areas, water is supplied by a branched hierarchical open channel flow network, with no water reuse.

The application of the 'bucket' mass balance approach requires the conceptualization of the systems using topological flow diagrams. After that, the model computes daily water balances for the irrigation units, based on the aggregation of the paddy fields that are served by each secondary canal. The water balance components are evapotranspiration, percolation, surface drainage (if present), precipitation and irrigation. Available data of actual water supply were used to evaluate the model, which will be used to examine the impact at district scale of the implementation of on-farm water saving practices.

**Keywords:** 'bucket' model, water balance, irrigation, rice.

## 1. Introduction

The rice irrigation management improvements studied within the scope of the MEDWATERICE project include different options: dry seeding, AWD (alternate wetting and drying) irrigation, surface and subsurface drip irrigation, multi-outlet hybrid irrigation, or drainage water recycling.

To upscale those on-farm improvements to the irrigation district scale, different methodologies have been applied, including the 'bucket' mass balance approach (Mateos et al., 2000). This approach was applied to most of the study cases in the project. In this paper, we report the application to (i) Quinta do Canal, in the Lower Mondego irrigation district (Portugal), supplied by the Mondego River; and (ii) the west side of the Bafra irrigation district (Turkey), supplied by the Kızılırmak River.

The two areas are traditionally rice growing areas, and a good part of their economy is dependent on rice production. In both cases, water is supplied by a branched hierarchical open channel network, with no water reuse.

The Quinta do Canal pilot area devotes 322 ha to rice production (Figure 1), part of the 5000 ha of rice grown in the Lower Mondego irrigation district. Water is supplied by 4 secondary canals deriving for the district main canal. Quinta do Canal faces poor soil drainage and relatively high salinity. Rice cycle is around 5 months, typically from April/May to September/October. The area is characterized by a small size of the holdings (only about 20% of the agricultural holdings have an area larger than 2.5 ha) and relatively low yield (6 t/ha/year), which forces the need for a complementary family income. Irrigation is traditionally by flooding, and it is estimated that the current irrigation practice requires on average about 16,390 $m^3$/ha/year (e.g., Oliveira et al., 2022), at the irrigation district scale.

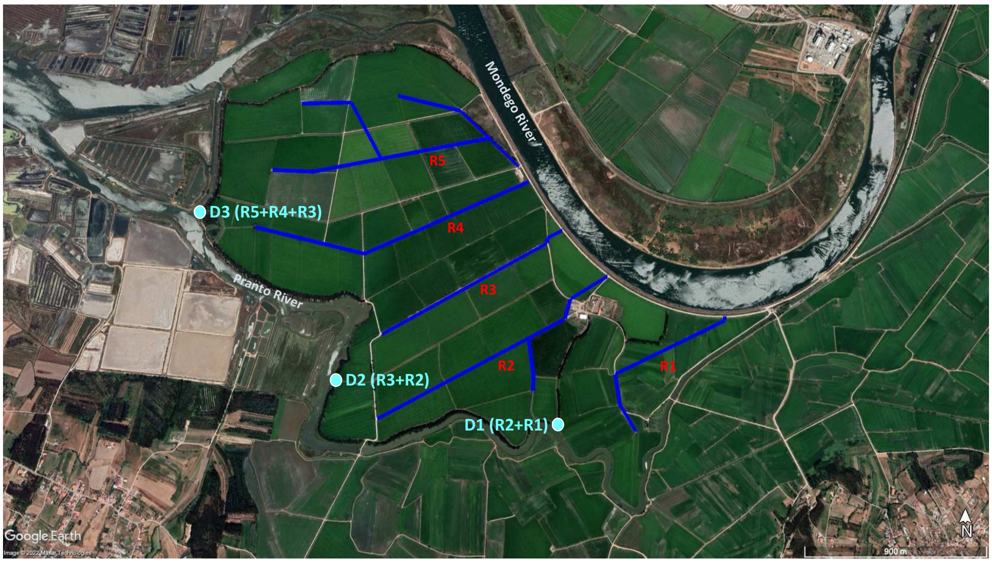


**Figure 1. Area of Quinta do Canal and identification of the five inlets from the main irrigation canal, the secondary canals (R) and 3 drainage outlets (D) to the Pranto River (Source: Google Maps, 2022).**

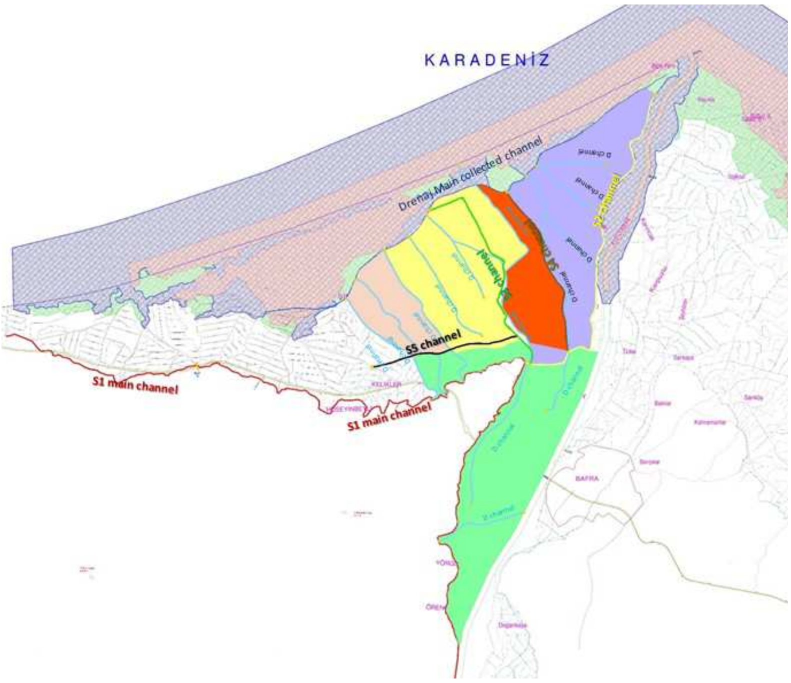


**Figure 2. Bafra plain and irrigation sectors (in colour) in the Bafra Plain west side Irrigated Area.**

The west side of the Bafra irrigation district (Figure 2) encompasses 6200 ha of irrigated land, including rice, maize, and horticulture, of which 5100 ha are devoted to rice cultivation.

Irrigation water used in the flooded irrigated rice fields is about 24,000 $m^3$/ha according to the General Directorate of State Hydraulic Works. The fields are bordered to prevent surface drainage, while a subsurface drainage system evacuates field water percolation through a drainage ditch network. Crop rotation is a common practice in the area mainly to prevent the soil from a long exposition to anaerobic conditions. Usually, rice is cultivated continuously during 5 to 7 years, and then the land is rotated to another crop.

## 2. Materials and methodology

Water circulation in the two study sites has been modelled with the 'bucket' mass balance approach (Mateos, 2008). The application of the 'bucket' approach requires first a conceptualization of the systems using topological flow diagrams. This diagram is determined by the layout of the hierarchical branched distribution networks and of the drainage network that collects return flows from the fields. The fields that share irrigation canal and drainage ditch are aggregated into irrigation units.

The water balance model computes daily balance components for each irrigation unit. These components are evapotranspiration, percolation, surface drainage (if present), precipitation and irrigation. Figure 3 shows a diagram of the water balance components computed for an irrigation unit.

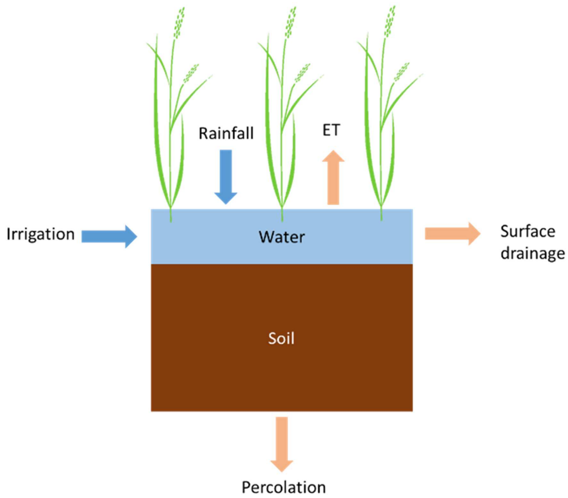


**Figure 3. Water fluxes in a paddy field.**

**Crop evapotranspiration ($ET_{ci}$)** is calculated with the single crop coefficient method. The daily crop coefficient will be considered as 1.05 when the paddy is flooded and before rice plants emerge above the water surface, increasing to 1.20 when the crop is fully developed, and dropping to 0.6, just before harvest, according to FAO (Allen et al., 1998). The **rainfall daily value ($R_i$)** and crop evapotranspiration daily value ($ET_{ci}$) are expressed in cubic meters in the irrigated unit. The $i$ subindex in all the equations represents the day in the balance, and $i-1$ indicates the value of the day before. Daily data for reference evapotranspiration and daily rainfall is available in both study cases from nearby weather stations.

**Percolation ($P_i$)** is estimated from a daily rate (K) introduced as a soil property expressed in mm of percolation per day and unit of area. $P_i$ , expressed in cubic meters, is:

$$P_i = Area * K$$

When the soil is saturated, percolation rate is equal to *K*, and when it is not saturated, percolation rate is considered zero.

For the balance purposes, the profile is divided into two layers, (1) the soil layer, which has a **soil water content ($SWC_i$)**, expressed in cubic meters, and (2) the free water layer, with a volume named **free water volume ($FWV_i$).**

The water balance accounts for management practices, through a parameter **called target free water depth ($TFWD_i$)** that measures the level of required free water layer in the field. This is a daily management input that varies depending on the area and the farmer. The $TFWD_i$ is transformed into **a target free water volume ($TFWV_i$)** using the area of the irrigation unit.

In the Quinta do Canal case study, **surface drainage ($D_i$)** is only used when the paddy field needs to be emptied. Then, the model simulates drainage by lowering $TFWD_i$ along 14 days. In the Bafra case study, there is no surface drainage (fields are emptied through percolation).

The daily **irrigation needs ($I_i$)** are calculated through the water balance with the objective of reaching $TFWV$ of the day:

$$I_i = TFWV_i - FWV_{i-1} + SWC_{SAT} - SWC_{i-1} + ETc_i - R_i + P_i + D_i$$

However, the resulting **irrigation ($I_i$)** is subjected to two conditions:

- ✓ If the value obtained is lower than 0, then $I_i$ remains 0.
- ✓ If the value obtained is higher than the maximum supply capacity, $I_i$ will be the maximum supply capacity.

Finally, $SWC_i$ and $FWV_i$ are calculated as follows:

$$SWC_i = SWC_{i-1} + FWV_{i-1} - ETc_i - P_i + R_i + I_i - D_i$$

If $SWC_i < SWC_{SAT}$, then $FWV_i = 0$

If $SWC_i > SWC_{SAT}$, then $SWC_i = SWC_{SAT}$

and $FWV_i = FWV_{i-1} - SWC_{SAT} + SWC_{i-1} - ETc_i - P_i + R_i + I_i - D_i$

Data used to run the model included cropped area by irrigation unit, weather data from a nearby station, and some measurements of soil texture. In Quinta do Canal, Sentinel-2 satellite imagery of the study area, with 10 m full spatial resolution and already atmospheric corrected, was downloaded from the Copernicus open-access website (https://sci-hub.copernicus.eu) and used to derive site specific crop coefficients derived from the vegetation index NDVI (Mateos et al., 2013; González-Dugo et al., 2013).

Irrigation district estimations of the water supply for the different irrigation units were used to evaluate the results of the model.

## 3. Results and discussion

### 3.1. Conceptualization of the case studies

Figures Figure 4 and Figure 5 represent the layout of the two case studies modelled with the 'bucket' approach.

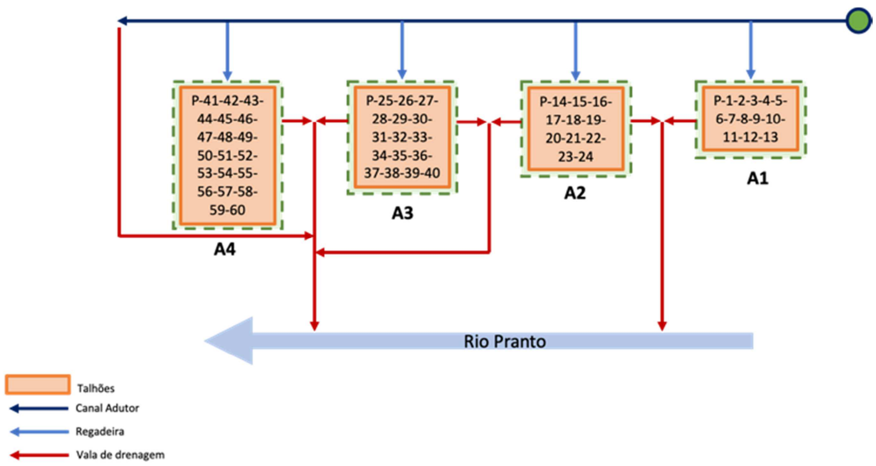


**Figure 4. Conceptual layout of the hydraulic arrangement for the 'bucket' modelling approach applied to the Quinta do Canal. See Figure 1 for relating the case study map with the mass circulation diagram.**

Figure 4 shows the four irrigation units defined for the Quinta do Canal case study. Water flow from the main canal is represented with a dark blue arrow, and the flow diverted into the four secondary canals is represented with light blue arrows. The fields supplied by each secondary canal were grouped into irrigation units A1 to A4. Surface drainage and percolation that ends up in the surface drainage network through lateral fluxes is represented by the red arrows that lead to the Pranto River.

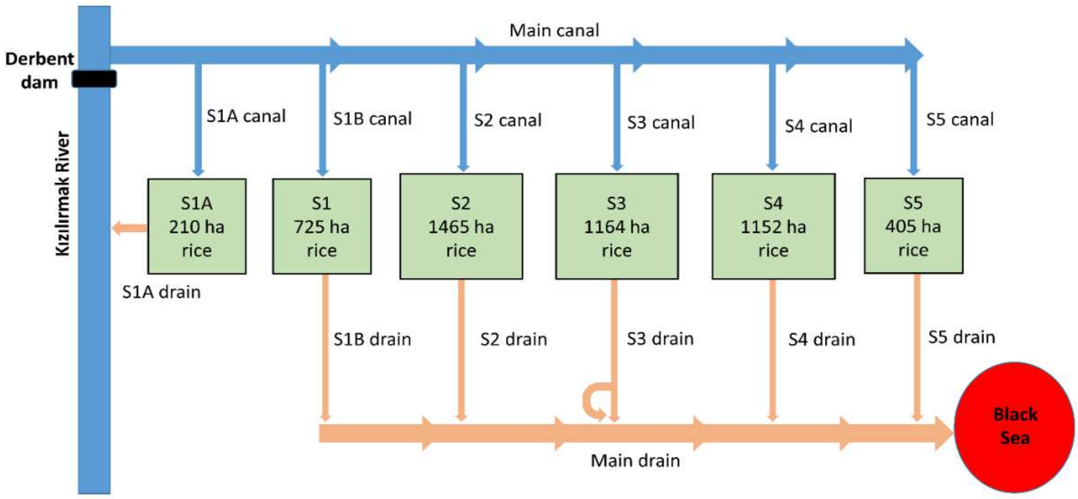


**Figure 5. Conceptual layout of the hydraulic arrangement for the 'bucket' modelling approach applied to the Bafra Plain west Side Irrigated Area. See Figure 2 to relate with case study map.**

Figure 5 shows the six irrigation units defined for the Bafra Plain west side case study. Water flows from the main canal and is diverted into six simplified secondary canals (represented by light blue arrows). The secondary canals serve the irrigation units S1A to S5. Percolation that ends up in the drains through lateral fluxes is represented by the orange arrows that lead to the Kızılırmak River or to the Black Sea.

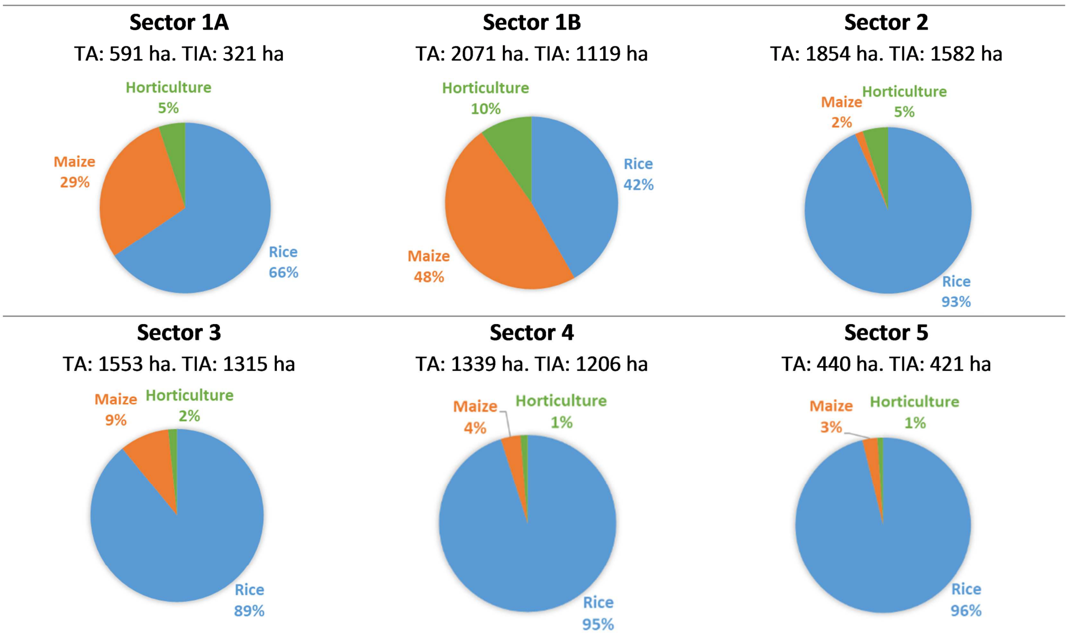


**Figure 6. Irrigated crop distribution in the 6 irrigation units of Bafra Plain west side. TA refers to total area, and TIA is the total irrigated area.**

The cropping pattern in the Bafra west side case study included: rice, barley, Vicia sativa, maize, melon, cauliflower, wheat, and many others. Some crops are not irrigated, although some supplementary irrigation might be applied when the weather is not optimal for the crop development. To model the water balance, irrigated crops have been classified in three groups: rice, maize, and horticulture. The cropping areas obtained are shown in Figure 6.

### 3.2. Water balance results in Quinta do Canal

The water fluxes obtained with the application of the water balance model to each irrigation unit of Quinta do Canal are presented in Figure 7. And the aggregated values are presented in Figure 8.

Table 1 presents total values for the modelled year. The average irrigation obtained is 1,442 mm/year.

Surface drainage occurs at two times, in June for pesticides treatment and before harvest. Irrigation has the higher peak at the beginning of the season when the paddies are filled up with water.

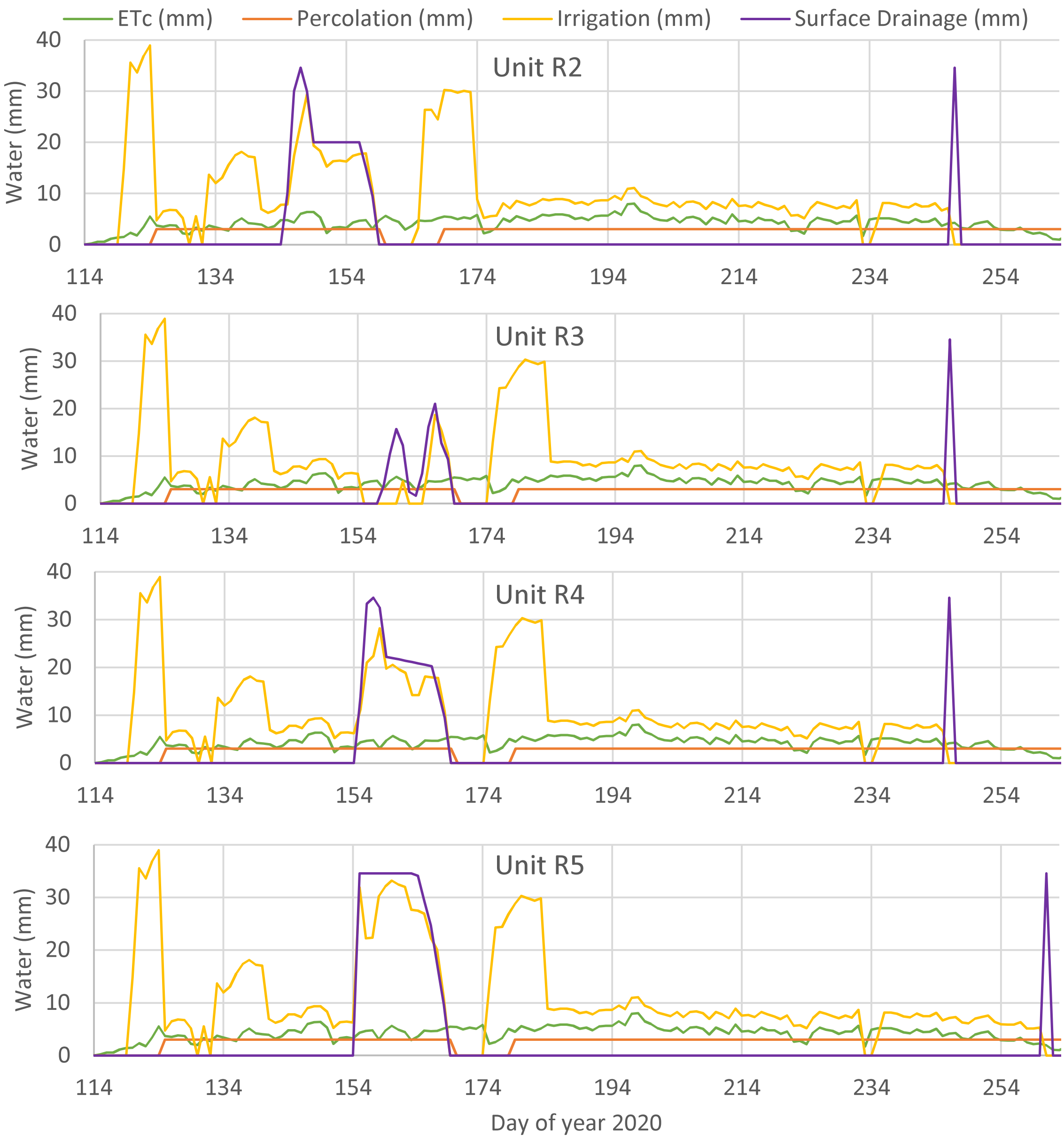


**Figure 7. Water balance results for irrigation units in Quinta do Canal (Portugal).**

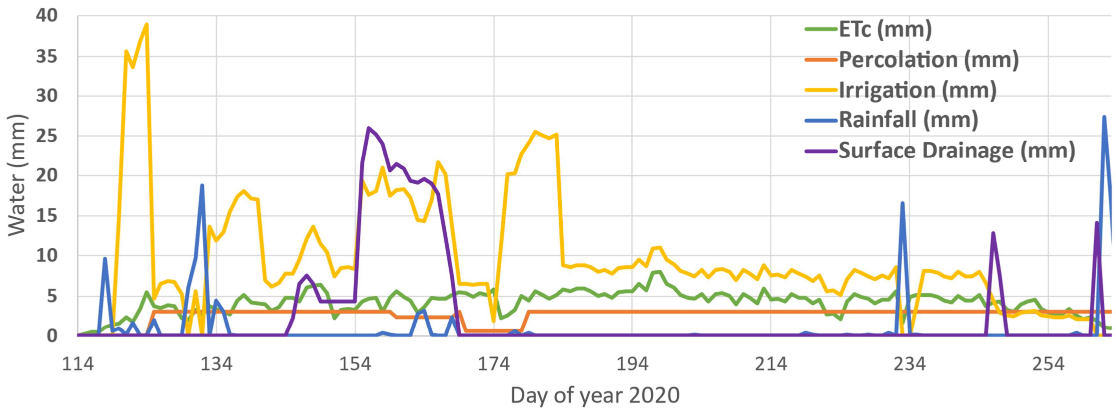


**Figure 8. Results for total daily water fluxes obtained from the mass balance in Quinta do Canal (Portugal).**

**Table 1. Modelled water balance fluxes for the irrigation season 2020 in Quinta do Canal.**

| **Total values** | **Water (mm)** |
|---:|---:|
| **ETc** | 633 |
| **Rainfall** | 134 |
| **Percolation** | 402 |
| **Surface drainage** | 358 |
| **Irrigation** | 1442 |
| **Increase in water content** | 183 |

### 3.3. Water balance results in Bafra

Table 2 shows total simulated water balance fluxes for year 2020. The values presented in the table encompasses all three simulated crop types. Average supply modelled for rice is highest, with an average value of 3,508 mm/year.

**Table 2. Modelled water balance fluxes for the irrigation season 2020 in Bafra plain west side.**

| | ETc ($m^3$/ha) | Perc ($m^3$/ha) | Irrig ($m^3$/ha) | Rain ($m^3$/ha) |
|---|---:|---:|---:|---:|
| S1A | 534 | 1,153 | 17,42 | 85 |
| S1B | 525 | 3,845 | 43,96 | 87 |
| S2 | 541 | 1,625 | 22,99 | 78 |
| S3 | 542 | 2,593 | 32,71 | 80 |
| S4 | 544 | 1,662 | 23,48 | 78 |
| S5 | 545 | 1,681 | 23,79 | 78 |

Detailed graphs of water balance components for the different irrigation units are presented in Figure 9. Daily values resulting from the water balance are shown in Figure 10. FWV represents the variation of the water level in the rice fields (determined by management decisions) and explains the three peaks that appear in the irrigation curve, to fill up the paddies.

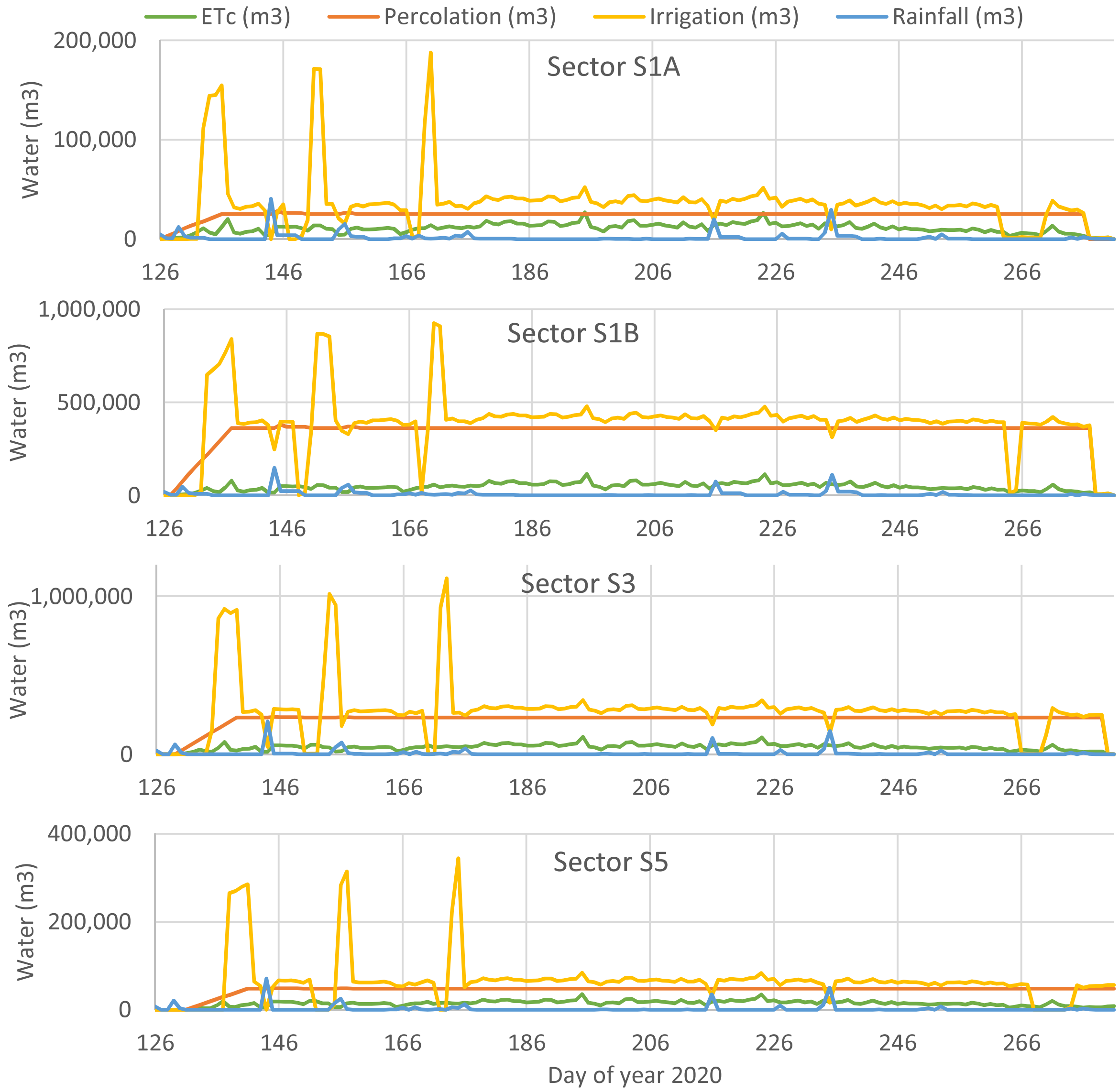


**Figure 9. Results of the daily water balance in some of the sectors in Bafra Plain left Side (Turkey).**

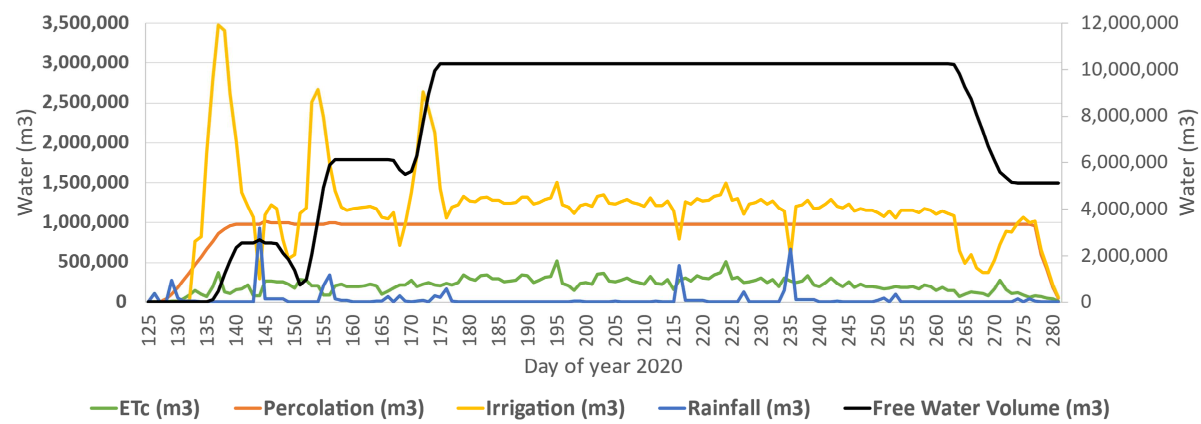


**Figure 10. Results of the total estimated daily water fluxes after the mass balance in Bafra Plain west side (Turkey). Free water volume (FWV) values correspond to the y axis on the right, the rest of the results represented correspond to the y axis on the left.**

### 3.4. Discussion

Available data on estimated water supply were used to evaluate the model, which could be used to upscale on-farm current management at district scale. Daily supply data in the Quinta do Canal case study was compared with the modelled irrigation requirement (Figure 11).

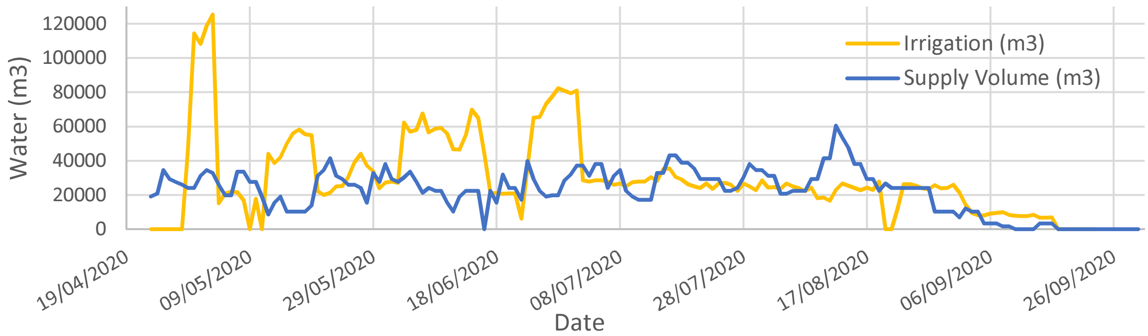


**Figure 11. Comparison of estimated and modelled data on irrigation supply for Quinta do Canal, rice cultivation season 2020.**

**Table 3. Modelled and estimated total supply volumes in Quinta do Canal, season 2020.**

| | R2 ($m^3$) | R3 ($m^3$) | R4 ($m^3$) | R5 ($m^3$) | Total ($m^3$) | Total ($m^3$/ha) | Total (l/s/ha) |
|---|---|---|---|---|---|---|---|
| **Estimated** | 639,360 | 453,600 | 864,000 | 1,595,592 | 3,552,552 | 11,033 | 0.829 |
| **Simulated** | 962,036 | 571,138 | 998,688 | 2,110,644 | 4,642,506 | 14,418 | 1.084 |

Table 3 includes the seasonal estimated and modelled water supply for each irrigation unit and the total value. Estimated supply values (11,033 $m^3$/ha/year for the entire study area) were lower than simulated ones, 3,400 $m^3$/ha/year on average. This difference could be due to inaccurate estimation of the percolation rate, which has been estimated from two soil texture analyses. But it could also be caused by an inaccurate estimation of the water supplied to the irrigation units, used to evaluate the model. As mentioned in the introduction section studies such as Oliveira et al. (2022) estimate rice irrigation in the area in 16,390 $m^3$/ha/year whereas our estimates reach only 11,033 $m^3$/ha/year. A better understanding of percolation in the area would help understand if the water balance model is simulating correctly the processes occurring in the field.

**Table 4. Estimated and modelled water flows, irrigation season 2020 in Bafra plain west side.**

| Sector | Irrigated area (ha) | Estimated water supply ($m^3$/ha/year) | Modelled water supply ($m^3$/ha/year) | Total volume of estimated supply ($m^3$/year) | Total volume of modelled supply ($m^3$/year) |
|---|---|---|---|---|---|
| **S1A** | 320.9 | 79,416 | 17,422 | 25,484,586 | 5,590,818 |
| **S1B** | 1118.6 | 79,416 | 43,958 | 88,834,710 | 49,171,720 |
| **S2** | 1581.8 | 36,086 | 22,989 | 57,081,024 | 36,364,653 |
| **S3** | 1315.4 | 31,201 | 32,715 | 41,041,728 | 43,033,490 |
| **S4** | 1206.0 | 18,776 | 23,479 | 22,643,712 | 28,315,293 |
| **S5** | 421.0 | 59,388 | 23,794 | 25,002,432 | 10,017,151 |
| **Global** | 5963.7 | 43,611.9 | 27,393 | **260,088,192** | **172,493,126** |

In the Bafra plain west side case study, available supply data were an average seasonal value of discharge in the distribution open channels, based on the design of the channels and assuming a constant water depth. The comparison between the estimated and modelled values is shown in

Table 4. Globally, modelled supply water was lower than the estimated supply. One possible reason for this discrepancy is that the channels might not always work at their full capacity.

Nevertheless, simulated results are of the same order than the supply data, but the quantity differs by more than a third. Particularly, sector S1A and S1B have very high estimates, which might be because those estimates correspond to the main channel, that continues further where the irrigation system is still under construction, thus its capacity overestimates actual discharge.

In general, crop water allocation is higher in Bafra plain than in Quinta do Canal, which is consistent with their climates and their water stress. Moreover, percolation is higher in Bafra plain than in Quinta do Canal, which will reinforce the difference in irrigation needs between the two areas.

## 4. Conclusions

The study cases of Quinta do Canal (Portugal), with 322 ha, and the west side of the Bafra irrigation district, with 6200 ha, have been modelled with the 'bucket' mass balance approach. A conceptualization of each system was first carried to apply the model. Results for the irrigation season 2020 showed a response to climate conditions and soil characteristics. Modelled results estimate irrigation needs of 14,420 $m^3$/ha/year for the Quinta do Canal area and 27,393 $m^3$/ha/year for the west side of the Bafra irrigation district.

Comparison with available supply data show a discrepancy with the modelling results, but the order of magnitude is the same. The reason for this gap is unknown due to the uncertainty in the estimated supply data available for model evaluation, and in some of the parameters used for the modelling exercise, which would in some cases require a more intense monitoring activity; this is particularly true for the percolation rates.

There is a considerable amount of potential work to be carried in the two areas to improve the results and obtain more information, such as monitoring discharges and solutes at certain locations upstream and downstream; this would allow to improve the water mass balance and introduce the solute mass balance in the modelling process.

**Acknowledgements:** This work is included in the framework of the MEDWATERICE project *Towards a sustainable water use in Mediterranean rice-based agro-ecosystems*, funded by the PRIMA program (Agencia Estatal de Investigación, PCI2019-103714; Fundação para a Ciência e a Tecnologia, PRIMA/2018/0006).

## References

Allen, R.G., Pereira, L.S., Raes, D. and Smith, M., (1998). Crop evapotranspiration - Guidelines for computing crop water requirements. *FAO Irrigation and Drainage Paper 56*. FAO, Rome.

González-Dugo, M.P., Escuin, S., Cano, F., Cifuentes, V., Padilla, F.L.M., Tirado, J.L., Oyonarte, N., Fernández, P. and Mateos L., (2013) Monitoring evapotranspiration of irrigated crops using crop coefficients derived from time series of satellite images. II. Application on basin scale. *Agricultural Water Management*. 125: 92-104

Mateos L, Young CA, Wallender WW, Carlson HL (2000) Simulating spatially distributed water and salt balances. *J Irrig Drain Engrg* 126:288–295

Mateos, L. (2008) Identifying a new paradigm for irrigation system performance. *Irrigation Science* 27:25-34

Mateos, L., González-Dugo, M.P., Testi, L., Villalobos, F.J., (2013) Monitoring evapotranspiration of irrigated crops using crop coefficients derived from time series of satellite images. I. Method validation. *Agricultural Water Management*. 125: 81-91

Oliveira, M.D., Oliveira, S., Russo, A.T., Bahcevandziev, K., Lopes, A.B., Jordão, A.J., Gonçalves, J.M., Nunes, M., Reis, P.A., (2022) Sustainability of Rice Production at Baixo Mondego, Portugal: Drivers, Risks, and System Improvements. *Impacts of Climate Change and Economic and Health Crises on the Agriculture and Food Sectors*; Martinho, V., Ed.; IGI Global: Pennsylvania, PA, USA, pp. 266–287.